molecules

Review

Structure and Biological Activity of Ergostane-Type Steroids from Fungi

Vladimir N. Zhabinskii [1,*], Pavel Drasar [2] and Vladimir A. Khripach [1]

[1] Institute of Bioorganic Chemistry, National Academy of Sciences of Belarus, Kuprevich Str., 5/2, 220141 Minsk, Belarus; khripach@iboch.by
[2] Department of Chemistry of Natural Compounds, University of Chemistry and Technology, Technicka 5, CZ-166 28 Prague, Czech Republic; pavel.drasar@vscht.cz
* Correspondence: vz@iboch.by; Tel.: +375-297-579-811

Abstract: Mushrooms are known not only for their taste but also for beneficial effects on health attributed to plethora of constituents. All mushrooms belong to the kingdom of fungi, which also includes yeasts and molds. Each year, hundreds of new metabolites of the main fungal sterol, ergosterol, are isolated from fungal sources. As a rule, further testing is carried out for their biological effects, and many of the isolated compounds exhibit one or another activity. This study aims to review recent literature (mainly over the past 10 years, selected older works are discussed for consistency purposes) on the structures and bioactivities of fungal metabolites of ergosterol. The review is not exhaustive in its coverage of structures found in fungi. Rather, it focuses solely on discussing compounds that have shown some biological activity with potential pharmacological utility.

Keywords: ergosterol; ergosteroids; fungi; mushrooms; anticancer; antiviral; cytotoxicity

check for updates

Citation: Zhabinskii, V.N.; Drasar, P.; Khripach, V.A. Structure and Biological Activity of Ergostane-Type Steroids from Fungi. *Molecules* **2022**, 27, 2103. https://doi.org/10.3390/molecules27072103

Academic Editors: Jacques Lebreton and Lillian Barros

Received: 28 February 2022
Accepted: 23 March 2022
Published: 24 March 2022

1. Introduction

Fungi are a rich source of chemical compounds with a wide spectrum of biological activity [1]. To survive in the environment in which they exist, they need to protect themselves from fungal infections. Therefore, it is not surprising that antimicrobial or antiviral compounds beneficial to humans can be isolated from many fungi [2]. A large number of currently used drugs have their origins in fungi [3]. Steroids occupy an important place among fungal constituents. The vast majority of them are ergosterol metabolites. The latter is the main sterol of fungi involved in the regulation of membrane fluidity and structure as well as performing immunological functions [4]. Fungal ergosterol derivatives are often referred to as "ergostane-type steroids" [5–12] or "ergosteroids" [13–17]. One should bear in mind, however, that the application of the term "ergosteroids" can be confusing, as it was also suggested by Lardy et al. [18] to structurally different dehydroepiandrosterone derivatives based on their mode of action (influence on energy metabolism).

Ergostane-type steroids are characteristic not only of fungi but also of plants [19–21] and sponges [22]. These steroids are not a focus of the present paper. The purpose of this review is to highlight current knowledge on the structures and biological activities of fungal constituents, built on an ergostane skeleton **1** (Figure 1) or structures of which can be traced back to it. Currently, there are a number of reviews in this area dedicated to certain aspects or groups of ergostanes. A nice review on chemistry, biology, and medicinal aspects of rearranged ergostane-type natural products has been published recently by Heretsch et al. [23]. A detailed literature survey by Merdivan and Lindequist was dedicated to the consideration of biological activities of a single compound (ergosterol 5α,8α-endoperoxide) [24]. Many reviews discuss ergostane-type steroids as a part of fungal compositional diversity constituents [25–32].

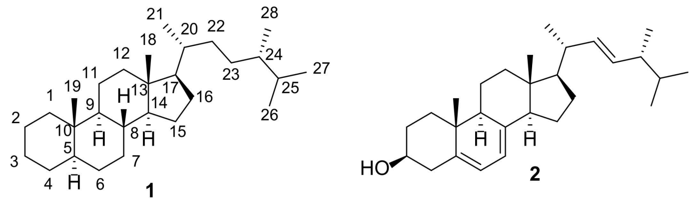

Figure 1. 5α-Ergostane skeleton **1** and structure of ergosterol (**2**).

2. Sterols

2.1. Ergosterol

Detailed studies of the biological effects of fungi have shown that some of them can be attributed to ergosterol (**2**) [33–38]. That is why ergosterol itself has attracted considerable attention as a potential lead for the development of new therapeutics. Its anticancer properties were investigated on the lungs [39], liver [40,41], breast [42], human gastric [43], and prostate [44] cancer cell lines.

Ergosterol treatment of mice inoculated with breast cancer cells prolonged mouse survival [42]. Suppression of cancer cell viability was explained by apoptosis and by up-regulating Foxo3 and Foxo3 downstream molecules Bim, Fas, and Fas L.

The antitumor potential of ergosterol was studied upon its application with amphotericin B [40]. The latter is a macrolide antifungal agent that is also used to reverse chemotherapeutic drug resistance. The combined treatment of liver cancer cell lines with ergosterol followed by amphotericin B resulted in a significant decrease of their viability as a result of necrotic cell death.

Experiments on reversing multidrug resistance in cancer cells were also performed using drug-sensitive human gastric carcinoma cell line SGC7901 and its adriamycin-resistant counterpart SGC7901/Adr. Ergosterol at concentrations below 5 μM has been shown to enhance the cytotoxicity of adriamycin on SGC7901/Adr cells [43].

In experiments with Hep2 cancer cells, it was shown that ergosterol inhibited cell growth with IC_{50} value of 40 μM/mL [41]. The observed effect was explained by the pro-oxidant properties of ergosterol on the Hep2 cells.

Different effects have been noted for androgen-dependent LNCaP and androgen-independent DU-145 prostate cancer cells [44]. While ergosterol exerted an antiproliferative action on LNCaP, it promoted cell proliferation on DU-145. The authors [44] suggested that the observed difference may be related to the ability of ergosterol to act as a ligand for the androgen receptor.

Experiments with rats fed with a diet containing 0.1% ergosterol have shown a certain bladder carcinogenesis-preventing effect [45]. It was supposed that the observed effect is due to an androgen receptor expression-reducing action of brassicasterol (metabolite of ergosterol) on bladder epithelial cells.

Several studies have reported the anti-inflammatory effects of ergosterol. Its treatment of RAW 264.7 macrophages inhibited lipopolysaccharide-induced inflammation by suppressing the production of tumor necrosis factor-α and expression of cyclooxygenase-2 [46]. The inhibitory effect of ergosterol on degranulation of mucosal-type murine bone marrow-derived mast cells [47] or basophilic leukemia (RBL-2H3) cells [48] was associated with inhibition of β-hexosaminidase and histamine release in antigen-stimulated cells and was of interest for the treatment of allergic diseases dependent on mast cells.

Pretreatment of mice with ergosterol at doses of 25 and 50 mg/kg reduced lipopolysaccharide-induced histopathological changes in the lungs [49]. In addition, inhibition of inflammatory cells and pro-inflammatory cytokines, including tumor necrosis factor-α and interleukin-6, was observed. Similar effects were found on cigarette smoke-induced chronic obstructive pulmonary disease (COPD) in mice [50]. Besides inhibiting pro-inflammatory cytokines, ergosterol restored the activities of superoxide dismutase and reduced the content of malondialdehyde in serum and in the lung. Another study of ergosterol's protective effect against the cigarette smoke extract-induced COPD suggested that protective effects may be related to the NF-κB/p65 signaling pathway [51].

The transcription factor Nrf2 plays an important role in controlling the expression of antioxidant genes, which ultimately leads to anti-inflammatory effects. Activation of the Nrf2 signaling pathway by ergosterol was shown to enhance cardiomyocyte resistance to oxidative stress in lipopolysaccharide- or isoproterenol-induced myocardial injury [52,53]. Oral administration of ergosterol (25 mg/kg/day) to mice for two weeks effectively delayed the progression of osteoarthritis through a mechanism involving activation of the Nrf2 pathway in primary chondrocytes [54].

Diabetic nephropathy is a chronic loss of kidney function in patients with diabetes mellitus. Ergosterol has been shown to attenuate kidney damage in diabetic mice [55,56]. It restored blood glucose and serum insulin levels and improved most biochemical and renal functional parameters. Xiong et al. [57] considered ergosterol as a potential hypoglycemic agent for the treatment of type 2 diabetes mellitus based on the discovery that it could promote glucose transporter type 4 translocation and expression, as well as glucose uptake via the PI3K (phosphatidylinositol 3-kinase) and Akt (protein kinase B) pathways. Hyperglycemia promotes the formation of advanced glycation end products (AGE) by crosslinking proteins and carbohydrates. Ergosterol prevented the suppression of oxidative stress in HSC-T6 cells and prevented age-related diseases such as liver fibrosis and diabetes [58].

An inhibitory effect of ergosterol against human recombinant aromatase (IC_{50} 8.1 μM) was observed in aromatase inhibitory assay [59]. Potential beneficial effects against ethanol hepatotoxicity were predicted by density functional theory calculations based on the ability of ergosterol to scavenge the •$CH(OH)CH_3$ radical [60].

The following pharmacokinetic parameters were measured after a single oral administration (100 mg/kg) of ergosterol to rats: the area under the plasma concentration versus time curve from time 0 h to 36 h ($AUC_{0–36}$) was 22.3 μg h mL^{-1}, peak plasma concentration (C_{max}) was 2.27 μg/mL, the elimination half-life ($t_{1/2}$) was 5.90 h, and time to C_{max} (T_{max}) was 8.00 h [61].

Ergosterol is an easily crystallized compound with low water and oil solubility. To increase its bioavailability, nano-sized delivery vehicles were suggested to overcome this limitation. Poly(lactide-co-glycolide) nanoparticle encapsulation allowed a 4.9-fold increase of oral bioavailability compared to free ergosterol [62]. The relative oral bioavailability of ergosterol-loaded nanostructured lipid carriers prepared using glyceryl monostearate and decanoyl/octanoyl glycerides by hot emulsification-ultrasonication was 277% higher than that of ergosterol itself [63].

In addition to being used as an active ingredient, ergosterol has also been tested as part of other drug delivery systems. The study of cellular uptake and in vitro cytotoxicity of cyclic arginine-glycine-aspartic and octa-arginine peptide-modified ergosterol-combined cisplatin liposomes showed their stability in serum and the strongest anti-lung cancer effect [39]. The encapsulation of chlorin e6 in self-assembled ergosterol nanoparticles resulted in a novel supramolecularly assembled photosensitizer [64]. When applied to cancer cells 4T1 and MCF-7, it showed remarkable in vitro phototoxicity with cell inhibition of about 73% and 92%, respectively. Evident in vitro antiproliferative activity was demonstrated for a mixture of sterols (consisting mainly of ergosterol and 22,23-dihydroergosterol) from popular edible mushroom *Flammulina velutipes* [65]. Encapsulation of the mixture increased the relative bioavailability of ergosterol and 22,23-dihydroergosterol to 163 and 244%, respectively.

Another way to increase the bioavailability of ergosterol is the preparation of its derivatives. Direct esterification of ergosterol and lauric acid led to the coupling product ergosterol laurate (**3a**) (Figure 2) with solubility in vegetable oil above 5.7 g/100 mL, while for ergosterol it was below 0.9 g/100 mL [66]. Esters of unsaturated fatty acids, ergosterol oleate (**3b**), ergosterol linoleate, and ergosterol linolenate were prepared by transesterification reaction using *Proteus vulgaris* K80 lipase [67]. Their solubility in the tricaprylin solvent was 11–16 times higher than that of the initial sterol. Another ergosterol ester, α-linolenic acid derivative, was prepared using *Candida* sp. 99-125 lipase as a biocatalyst [68].

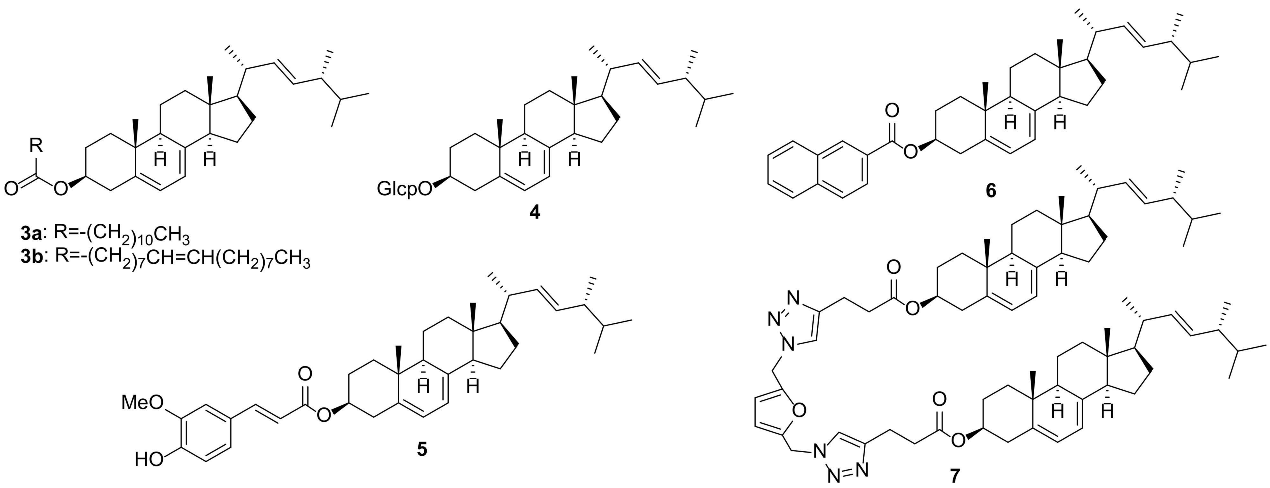

Figure 2. Structures of ergosterol *O*-derivatives.

The glucopyranosyl derivative **4** showed slightly higher activity in inhibiting LPS-induced NO production than ergosterol (**1**) (IC_{50} 16.6 and 14.3 μM, respectively) [69]. On the other hand, COX-1 enzyme inhibitory activity of **4** was weaker compared with that of the aglycone **1** [70].

Ergosterol adduct, ferulate **5**, was studied for the HMG-CoA reductase inhibitory activity, which was 1.93 times higher than that of oryzanol [71]. Another adduct **6**, derived from 2-naphthoic acid and ergosterol, showed stronger anti-tumor [72] and antidepressant [73] activities in vivo compared to ergosterol.

The antiproliferative effects of some ergosterol dimers have been studied against the HT29 and MCF-7 cancer cell lines [74]. The most effective was dimer **7** for the HT29 cancer cell line with an IC_{50} value of 160 μM. Unfortunately, the results of comparing the activity with ergosterol itself were not reported.

2.2. Other Fungal Sterols

Sterol fraction of fungi is typically a mixture of sterols [75]. As a rule, ergosterol has been considered to be its dominant component. However, this is not true in all cases. There are at least four other taxon-specific sterols (cholesterol, 24-methylenecholesterol, 24-ethylcholesterol, and brassicasterol), which may be the main sterols in some fungal species [76]. Research on the biological or pharmaceutical uses of ergostane sterols has received much less attention compared to ergosterol or functionalized ergostanes. Only sterols that have attracted attention as objects for the further in-depth study will be considered here.

5,6-Dihydroergosterol or stellasterol (**8**) (Figure 3) is widely found as a minor ergostane constituent of many fungi, including sclerotia of *Polyporus umbellatus* [77], mycelium of *Cordyceps jiangxiensis* [78], *Stereum insigne* [79], *Eurotium rubrum* [80], fruiting bodies of *Stropharia rugosoannulata* [81], *Amauroderma amoiensis* [82], *Amauroderma subresinosum* [83], *Lasiosphaera fenzlii* [84], *Cortinarius xiphidipus* [85], *Pleurotus eryngii* [59], *Trametes versicolor* [86]. For practical purposes, a more suitable source of stellasterol (**8**) is its chemical synthesis from ergosterol [69,87].

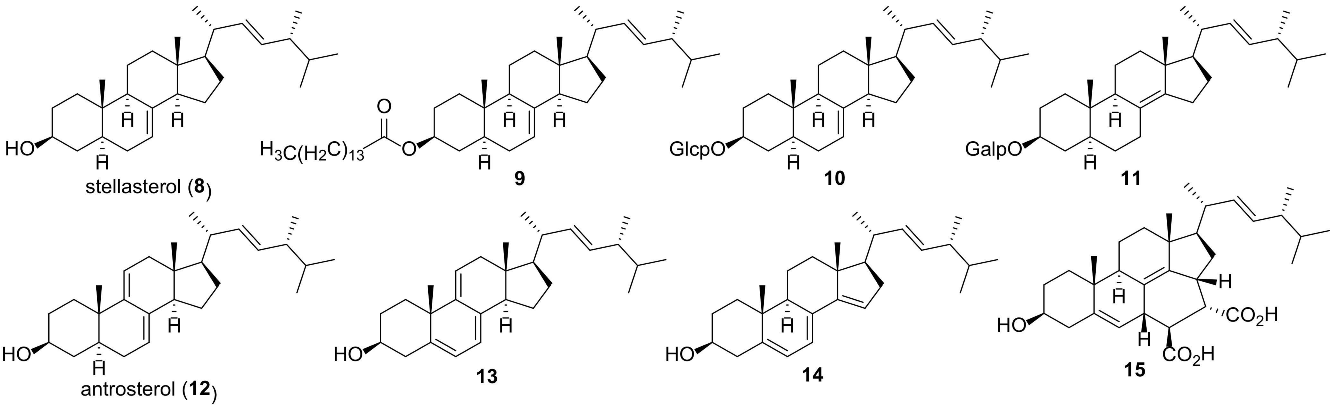

Figure 3. Structures of some fungal sterols and their derivatives.

Andrade et al. studied the effect of the purified *Marthasterias glacialis* extract and stellasterol (**8**) as its sterol constituent on inflammation in LPS-treated RAW 264.7 cells [88] and against human breast cancer (MCF-7) and human neuroblastoma (SH-SY5Y) cell lines [89]. The maximum anti-inflammatory effect was achieved when used in combination with unsaturated fatty acids [88]. In experiments with cancer cells, treatment with the extract markedly affected their growth, with stellasterol being responsible for the cell cycle arrest [89]. Yang et al. reported decreased NO production in LPS-treated RAW 264.7 cells with IC_{50} value of 15.1 μM and inhibition of iNOS and COX-2 [90].

The oxygen radical antioxidant capacity (ORAC) assay of components of the edible mushroom *Meripilus giganteus* revealed the highest antioxidant activity (4.94 mmol TE/g) for stellasterol (**8**) [91].

The study of the mechanism of anti-diabetic activity of the cosmopolitan woody polypore fungus *Ganoderma austral* showed that this may be due to its major component, stellasterol [92]. Its IC_{50} as an α-glucosidase inhibitor (315 μM) was close to that of acarbose (208 μM), which is an anti-diabetic drug used to treat diabetes mellitus.

Stellasterol was also isolated from fruiting bodies of *Ganoderma lucidum* as pentadecanoate ester (**9**), which at a dose 100 mg/kg bw demonstrated moderate anti-inflammatory activity (60% inhibition) in carrageenan-induced paw edema [93].

Kim et al. conducted an extensive study of the effects of synthetically obtained stellasterol glucoside (**10**) and its analogs on skin inflammation [69,94–96]. It has been shown that **10** exhibits strong inhibitory activity against the production of nitric oxide (NO), which is a molecular mediator involved in inflammation. In addition, glucoside **10** suppressed the production of Th2-type chemokines CCL17 and CCL22. It was not cytotoxic up to a concentration of 100 μM, which makes it possible to consider **10** as a potential therapeutic agent for atopic dermatitis. Further studies in this area led to the discovery of galactosyl $\Delta^{8(14)}$-ergostenol (**11**) as the best candidate for the treatment of arthritis [97].

Ergostatrienol **12** (also named as antrosterol or EK100) is a quite common steroid in fungal sources. In particular, it was isolated from *Antrodia camphorate* [98–100], *Coprinus setulosus* [101], *Cordyceps militaris* [102], *Ganoderma resinaceum* [103], *Nigrospora sphaerica* [104], *Xylaria nigripes* [105].

Shih et al. showed that antrosterol (**12**) may be useful in the treatment of type 2 diabetes associated with hyperlipidemia [98]. Its use has led to a decrease in blood glucose and total cholesterol and triglyceride levels, an increase in the GLUT4 protein in skeletal muscle, and an improvement in insulin resistance.

The anti-inflammatory properties of *Antrodia camphorata* mycelium, used in traditional Chinese medicine, are at least partially determined by the presence of antrosterol as one of its constituents. Similar to the action of corticosteroids, compound **12** reduced the expression of IL-6 and IL-1β in macrophages [106]. The mechanism of anti-inflammatory effect of **12** has also been studied by Kuo et al. [107]. Authors explained the observed effect by an increase in the activity of antioxidant enzymes such as catalase, superoxide dismutase, and glutathione peroxidase in liver tissue, and the reduction of the expression of iNOS and cyclooxygenase-2. The studies [108,109] also noted a decrease in the expression of the inflammatory factor NF-κB and inflammatory cytokines IL-6 and TNF-α. The mechanism of anti-inflammatory action of **12** was also investigated in LPS-stimulated RAW264.7 cells and *Drosophila* [102].

In experimental acute ischemic stroke model, antrosterol (**12**) reduced ischemic brain damage by decreasing the expression of p65NF-κB and caspase 3 and promoted neurogenesis and neuroprotection by activating PI3k/Akt-associated inhibition of GSK3 and activation of β-catenin [110]. Compound **12** was proposed as a potential therapeutic agent in intracerebral hemorrhage [111]. It had an inhibitory effect on the activation of the microglial c-Jun N-terminal kinase and attenuated the expression of brain cyclooxygenase, activation of matrix metalloproteinase and brain injuries in a model of intracerebral hemorrhage in mice. Long-term daily administration of **12** was shown to be safe and can be used as a potential ergogenic aid [112].

Hu et al. showed a strong cytotoxic effect of **12** against human U2OS lung osteosarcoma cells with IC_{50} value of 0.93 μM [105].

Cholesterol is a vital component of eukaryotic cells and its trafficking is an important issue for their proper functioning. 9-Dehydroergosterol (**13**) has proven to be a very convenient biochemical tool for studying cholesterol transport in living cells [113–115]. First of all, this is due to its own fluorescence because no additional moieties covalently attached to cholesterol are required. Second, 9-dehydroergosterol (**13**) mimics cholesterol very well, which is a consequence of its ability to stand upright in the membrane, almost identical to cholesterol.

Ano et al. found that extracts of dairy products fermented with *Penicillum candidum* have potent anti-inflammatory effect on microglia [116]. Repeated purification of the extracts led to the isolation of 9-dehydroergosterol (**13**) as an active principle responsible for the observed effect. Compound **13** significantly inhibited neurotoxicity and neuronal cell death induced by over-activated microglia, making it a valuable agent for the prevention of dementia.

Dendritic cells play a key role in regulating the balance between tolerance and immune response. It has been shown that 14-dehydroergosterol (**14**) induces the transformation of dendritic cells in the bone marrow of mice and differentiates them into a tolerogenic type [117]. It can be helpful in preventing chronic inflammatory and autoimmune diseases.

She et al. isolated from the mangrove-derived fungus *Aspergillus* sp. two steroids having a 6/6/6/6/5 pentacyclic steroidal system [118]. Ergosterdiacid A (**15**) was supposed to be a natural Diels-Alder product derived from fumaric acid and ergostatetraene **14**. In vitro experiments showed that adduct **15** was active against *Mycobacterium tuberculosis* tyrosine phosphatase B (IC_{50} 15.1 μM) and had a strong anti-inflammatory effect by suppressing NO production at 4.5 μM.

A number of hybrids of 9-dehydroergosterol with polyketides have been isolated from natural sources. Two anthraquinone derivatives, evantrasterol A and B (**16** and **17**) (Figure 4), have been found in the endophytic fungus *Emericella variecolor* [119].

Elsebai et al. isolated nitrogenous metabolites of phenalenone, conio-azasterol (**18**), and S-dehydroazasirosterol (**19**), from the marine endophytic fungus *Coniothyrium cereal* [120]. Another nitrogenous hybrid of 9-dehydroergosterol fused through the morpholine ring with alternariol, pestauvicomorpholine A (**20**), was isolated from the fermentation product of the fungus *Pestalotiopsis uvicola* [121]. No cytotoxicity was detected for any of the tested compounds **16–20**.

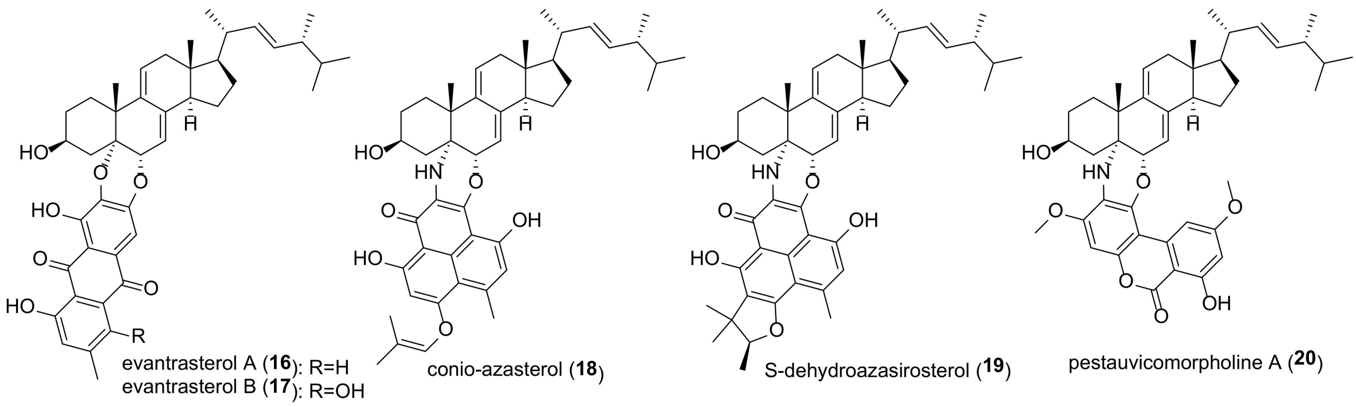

Figure 4. Structures of natural hybrids of 9-dehydroergosterol with polyketides.

3. Endoperoxides

Compounds containing a peroxide group are quite widespread among various natural substances, and steroids are not an exception [27]. Two 5α,8α-endoperoxides, ergosterol peroxide (EP, **21a**) and 9,11-dehydroergosterol peroxide (DHEP, **22a**) (Figure 5), are the most typical representatives of fungal steroids. Publications up to 2016 on the biological activity of EP (**5a**) have been thoroughly reviewed by Merdivan and Lindequist [24], and only the more recent literature regarding this compound will be discussed here.

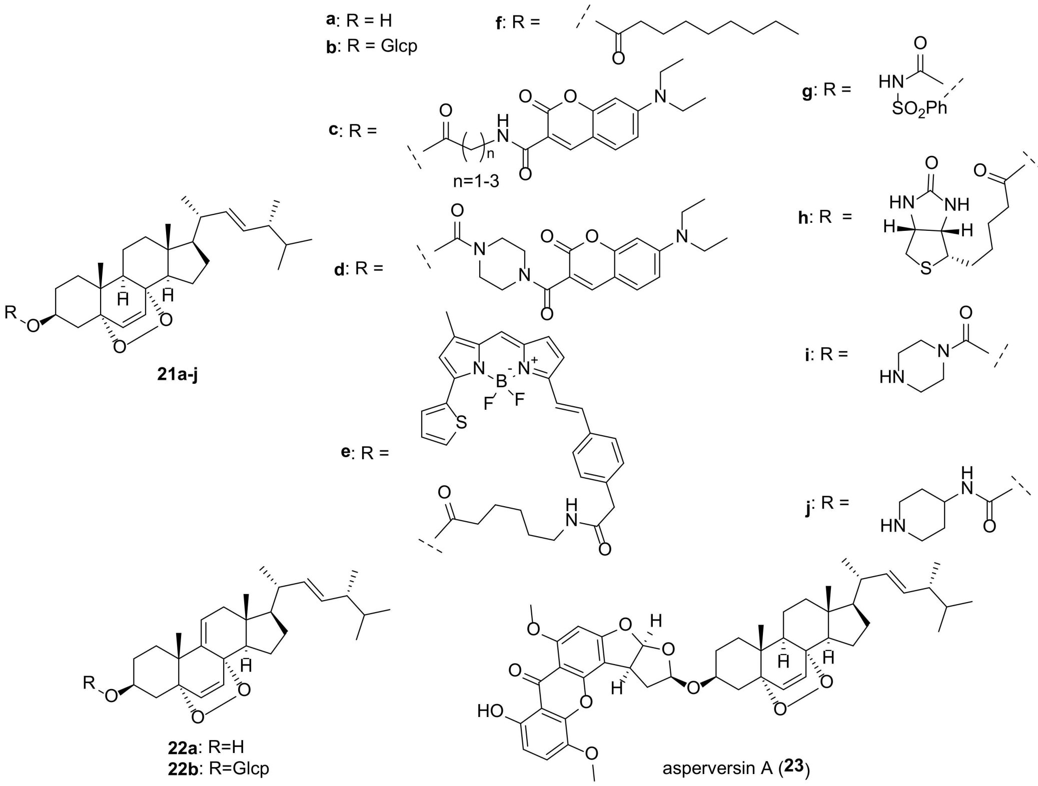

Figure 5. Structures of fungal 5α,8α-endoperoxides and their *O*-derivatives.

Biological studies of endoperoxides **21a** and **22a** have been aimed primarily at assessing their cytotoxic potential. Both compounds revealed quite high level of cytotoxicity in a wide range of cancer cells (Table 1). It should be noted that measurements of cell toxicity often vary significantly from laboratory to laboratory. Thus, for EP and cell line MCF-7 the values of IC_{50} varied from IC_{50} 1.18 μM [122] to 151 μM [123].

Attempts have been made to understand the cytotoxicity mechanism for **21a**, and some authors have concluded that more than one mechanism is at work. Obviously, the peroxide bridge plays a crucial role, bearing in mind that ergosterol is not cytotoxic. It was assumed that induction of apoptosis is the main cause of cytotoxicity [24]. Homolytic cleavage of the peroxide moiety in a reducing medium leads to the formation of reactive oxygen species (ROS), which are powerful internal stimuli for apoptosis. This has been confirmed, in particular, in experiments with MCF-7 cells [124]. Their treatment with **21a** at concentrations of 40–80 μg/mL led to an increase in the production of ROS in a dose-dependent manner and to the induction of apoptosis. The inhibitory properties of **21a** against A549 lung cancer cells were mediated by mitochondria-dependent apoptosis and autophagy [125]. EP also reduced LPS/ATP-induced proliferation and migration of A549 cells. A synergistic effect was observed when using EP with kinase inhibitor Sorafenib.

Based on ID_{50} values for the MCF-7 cell line (1.18 μM) compared to the MDA-MB-231 cell line (12.82 μM), EP (**21a**) was hypothesized to target estrogen receptors [122]. Its possible role as an ERα antagonist was suggested by Kim et al. based on the suppression of the increase in the viability of MCF-7 cells caused by 17β-estradiol [126].

Ergosterol peroxide (**21a**) and 9,11-dehydroergosterol peroxide (**22a**) were often isolated from the same fungal material, and on the whole both compounds exhibit similar biological properties. DHEP (**22a**) was slightly more cytotoxic than EP (**21a**) on the Hep 3B cell viability (IC_{50} 16.7 and 19.4 μg/mL, respectively) [127]. In experiments with BV-2 microglia cells, compound **22a** did not damage cell viability, although EP was cytotoxic to these cells [128]. Kobori et al. showed that **22a** selectively inhibits the growth of HT29 human colon adenocarcinoma cells without affecting normal human WI38 fibroblasts [129]. The inhibition was attributed to the induction of expression of an inhibitor of cyclin-dependent kinase 1A, thus causing cell cycle arrest and apoptosis. The rather strong cytotoxic effect of **22a** (IC_{50} 8.58 μM) on HeLa human cervical carcinoma cells was associated with the regulated expression of stathmin 1, a protein that is critical for the regulation of the cell cytoskeleton [130]. The mechanisms of **22a** cytotoxicity in A375 melanoma cells have been shown to be caspase-dependent and mediated via the mitochondrial pathway and include targeting of the induced differentiation protein of myeloid leukemia cells Mcl-1, release of cytochrome c, and activation of caspase-9 and -3 [131].

In experiments with a large number of cell lines EP possessed cytotoxic activity at the level of 1 μM and was more active in comparison with DHEP [132]. On the other hand, in the aromatase inhibitory assay 9(11)-double-bond enhances the inhibitory activity (IC_{50} > 100 μM vs. 32.6 μM for EP and DHEP, respectively) [59].

EP was thought to be one of the main compounds responsible for the antiproliferative effect of an ethanolic extract of the native New Zealand mushroom *Hericium novaezealandiae* [133]. Two possible mechanisms of the observed effect have been proposed: apoptosis based on upregulation of CASP3, CASP8, CASP9, and anti-inflammation, as follows from downregulation of IL6 and upregulation of IL24.

Studying the cytotoxic effects on renal cell carcinoma cells, Zhang et al. found that EP treatment suppressed cell growth, colonization, migration and invasion, arrested the cell cycle, and triggered apoptosis [134]. This also means that several mechanisms can act for the same effect.

A similar situation with multiple pathways was observed in experiments with ovarian cancer cells [135]. Their treatment with **21a** inhibited nuclear β-catenin, thus decreasing the expression levels of cyclin D1 and c-Myc. Meanwhile, the level of protein tyrosine phosphatase SHP2 was increased in the treated cells, while the activity of Src kinase was suppressed. Thus, the antitumor effect of **21a** on ovarian cancer cells is due to both the β-catenin and STAT3 signaling pathways.

Significant inhibition of the formation of experimental lung metastases in vivo was found for EP (**21a**) [136]. The effect was attributed to inhibition of the NF-κB and STAT3 inflammatory pathways in 4T1 breast cancer cells.

EP was more effective than cisplatin in a mouse tumor model, inhibiting CT26 cell growth and improving the survival of tumor mice with no obvious side effects [137]. The growth of tumor cells of the gastrointestinal tract was suppressed due to the induction of apoptosis by the stress of the endoplasmic reticulum and mitochondria-dependent pathway.

Table 1. Cytotoxicity of fungal endoperoxides on different cell lines.

Compound	Cell Line	Origin *	Effect [Ref.]
21a	4T1	Mouse breast cancer	IC_{50} 9.06 µM [138]
	A549	Lung carcinoma	IC_{50} 17.04 µM [138], IC_{50} 17.2 µM [84], IC_{50} > 20 µM [139], IC_{50} 23 µM [125], IC_{50} 57 µM [140]
	B 16	Murine melanoma	IC_{50} 78.77 µM [141]
	B16F10	Murine melanoma	IC_{50} 55.8 µM [142]
	BGC823	Gastric cancer	IC_{50} 35.23 µg/mL [137]
	Eca-109	Esophageal carcinoma	IC_{50} 23.17 µg/mL [137]
	DU145	Prostate cancer	IC_{50} 21 µg/mL [133]
	HCT116	Colorectal carcinoma	IC_{50} 80.72 µM [142]
	HeLa	Cervical carcinoma	IC_{50} 13.6 µM [84], IC_{50} > 20 µM [139], IC_{50} 31 µM [125], IC_{50} > 50 µM [143], IC_{50} > 50 µM [138]
	Hep 3B	Hepatocellular carcinoma	IC_{50} 35.2 µg/mL [144]
	HepG2	Liver carcinoma	IC_{50} 13.19 µM [138], IC_{50} > 20 µM [139], IC_{50} 23.15 µM [145], IC_{50} 23.5 µM [146], IC_{50} 34 µM [147], IC_{50} 46.9 µM [144], IC_{50} 113 µM [123]
	HL-60	Promyelocytic leukemia	IC_{50} 39.4 µM [143]
	HT-29	Colon adenocarcinoma	IC_{50} 25.47 µM [137], IC_{50} > 50 µM [138]
	J5	Hepatocellular carcinoma	IC_{50} 33 µM [125]
	L1210	Mouse lymphotic leukemia	IC_{50} 36.40 µM [138]
	LNCap	Prostate cancer	IC_{50} 15 µg/mL [133], IC_{50} 35.53 µg/mL [141]
	LS180	Colon adenocarcinoma	IC_{50} 17.3 µg/mL [148]
	MDA-MB-231	Breast carcinoma	IC_{50} 12.82 µM [122], EC_{50} 18 µM [149], IC_{50} 24.75 µM [146], IC_{50} 44.6 µM [147]
	MCF-7	Breast cancer	IC_{50} 1.18 µM [122], IC_{50} 9.01 µM [138], IC_{50} 26 µM [140], IC_{50} 26.06 µM [145,146], IC_{50} 29 µM [125], IC_{50} 38.2 µM [143], IC_{50} 40 µM [124], IC_{50} 98.12 µM [142], IC_{50} > 100 µM [126,144], IC_{50} 151 µM [123]
	MGC-803	Gastric carcinoma	IC_{50} 15.2 µM [84]
	NCI 60 panel		significant activity against most tumor cell lines tested [132]
	PC3	Prostate cancer	IC_{50} 42 µg/mL [133]
	PC-3M	Prostatic carcinoma	IC_{50} 23.15 µM [123]
	RCC	Renal carcinoma	IC_{50} 30 µM [134]
	SK-Hep1	Liver cancer	IC_{50} 19.25 µM [145], IC_{50} 19.71 µM [146]
	SUM-149	Breast cancer	EC_{50} 9 µM [149], EC_{50} 20 µM [150]
	T-47D	Breast cancer	EC_{50} 19 µM [149]
21b	A549	Lung carcinoma	IC_{50} 14.21 µM [151]
	HCT-15	Colon adenocarcinoma	IC_{50} 17.49 µM [151]
	SK-MEL-2	Skin melanoma	IC_{50} 9.01 µM [151]
	SK-OV-3	Ovary malignant ascites	IC_{50} 15.11 µM [151]
	U87	Glioblastoma	20.1% inhibition at 100 µM [152]
21c	HepG2	Liver carcinoma	IC_{50} 12.34 (n = 1), 9.46 (n = 2), 6.74 (n = 3) µM [145]
	MCF-7	Breast cancer	IC_{50} 14.80 (n = 1), 13.70 (n = 2), 7.45 (n = 3) µM [145]
	SK-Hep1	Liver cancer	IC_{50} 10.43 (n = 1), 11.70 (n = 2), 5.92 (n = 3) µM [145]
21d	HepG2	Liver carcinoma	6.60 µM [145]
	MCF-7	Breast cancer	10.62 µM [145]
	SK-Hep1	Liver cancer	8.10 µM [145]
21e	MDA-MB-231	Breast carcinoma	EC_{50} 7 µM [149]
	SUM-149	Breast cancer	EC_{50} 2 µM [149]
	T-47D	Breast cancer	EC_{50} 16 µM [149]

Table 1. *Cont.*

Compound	Cell Line	Origin *	Effect [Ref.]
21f	HCT-116	Colon carcinoma	IC_{50} 0.21 μM [153]
21g	SUM-149	Breast cancer	EC_{50} 12 μM [150]
21h	MDA-MB-231	Breast carcinoma	EC_{50} 10 μM [149]
	SUM-149	Breast cancer	EC_{50} 4 μM [149]
	T-47D	Breast cancer	EC_{50} > 10 μM [149]
21i	HepG2	Liver carcinoma	IC_{50} 0.85 μM [146]
	MCF-7	Breast cancer	IC_{50} 3.26 μM [146]
	MDA-MB-231	Breast carcinoma	IC_{50} 4.12 μM [146]
	SK-Hep1	Liver cancer	IC_{50} 1.75 μM [146]
21j	HepG2	Liver carcinoma	IC_{50} 2.83 μM [146]
	MCF-7	Breast cancer	IC_{50} 4.62 μM [146]
	MDA-MB-231	Breast carcinoma	IC_{50} 3.99 μM [146]
	SK-Hep1	Liver cancer	IC_{50} 0.92 μM [146]
22a	4T1	Mouse breast cancer	IC_{50} 9.31 μM [138]
	A375	Malignant melanoma	IC_{50} 9.46 μg/mL [131]
	A549	Lung carcinoma	IC_{50} 9.7 μM [84], IC_{50} 10.77 μM [138], IC_{50} 49 μM [125], IC_{50} 63 μM [140], IC_{50} 103.74 μM [154], IC_{50} 121.9 μM [155], No cytotoxicity [156]
	Calu-6	Lung carcinoma	IC_{50} 71.2 μM [155]
	Colo201	Colorectal adenocarcinoma	IC_{50} 13.02 μg/mL [131]
	H1264	Lung carcinoma	IC_{50} 92.3 μM [155]
	H1299	Lung carcinoma	IC_{50} 50.6 μM [155]
	HeLa	Cervical carcinoma	IC_{50} 7.6 μM [84], IC_{50} 8.58 μM [130], IC_{50} 35.82 μM [138], IC_{50} 37 μM [125]
	Hep 3B	Hepatocellular carcinoma	IC_{50} 16.7 μg/mL [127]
	HepG2	Liver carcinoma	IC_{50} 10.93 μM [138], IC_{50} 44.5 μM [147], IC_{50} 64.95 μM[154]
	HGC27	Gastric carcinoma	IC_{50} 26.47 μM [16]
	HT-29	Colon adenocarcinoma	IC_{50} 30.76 μM [138]
	J5	Hepatocellular carcinoma	IC_{50} 36 μM [125]
	L1210	Mouse lymphotic leukemia	IC_{50} 29.31 μM [138]
	MCF-7	Breast cancer	IC_{50} 3.3 μM [140], IC_{50} 8.40 μM [138], IC_{50} 16.89 μg/mL [131], IC_{50} 34 μM [125], IC_{50} 67.89 μg/mL [131], IC_{50} > 100 μM [126]
	MDA-MB-231	Breast carcinoma	IC_{50} 72.68 μM [154], IC_{50} 99 μM [16], IC_{50} 328 μM [147]
	MGC-803	Gastric carcinoma	IC_{50} 7.8 μM [84]
	Panc-28	Pancreatic adenocarcinoma	No cytotoxicity [156]
	SW620	Colorectal adenocarcinoma	IC_{50} 32.87 μg/mL [131]
22b	A549	Lung carcinoma	No cytotoxicity [156]
	A549	Lung carcinoma	IC_{50} 15.42 μM [151]
	HCT-15	Colon adenocarcinoma	IC_{50} 19.32 μM [151]
	Panc-28	Pancreatic adenocarcinoma	No cytotoxicity [156]
	SK-MEL-2	Skin melanoma	IC_{50} 12.96 μM [151]
	SK-OV-3	Ovary malignant ascites	IC_{50} 18.26 μM [151]
27	A549	Lung carcinoma	IC_{50} 5.26 μg/mL [12]
	MCF-7	Breast cancer	IC_{50} 5.15 μg/mL [12]
28	A549	Lung carcinoma	IC_{50} 0.26 μg/mL [157]
	HSC-3	Oral squamous cell carcinoma	IC_{50} 1.72 μg/mL [157]
	HSC-4	Oral squamous cell carcinoma	IC_{50} 1.94 μg/mL [157]
	MKN45	Stomach adenocarcinoma	IC_{50} 0.34 μg/mL [157]

* Human, if not stated otherwise.

Compound **21a** can be used as a radiosensitizer in the treatment of cervical cancer to reduce the toxic effects that occur after ionizing radiation therapy. Loss of viability of the cervical cell lines HeLa and CaSki was observed with increasing dose of **21a** [158].

Biological effects of EP (**21a**) and its $\Delta^{9,11}$-counterpart **22a** are not limited to their cytotoxic and anticancer properties. A detailed study on the bioactivity of the components of the truffle *Reddellomyces parvulosporus* revealed a number of EP activities, including anti-tyrosinase, anti-urease, anti-α-glucosidase, and anti-α-amylase ones [159]. Tyrosinase is an enzyme involved in the biosynthesis of melanin in humans, and its inhibitors are of interest for preventing excessive melanin production, as being active ingredients of skin whitening agents. Tyrosinase inhibitory activity (IC_{50}: 202.37 μg/mL) of EP was also detected by Bai et al. [160].

Ng et al. reported the antidiabetic effect of **21a** that was due to the upregulation of glucose absorption and modulation of the PI3K/Akt, MAPK, and GLUT-4 signaling pathways [161].

EP was tested for its antileishmania activity against *Leishmania donovani* promastigotes and showed good activity with IC_{50} values of 9.43 μM [162]. The EP trypanocidal activity has been associated with its interaction with CYP51 [163]. The key structural moiety responsible for this is the peroxide bridge, which mediates interaction with the CYP51 heme binding site. At a later stage, this can cause the appearance of free radicals through homolytic cleavage at the O-O site, the pharmacophore responsible for the biological activity of **21a**.

Zhou et al. studied the immunoregulatory effect on inflammation caused by influenza A virus in human alveolar epithelial cells A549. EP (**21a**) was found to have anti-inflammatory effects and prevent virus-induced apoptosis by attenuating retinoic acid-inducible gene I signaling in infected cells [164].

Oral administration of EP to piglets infected with porcine delta-coronavirus resulted in a reduction in diarrhea, relief of intestinal damage, and a decrease in viral load in feces and tissues [165]. Wang et al. demonstrated that ergosterol peroxide prevents infection by suppressing porcine delta-coronavirus-induced autophagy via the p38 signaling pathway [166,167].

DHEP (**22a**) was found to exhibit strong anti-inflammatory effect in lipopolysaccharide-stimulated RAW264.7 cells [168–170]. It suppressed the production of NO even at 12.5 μM and pro-inflammatory cytokines interleukin 6 at 25 μM [168].

With age, mesenchymal stem cells in bone marrow tend to differentiate more into adipocytes than into osteocytes. Compounds **21a** and **22a** have been shown to inhibit the differentiation of mesenchymal stem cells toward adipocytes, which may be useful for the treatment of postmenopausal osteoporosis [171].

In experiments with 3T3-L1 mouse embryonic fibroblast cells, it was shown that EP inhibits triglyceride synthesis and reduces the accumulation of lipid droplets by suppressing adipogenesis [172].

The endoperoxides **21a** and **22a** were tested for their antibacterial activity [173–177]. The presence of a 9,11-double bond contributed to the increase in activity [173,177]. Thus, $\Delta^{9,11}$-derivative **22a** was more effective against *M. tuberculosis* H37Rv in comparison with **21a** (MIC 16 μg/mL and 64 μg/mL, respectively) [173]. Antitubercular activity of the fungus *Gliocladium* sp. MR41., was tested on M. tuberculosis. It was found to be due to EP (**21a**) with MIC 0.78 μg/mL [178].

Kim et al. isolated glucosides **21b** and **22b** from the Korean wild fungus *Xerula furfuracea* and tested their effects on adipogenesis and osteogenesis in a mouse mesenchymal stem cell line [10]. Both compounds were found to inhibit the differentiation of stem cells into adipocytes, which is of interest in the treatment of syndromes associated with menopause.

Significant antifungal and cytotoxic activities were reported for EP decanoate (**21f**) [153]. In disk diffusion test against *Candida albicans* culture, its MIC value was found to be 8.3 μg/disc that was comparable to clotrimazole (MIC 5.1 μg/disc). Compound **21f** showed also very good cytotoxicity against the HCT-116 cell line with IC_{50} value of 0.21 μM compared to doxorubicin (IC_{50} 0.06 μM).

In an attempt to improve antitumor activity, a number of derivatives of endoperoxide **21a** have been studied. Ergosterol peroxide sulfonamide **21g** was found to be more effective in reducing cancer cell viability than the parental endoperoxide **21a** [150]. Significantly, its toxicity to normal human BJ fibroblasts was minimal, indicating that **21g** targets cancer cells.

A series of EP analogs containing BODIPY or a biotin moiety was obtained by Rivas et al. as probes for cellular localization studies [149]. They demonstrated that EP is distributed across the cytosol with significant accumulation in the endoplasmic reticulum.

In addition, the resulting compounds were tested for antiproliferative activity in breast cancer cell models. The most active ones were analogs **21e** and **21h** (Table 1).

Several adducts of EP with 7-*N*,*N*-diethylaminocoumarins have been obtained by Bu et al. [145]. Analogues **21c** and **21d** exhibited increased cytotoxicity compared to **21a**, which was explained by their localization mainly in mitochondria, as followed from fluorescence imaging. In addition, the piperazine derivative **21d** suppressed the formation, invasion, and migration of cell colonies, induced arrest of HepG2 cells in the G2/M phase, and increased the level of intracellular reactive oxygen species.

A number of EP 3-carbamate derivatives were obtained by Hu et al. [146]. They exhibited antiproliferative activity, which was 6–28 times stronger than that of the initial endoperoxide **21a** (Table 1). The most active compounds **21i** and **21j** contain piperazinyl and piperidinyl fragments.

A steroid-xanthone heterodimer, asperversin A (**23**), was isolated from the culture of *Aspergillus versicolor*, an endophytic fungus isolated from the marine brown alga *Sargassum thunbergii* [179]. Compound **23** was tested for biological activities against some bacterial and fungal strains with no noticeable effect.

Further structural modifications of steroidal molecule with retention of the 5α,8α-endoperoxide scaffold included changes in the carbon skeleton of the side chain [180,181]. Thus, 7-dehydrocholesterol peroxide, its acetate and hemisuccinate showed improved anticancer activity and selectivity over the corresponding derivatives of EP [180].

In comparison with the compounds **21a** and **22a**, 5α,9α-endoperoxides have been studied much less due to their lower availability. Compounds **24** and **25** (Figure 6) were isolated from the edible mushroom *Grifola gargal* and evaluated in the osteoclast-forming assay [182]. They inhibited osteoclast formation, which may be of interest for the prevention of osteoporosis. Endoperoxide **26**, isolated from the fruiting bodies of *Stropharia rugosoannulata*, protected neuronal cells by attenuating endoplasmic reticulum stress caused by thapsigargin, an inhibitor of the Ca^{2+}-ATPase [81]. A significant cytotoxicity (Table 1) against A549 and MCF-7 cells was noted for the endoperoxide **27**, isolated from the fruiting body of a medicinal macro fungus *Ganoderma lingzhi* [12]. Agarol (**28**) was isolated as a tumoricidal substance from the mushroom *Agaricus blazei* [157]. Its cytotoxicity was evaluated against four cancer lines (Table 1). Agarol (**28**) was shown to induce apoptosis by increasing generation of ROS and release of apoptosis-inducing factor from the mitochondria to the cytosol.

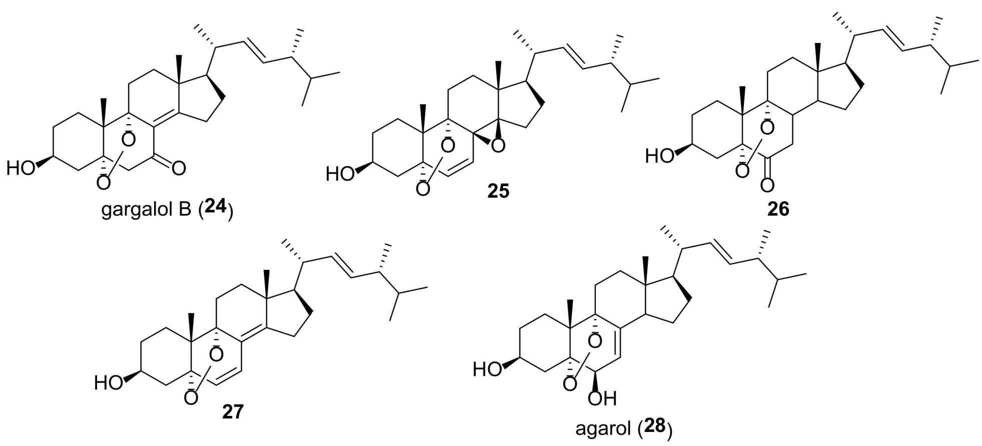

Figure 6. Structures of fungal 5α,9α-endoperoxides.

4. Epoxides

The majority of compounds of this group are 5α,6α epoxides (Figure 7). Almost all of them contain a hydroxy- or keto group at C-7, $\Delta^{8(9)}$-, or $\Delta^{8(14)}$-double bond, and some 5α,6α-epoxides have a functionalized ring D. Other epoxides (4,5-, 5β,6β-, 8,9-, 8,14-, and 9,11-derivatives) are much less common in fungi (Figure 8). Compounds **29–59** were tested in various assays, including AChE inhibitory, cytotoxic, α-glucosidase inhibition, NO production inhibition, etc., (Table 2).

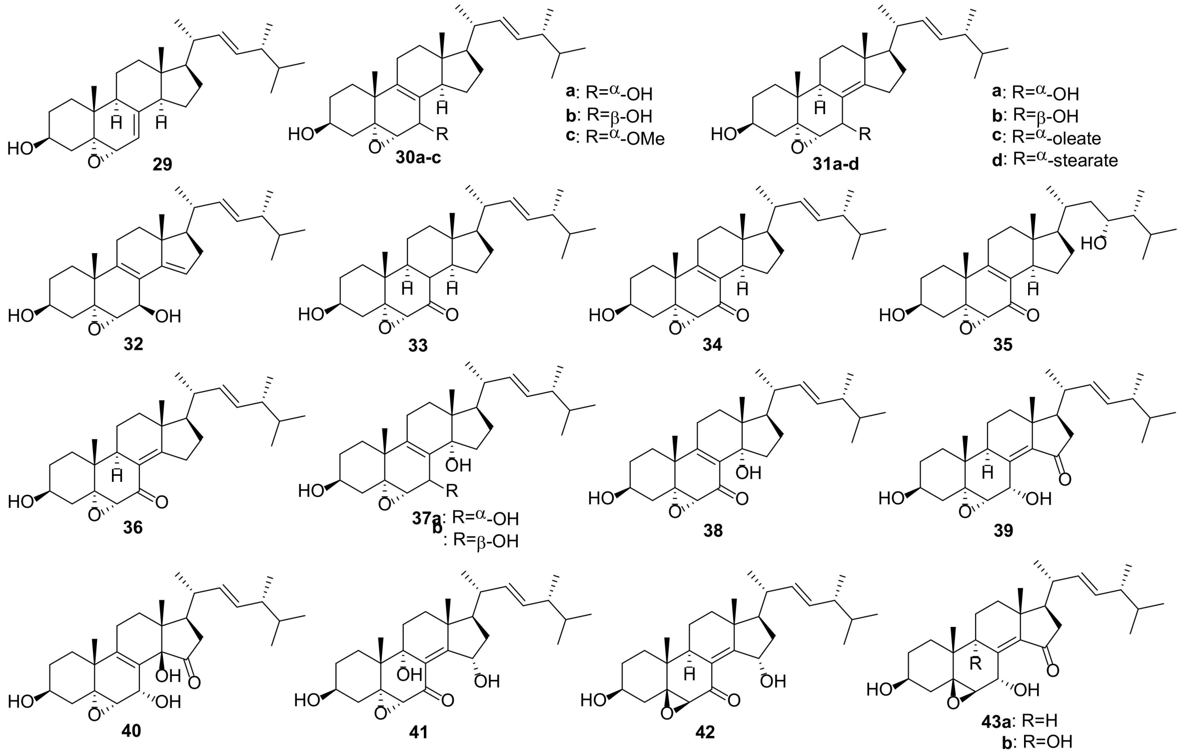

Figure 7. Structures of fungal 5,6-epoxides.

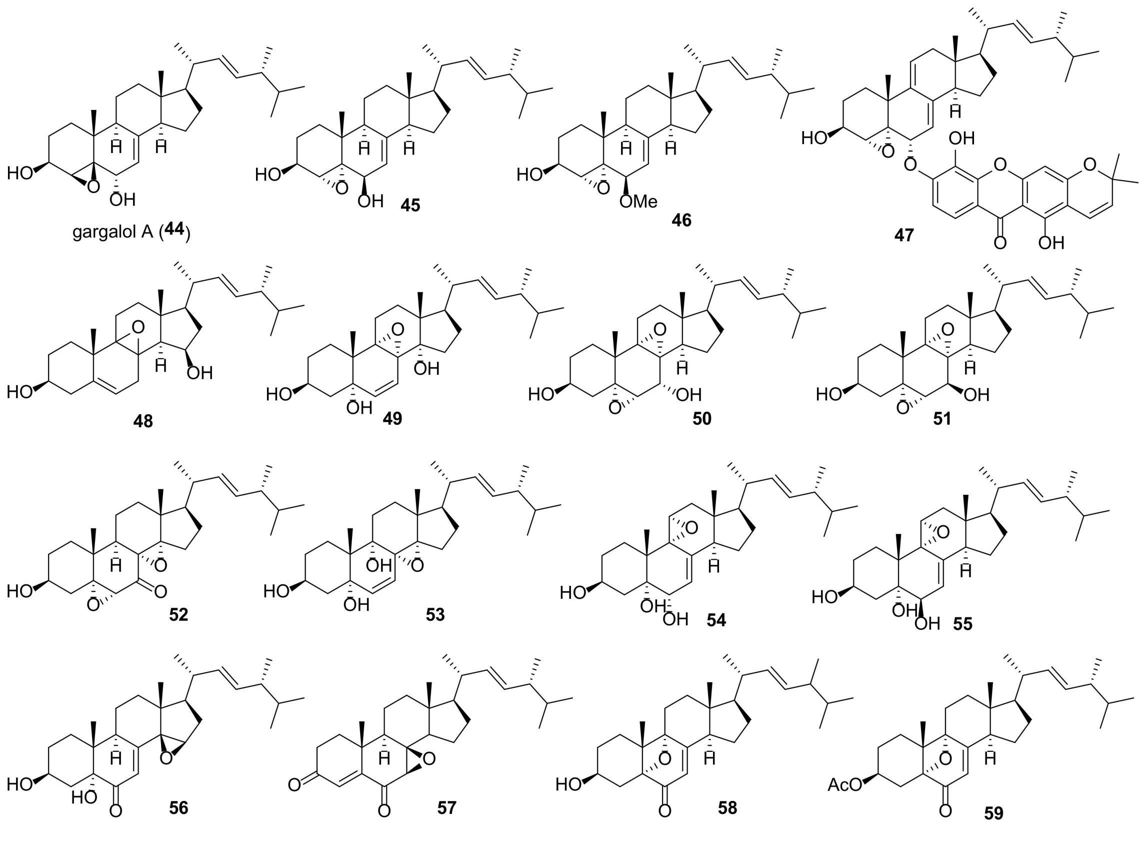

Figure 8. Structures of other fungal epoxides.

Bae et al. noted that the presence of an epoxy group in the tetracyclic skeleton of ergosterol derivatives increases their cytotoxic properties [183]. Isolation of a series of 5α,6α-epoxides from the macrofungus *Omphalia lapidescens* allowed to establish some structure activity relationship correlations [15]. The greatest cytotoxicity against a human gastric cancer cell line, HGC-27, was noted for the compound **30a** and **31a** containing an α-oriented hydroxyl group at C-7 and $\Delta^{8(9)}$- or $\Delta^{8(14)}$-double bond (Table 2). The transition to 7-ketones **33** and **36** led to a decrease in activity, and of both compounds, the derivative **33** without a double bond in the BC cycles was less active. The diepoxide **52** showed the least activity, which indicates the importance of the double bond for cytotoxic activity.

Epoxides **41**, **43a**, and **43b**, isolated from the culture of Basidiomycete *Polyporus ellisii*, were evaluated for cytotoxicity against five human cancer cell lines [184]. The first two compounds were practically inactive, while epoxide **41** exhibited strong activity against all tested cell lines with IC_{50} in the range from 1.5 to 3.9 μM (Table 2).

Ferreira et al. performed virtual screening experiments on low-molecular weight fungal constituents as potential MDM2 inhibitors [185]. The latter is an important negative regulator of the p53 tumor suppressor, and its inhibitors have significant anti-tumor activity. From the compounds studied, epoxide **29** returned one of the best docking scores.

Epoxide **31b** was found to exhibit potent inhibitory activity on the expression of mRNA of proprotein convertase subtilisin/kexin type 9 (PCSK9) [186]. The latter affects the low density lipoprotein receptor on the surface of liver cells, resulting in high level of low density lipoprotein cholesterol (LDL-C). PCSK9 inhibitors have been proposed as novel LDL-C-lowering agents for the treatment of hyperlipidemia. Compound **31b** showed activity with IC_{50} values of 8.23 μM, which was comparable with berberine (IC_{50} 8.04 μM) used as a positive control.

A number of epoxides were tested for their anti-inflammatory activity. As a rule, inhibition of TNF-α and NO production in LPS-stimulated RAW264.7 macrophage cells was used to evaluate anti-inflammatory effects. Epoxide **30c** showed superior inhibitory activity on NO production with IC_{50} value of 3.24 μM [103]. In the same experiment, the positive control L-NMMA, nitric oxide synthase inhibitor, revealed IC_{50} value of 49.86 μM. TNF-α secretion decreased after treatment of macrophage cells with epoxide **49**, which at 10 μM exhibited activity with inhibition value of 37.5% [187]. This was comparable to the positive control (52.5% at 1 μM) exerted by celecoxib, the cyclooxygenase-specific inhibitor.

Table 2. Sources and biological activity of fungal epoxides.

Compound	Fungal Source [Ref.]	Assays (Activity) [Ref.]
29	*Hericium erinaceus* [187,188], *Chaetomium* sp. M453 [189], *Colletotrichum* sp. YMF432 [190], *Cordyceps sinensis* [191], *Stereum insigne* CGMCC5.57 [79]	**AChE inhibitory assay** (IC_{50} 67.8 μM) [190], **nematicidal and antibacterial assays** (no activity) [79]
30a	*Amauroderma subresinosum* [83], *Ganoderma lucidum* [147], *G. resinaceum* [103], *Grifola frondosa* [154], *Omphalia lapidescens* [15], *Simplicillium* sp. YZ-11 [192], *Stropharia rugosoannulata* [193], *Pleurotus eryngii* [6]	**α-glucosidase inhibition assay** (IC_{50} > 100 μM) [154], **cytotoxic assay** (HGC-27, IC_{50} 11.69 μM) [15], (MCF-7, IC_{50} 24.3 μM; NCI-H460, IC_{50} 19.8 μM; SF-268, IC_{50} 15.5 μM) [194], (A549, IC_{50} 35.99 μM; HepG2, IC_{50} 25.81 μM; MDA-MB-231, IC_{50} 29.73 μM) [154], (HepG2, IC_{50} 22.1 μM; MDA-MB-231, IC_{50} 20.3 μM) [147], **lettuce hypocotyl growth assay** (65–80% inhibition) [193], **NO production inhibition assay** (IC_{50} 12.4 μM) [6], (IC_{50} 19.77 μM) [103]
30b	*Ganoderma resinaceum* [103], *Stropharia rugosoannulata* [81]	**anti-fungal assay** (MIC 250 μM) [81], **NO production inhibition assay** (IC_{50} 17.23 μM) [103], **osteoclast-forming assay** [81]
30c	*Amauroderma amoiensis* [82], *Ganoderma resinaceum* [103]	**NO production inhibition assay** (IC_{50} 3.24 μM) [103]

Table 2. *Cont.*

Compound	Fungal Source [Ref.]	Assays (Activity) [Ref.]
31a	*Cortinarius glaucopus* [195], *Ganoderma lucidum* [147], *G. resinaceum* [103], *G. sinense* [196], *Grifola frondosa* [154], *Hygrophorus russula* [183], *Leptographium qinlingensis* [197], *Omphalia lapidescens* [15], *Simplicillium* sp. YZ-11 [192], *Stropharia rugosoannulata* [193], *Phellinus linteus* [198], *Pleurotus eryngii* [6], *Termitomyces microcarpus* [132]	**α-glucosidase inhibition assay** (IC_{50} > 100 μM) [154], **cytotoxic assay** (HGC-27, IC_{50} 18.97 μM) [15], (MCF-7, IC_{50} > 50 μM; NCI-H460, IC_{50} > 50 μM); SF-268, IC_{50} > 50 μM)-194], (A549, IC_{50} 69.11 μM; HepG2, IC_{50} 38.87 μM; MDA-MB-231, IC_{50} 46.76 μM) [154], (A549, IC_{50} 15.3 μg/mL; XF498, IC_{50} 15.1 μg/mL) [183], (HepG2, IC_{50} 50.6 μM; MDA-MB-231, IC_{50} 46.7 μM) [147], **HNE inhibitory assay** (IC_{50} 28.2 μM) [198], **lettuce hypocotyl growth assay** (61–78% inhibition) [193], **NCI 60 panel** [132], **NO production inhibition assay** (IC_{50} > 30 μM) [6], (IC_{50} 23.34 μM) [103], (IC_{50} > 40 μM) [196]
31b	*Ganoderma resinaceum* [103], *Hericium erinaceus* [187,188], *Sparassis crispa* [186,199], *Phellinus linteus* [198], *Pleurotus eryngii* [6]	**cytotoxic assay** (MCF-7, IC_{50} > 50 μM) [194], (NCI-H460, IC_{50} > 50 μM) [194], (SF-268, IC_{50} > 50 μM) [194], **NO production inhibition assay** (IC_{50} 14.3 μM) [6], (IC_{50} 17.23 μM) [103], **PCSK9 mRNA expression** (inhibition, IC_{50} 8.23 μM) [186]
31c	*Hericium erinaceum* [200]	**PPAR transactivation assay** (EC_{50} 8.2 μM) [200]
31d	*Hericium erinaceum* [200]	**PPAR transactivation assay** (EC_{50} 6.4 μM) [200]
32	*Pleurotus eryngii* [59]	**aromatase inhibitory assay** (IC_{50} 17.3 μM) [59]
33	*Hericium erinaceum* [187], *Omphalia lapidescens* [15]	**cytotoxic assay** (HGC-27, IC_{50} 29.34 μM) [15], **HNE inhibitory assay** (IC_{50} 75.1 μM) [198], **TNF-α secretion assay** (inhibition value of 37.5% at 10 μM) [187]
34	*Grifola gargal* [182]	**osteoclast-forming assay** [182]
35	*Amauroderma subresinosum* [83]	**AChE inhibitory assay** (20.9% at 100 μM) [83]
36	*Omphalia lapidescens* [15]	**cytotoxic assay** (HGC-27, IC_{50} 23.41 μM) [15]
37a	*Pleurotus eryngii* [201]	**cytotoxic assay** (RAW264.7, IC_{50} > 30 μM) [201]
37b	*Stropharia rugosoannulata* [81]	**osteoclast-forming assay** [81]
38	*Grifola gargal* [182]	**cytotoxic assay** (HepG2, IC_{50} 200.9 μM; MDA-MB-231, IC_{50} 189.4 μM) [147], **osteoclast-forming assay** [182]
39	*Amauroderma subresinosum* [83], *Polyporus ellisii* [184]	**cytotoxic assay** (HL-60, IC_{50} 32.1 μM; SMMC-7721, A549, MCF-7, SW480, IC_{50} > 40 μM) [184]
40	*Pleurotus eryngii* [201]	**cytotoxic assay** (RAW264.7, IC_{50} > 30 μM) [201], **NO production inhibition assay** (IC_{50} 13.2 μM) [201]
41	*Polyporus ellisii* [184]	**cytotoxic assay** (HL-60, IC_{50} 1.5 μM; SMMC-7721, IC_{50} 3.9 μM; A549, IC_{50} 2.7 μM; MCF-7, IC_{50} 3.1 μM; SW480, IC_{50} 2.9 μM) [184]
42	*Phomopsis* sp. [202]	**α-glucosidase inhibition assay** (IC_{50} > 100 μM) [202]
43a	*Polyporus ellisii* [184], *Phomopsis* sp. [202]	**antibacterial assay** (MIC 28.2 μM against *Micrococcus tenuis*) [202], **cytotoxic assay** (HL-60, IC_{50} 32.1 μM; SMMC-7721, A549, MCF-7, SW480, IC_{50} > 40 μM) [184]
43b	*Ganoderma resinaceum* [103], *Polyporus ellisii* [184], *Phomopsis* sp. [202]	**cytotoxic assay** (HL-60, IC_{50} 18.8 μM; SMMC-7721, A549, MCF-7, SW480, IC_{50} > 40 μM) [184]
44	*Grifola gargal* [182]	**osteoclast-forming assay** [182]
45	*Pleurotus eryngii* [6]	**NO production inhibition assay** (IC_{50} > 30 μM) [6]
46	*Ganoderma lucidum* [147]	**cytotoxic assay** (HepG2, IC_{50} 138.3 μM; MDA-MB-231, IC_{50} 176.1 μM) [147]
47	*Amauroderma amoiensis* [82]	**AChE inhibitory assay** (14.63% inhibition at 100 μM) [82]
48	*Trametes versicolor* [168]	(NO inhibitory activity at 12.5 μM, IL-6 inhibitory effect at 25 μM) [168]
49	*Hericium erinaceus* [187,188]	**TNF-α secretion assay** (37.5% inhibition at 10 μM) [187]
50	*Hericium erinaceus* [187,188], *Phellinus linteus* [198], *Stropharia rugosoannulata* [193]	**HNE inhibitory assay** (IC_{50} 35.2 μM) [198], **inhibition of lettuce hypocotyl growth** (no activity) [193]
51	*Ganoderma lucidum* [147], *Hericium erinaceum* [187]	**NO production inhibition assay** (moderate activity) [187]
52	*Aspergillus awamori* [203], *Omphalia lapidescens* [15]	**cytotoxic assay** (HGC-27, IC_{50} 58.43 μM) [15], (A549, IC_{50} 64 μM) [203]
53	*Hericium erinaceum* [187], *Pleurotus eryngii* [6]	**NO production inhibition assay** (IC_{50} > 30 μM) [6]
54	*Omphalia lapidescens* [15]	**cytotoxic assay** (HGC-27, IC_{50} 15.37 μM) [15]

Table 2. *Cont.*

Compound	Fungal Source [Ref.]	Assays (Activity) [Ref.]
55	*Pleurotus eryngii* [201]	**cytotoxic assay** (RAW264.7, IC_{50} > 30 μM) [201]
56	*Talaromyces stipitatus* [204]	**cytotoxic assay** (Hep3B, IC_{50} 4.75 μM; HepG2, IC_{50} 8.85 μM; Huh-7, IC_{50} 13.78 μM) [204]
57	*Aspergillus penicillioides* [205], *Ganoderma lingzhi* [12]	**antibacterial assay** (MIC 32 μg/mL against *Vibrio anguillarum*) [205], **cytotoxic assay** (A549, IC_{50} 8.57 μM; MCF-7, IC_{50} 6.09 μM) [12]
58	*Chaetomium* sp. [189]	**AChE inhibitory assay** (20–60% inhibition at 50 μg/mL) [189]
59	*Colletotrichum* sp. [206]	**AChE inhibitory assay** (18.2% inhibition at 100 μg/mL) [206]

Human neutrophil elastase (HNE) is a serine protease that can degrade extracellular matrix proteins such as collagen, fibronectin, etc. Inhibition of this enzyme can prevent the loss of skin elasticity, thereby preventing skin aging. Yoo et al. reported the HNE-inhibitory properties of *Phellinus linteus* mycelium components [198]. All three tested epoxides **31a, 34,** and **50** showed significant activity with ID_{50} ranging from 28.2 to 75.1 μM.

Epoxides **30a**, **31a,** and **33** were isolated after anaerobic incubation of ergosterol peroxide (EP, **21a**) with rat intestinal flora [207]. Two of them (**30a** and **33**) were found to be more active against human colorectal cancer cells than the original EP. This means that EP's strong anti-tumor properties may be (at least in part) due to its metabolic products.

A number of ergostane-type sterol fatty acid esters, including epoxides **31c** and **31d**, were isolated from the mushroom *Hericium erinaceum* and evaluated for their PPAR transactivational effects using a luciferase reporter system [200]. Oleyl and linoleyl esters **31c** and **31d** proved to be the most potent activators of the transcriptional activity of PPARs with EC_{50} values down to 6.4 μM.

5. Polyols

It should be kept in mind that the structures of ergostane-type steroids with hydroxyl and/or carbonyl group(s) given below do not fully reflect their diversity in fungal sources. A large number of compounds have been isolated before 2010; for a number of compounds isolated later, no data on biological activity are given, and for this reason they are not included in this review.

Many fungal ergostanes of this class are 5α-alcohols containing (an)other hydroxy (or a functionalized hydroxy) group(s) at C-6, C-9, and/or C-14 (Figure 9). 5α,6α Epoxides are their evident biosynthetic precursors. As a rule, rings A and B are trans-fused for most ergostanes of this group, with the exception of 5β-alcohols **77, 78, 84** (Figure 10). It should be noted that fomentarol B (**84**) has a cis-junction of ring B and C, which is rare among the ergostane type steroids [208].

Cerevisterol (**60**) is probably the best studied among 5α,6β-dihydroxy derivatives, as it is widespread in the fungal kingdom (Table 3). It should be noted that data on its cytotoxicity are inconsistent and sometimes contradictory. Thus, cerevisterol (**60**) showed significant activity with IC_{50} values of 1.1–1.9 μM against the BT-549, KB, SK-MEL, and SKOV-3 cancer cell lines [209]. On the other hand, it was practically inactive toward A549, HeLa, HepG2, and MCF-7 cells [210]. This inconsistence may be partly due to the diverse cell lines used by different authors. But a large difference was also observed in experiments with the same cell lines (e.g., reported IC_{50} values for HepG2 varied from 14.5 μM [211] to 174.6 μM [147]).

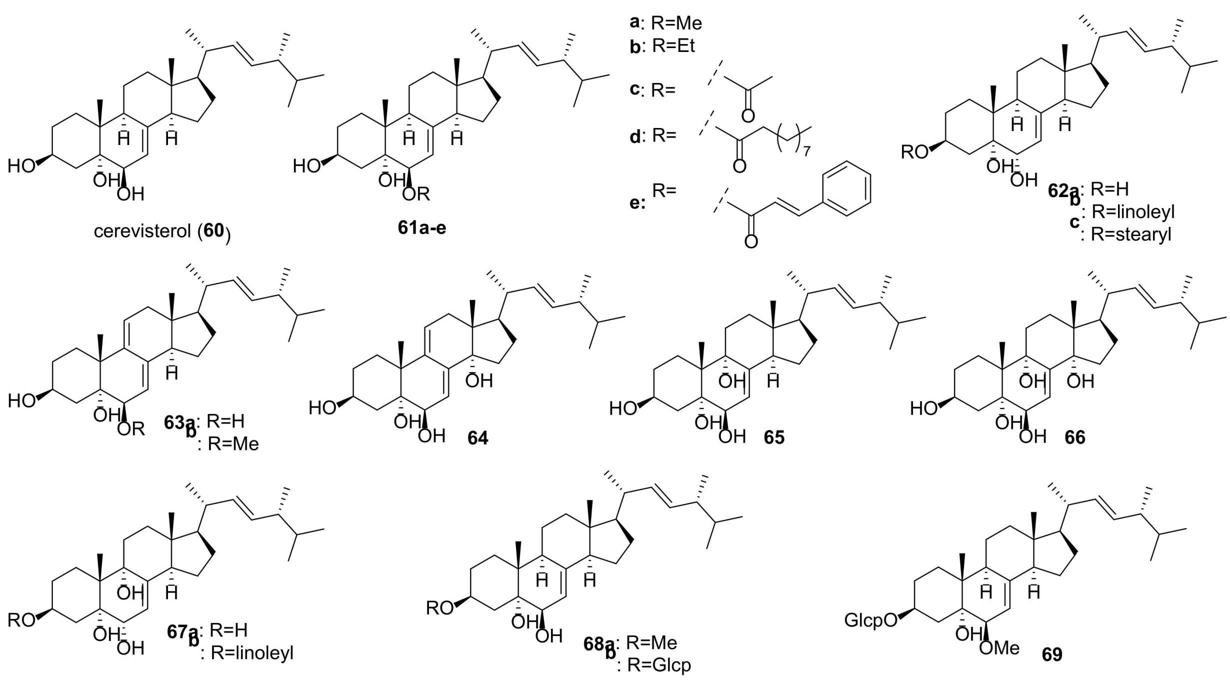

Figure 9. Structures of fungal steroids with a 5α,6-diol fragment and their *O*-derivatives.

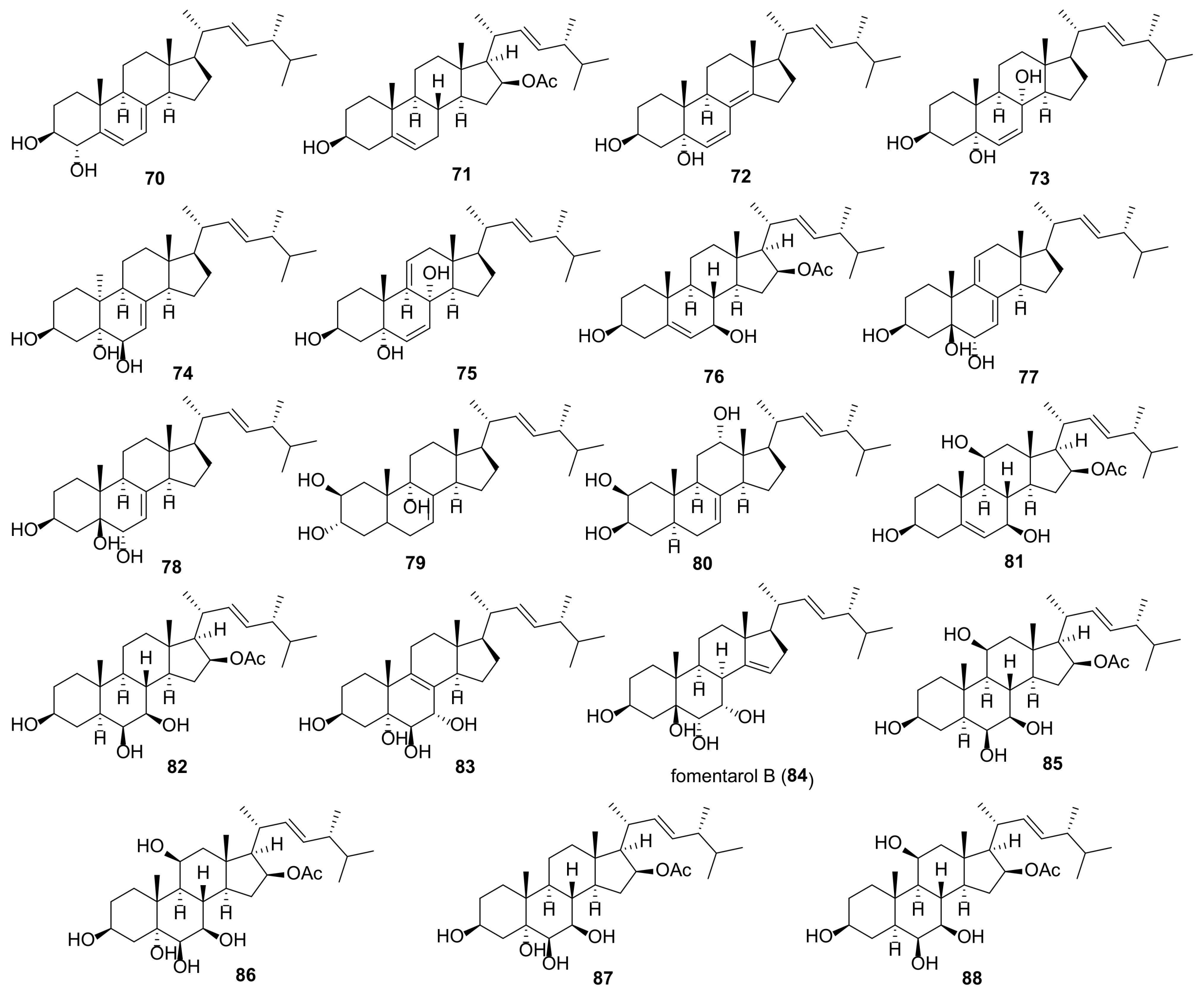

Figure 10. Structures of other fungal polyols.

The results of studies of antimicrobial activity also vary quite a lot. Thus, in the course of searching for biologically active constituents of wood decaying mushrooms, *Trametes gibbosa* and *Trametes elegans*, Agyare et al. isolated cerevisterol (**60**) as a compound responsible for their antimicrobial activity [212]. It inhibited the growth of a number of bacteria with MICs ranging from 25 to 50 μg/mL (ciprofloxacin MICs were between 0.31 and 3.50 μg/mL). The sub-inhibitory concentration of **60** (3 μg/mL) modified the activity of commonly used antibiotics (either potentiating or reducing). Similar results with respect to antimicrobial activity of **60** were obtained by Zhou et al. [213]. On the other hand, no antimicrobial activity for cerevisterol (**60**) was reported in works [214,215].

To access the anti-inflammatory activity of cerevisterol (**60**), Lee et al. measured the levels of NO and PGE_2 and the production of cytokines TNF-α, IL-1, and IL-6 in LPS-stimulated macrophages [216]. It was shown that **60** suppressed the LPS-induced production of NO and PGE2 and decreased the expression of pro-inflammatory cytokines.

Table 3. Sources and biological activity of fungal alcohols.

Compound	Fungal Source [Ref.]	Assays (Activity) [Ref.]
60	*Aspergillus fumigatus* [213], *A. versicolor* [179], *Cladosporium* sp. [217], *Clitocybe nebularis* [214], *Eurotium rubrum* [80], *Fomes fomentarius* [208], *Fusarium chlamydosporum* [209,218], *F. equiseti* [219], *F. solani* [216], *Ganoderma sinense* [196,220], *Glomerella* sp. [215], *Gomphus clavatus* [221], *Hericium erinaceum* [222,223], *Hypholoma lateritium* [224], *Lentinus polychrous* [225], *Leptographium qinlingensis* [197], *Leucocalocybe mongolica* [210], *Meripilus giganteus* [91], *Morchella esculenta* [226], *Omphalia lapidescens* [15], *Penicillium brasilianum* [227], *Pleurotus eryngii* [6], *P. tuber-regium* [228], *Polyporus umbellatus* [77,211], *Termitomyces microcarpus* [132], *Trametes gibbosa* and *T. elegans* [212], *Tricholoma populinum* [229], *Xylaria nigripes* [105]	**AChE inhibitory assay** (0.4% inhibition at 100 μg/mL) [80], **antibacterial assay** (no activity against *Streptococcus agalactiae*, *Staphylococcus epidermidis*, *Moraxella catarrhalis*, *Haemophilus influenzae*, and *Proteus mirabilis*) [214], (*S. typhi*, *S. aureus* and *A. niger*, MICs 25 μg/mL each, *E. faecalis*, MIC 50 μg/mL) [212], (*Bacillus subtilis* and *Escherichia coli*, MICs 64 μg/mL each; *Staphylococcus aureus*, MIC 32 μg/mL) [213], **cytotoxic assay** (A549, IC_{50} 94.75 μM; HeLa, IC_{50} 74.13 μM; HepG2, IC_{50} 46.58 μM; MCF-7, IC_{50} 63.76 μM) [210], (T47D, 50.2% inhibition at 30 μM) [229], (BT-549, 1.4 μM; KB, 1.90 μM; SK-MEL, 1.70 μM; SKOV-3, 1.1 μM) [209], (Caco-2, IC_{50} 37.56 μM; MCF-7, IC_{50} 32.4 μM; MDA-MB-231, IC_{50} 41.5 μM) [219], (HGC-27, IC_{50} 37.71 μM) [15], (MCF-7, IC_{50} 37.2 μM; PC-3, IC_{50} 80 μM) [221], (HepG2, IC_{50} 14.5 μM) [211], (HepG2, IC_{50} 174.6 μM; MDA-MB-231, IC_{50} 148.8 μM) [147], (SW1990, IC_{50} 32.81 μM; Vero, IC_{50} > 100 μM) [220], **NF-κB inhibitory assay** (IC_{50} 5.1 μM) [226], **HIV-inhibitory assay** (IC_{50} 9.3 μM) [230], **HNE inhibitory assay** (IC_{50} 77.5 μM) [198], **DPPH free radical-scavenging assay** (IC_{50} 11.38 μM) [222], **GIRK channel inhibitory assay** (13% inhibition at 10 μM) [224], **lipoxygenase inhibitory assay** (IC_{50} 5.46 μM) [218], **NO production inhibition assay** (IC_{50} > 40 μM) [196], (IC_{50} > 30 μM) [6], **ORAC assay** (antioxidant activity 1.94 mmol TE/g) [91], **PTP1B inhibitory activity assay** (IC_{50} 7.5 μg/mL) [77], **toxicity to *Pinus armandi* seedlings assay** (lethal rate 95% at 30 μg/mL) [197], **trap activity assay** (reduction to 28.1% from 332% in control cells) [223]
61a	*Aspergillus penicillioides* [205], *A. ustus* [231], *Aspergillus versicolor* [179], *Eurotium rubrum* [80], *Ganoderma lucidum* [232], *G. sinense* [233], *Hericium erinaceum* [223], *Omphalia lapidescens* [15], *Penicillium brasilianum* [227], *Pleurotus eryngii* [6], *Tricholoma populinum* [229], *Xylaria nigripes* [105]	**AChE inhibitory assay** (2.7% inhibition at 100 μg/mL) [80], **cytotoxic assay** (T47D, 23.7% inhibition at 30 μM; MDA-MB-231, 54.7% inhibition at 30 μM) [229], (U2OS, IC_{50} 6.0 μM) [105], (HGC-27, IC_{50} 4.17 μM) [15], [15], (HL-60, IC_{50} 22.4 μM; LLC, IC_{50} 55.3 μM; MCF-7, IC_{50} > 100 μM) [232], **HIV-inhibitory assay** (IC_{50} 3.8 μM) [230], **HNE inhibitory assay** (IC_{50} 14.6 μM) [198], **neuroprotective activity assay** (20.9% increase in cell viability against $A\beta_{25-35}$-induced injury in SH-SY5Y neuroblastoma cells at the concentration 10 μM) [105], **NO production inhibition assay** (IC_{50} 20.4 μM) [6], (108.2% inhibitory rate at 10 μM) [230], **trap activity assay** (reduction to 74.8% from 332% in control cells) [223]
61b	*Fomes fomentarius* [208], *Omphalia lapidescens* [15]	**cytotoxic assay** (HGC-27, IC_{50} 25.50 μM) [15]
61c	*Eurotium rubrum* [80], *Hericium erinaceum* [223]	**AChE inhibitory assay** (17.9% inhibition at 100 μg/mL) [80], **trap activity assay** (reduction to 81.8% from 332% in control cells) [223]
61d	*Fusarium chlamydosporum* [218]	**lipoxygenase inhibitory assay** (IC_{50} 3.06 μM) [218]
61e	*Hericium erinaceum* [223]	**ORAC assay** (antioxidant activity 8.01 mmol TE/g at 10 μM) [223]

Table 3. *Cont.*

Compound	Fungal Source [Ref.]	Assays (Activity) [Ref.]
62a	*Eurotium rubrum* [80], *Fomes fomentarius* [208], *Hericium erinaceum* [223], *Hygrophorus russula* [183], *Omphalia lapidescens* [15]	**AChE inhibitory assay** (2.4% inhibition at 100 µg/mL) [80], **cytotoxic assay** (HGC-27, IC_{50} > 100 µM) [15], (HepG2, IC_{50} 196.9 µM; MDA-MB-231, IC_{50} 114.2 µM) [147], (A549, >30 µg/mL; XF498, >30 µg/mL) [183], **trap activity assay** (reduction to 138.9% from 332% in control cells) [223]
62b	*Hericium erinaceum* [200]	**PPAR transactivation assay** (EC_{50} 18.7 µM) [200]
62c	*Hericium erinaceum* [200]	**PPAR transactivation assay** (EC_{50} 20.6 µM) [200]
63a	*Ganoderma lucidum* [147], *Pleurotus eryngii* [6]	**cytotoxic assay** (HepG2, IC_{50} 62.5 µM; MDA-MB-231, IC_{50} 56.3 µM) [147], **NO production inhibition assay** (IC_{50} 29.8 µM) [6]
63b	*Ganoderma sinense* [220]	**cytotoxic assay** (SW1990, IC_{50} 5.05 µM; Vero, IC_{50} 22.59 µM) [220]
64	*Fomes fomentarius* [208], *Ganoderma lucidum* [147], *Hericium erinaceum* [187]	**cytotoxic assay** (HepG2, IC_{50} 156.4 µM; MDA-MB-231, IC_{50} 168.9 µM) [147], **TNF-α secretion assay** (33.7% inhibition at 10 µg/mL) [187]
65	*Clitocybe nebularis* [214], *Fomes fomentarius* [208], *Hericium erinaceum* [223], *Hygrophorus russula* [183], *Leptographium qinlingensis* [197], *Naematoloma fasciculare* [151], *Stropharia rugosoannulata* [81], *Tricholoma populinum* [229]	**antibacterial assay** (no activity against *Streptococcus agalactiae*, *Staphylococcus epidermidis*, *Haemophilus influenzae*, and *Proteus mirabilis*, marginal activity against *Moraxella catarrhalis*) [214], **anti-fungal assay** (MIC 500 µM) [81], **cytotoxic assay** (MCF-7, MDA-MB-231, T47D, no activity) [229], (HepG2, IC_{50} 129.7 µM; MDA-MB-231, IC_{50} 148.2 µM) [147], (A549, 17.1 µg/mL; XF498, 16.5 µg/mL) [183], (A549, 10.83 µM; HCT-15, 13.2 µM; SK-MEL-2, 10.39 µM; SK-OV-3, 12.16 µM;) [151]
66	*Ganoderma lucidum* [147]	**cytotoxic assay** (HepG2, IC_{50} 286.4 µM; MDA-MB-231, IC_{50} 216.5 µM) [147]
67a	*Omphalia lapidescens* [15]	**cytotoxic assay** (HGC-27, IC_{50} 12.71 µM) [15], (HepG2, IC_{50} 184.6 µM; MDA-MB-231, IC_{50} 224.2 µM) [147]
67b	*Hericium erinaceum* [200]	**PPAR transactivation assay** (EC_{50} 22.3 µM) [200]
68a	*Omphalia lapidescens* [15]	**cytotoxic assay** (HGC-27, IC_{50} 26.74 µM) [15]
68b	*Fomes fomentarius* [208]	**cytotoxic assay** (A549, IC_{50} 29.8 µM; MCF-7, IC_{50} 26.1 µM; NUGC-3, IC_{50} 24.1 µM) [208]
69	*Pleurotus eryngii* [6]	**NO production inhibition assay** (IC_{50} > 30 µM) [6]
70	*Hericium erinaceus* [187,188]	**TNF-α secretion assay** (25% inhibition at 10 µg/mL) [187]
71	*Penicillium granulatum* [234]	**cytotoxic assay** (no activity) [234]
72	*Hericium erinaceum* [187]	**TNF-α secretion assay** (36.7% inhibition at 10 µg/mL) [187]
73	*Coprinus setulosus* [101], *Ganoderma lipsiense* [235], *G. resinaceum* [103], *Xylaria nigripes* [105]	**antigiardial assay** (93.6% inhibition against *Giardia duodenalis* throphozoites) [235], **NO production inhibition assay** (IC_{50} 27.6 µM) [105], (IC_{50} 22.76 µM) [103], **tyrosinase inhibitory assay** (IC_{50} 6.9 µM) [236]
74	*Eurotium rubrum* [80]	**AChE inhibitory assay** (23.1% inhibition at 100 µg/mL) [80]
75	*Ganoderma resinaceum* [103]	**NO production inhibition assay** (IC_{50} 22.76 µM) [103]
76	*Penicillium granulatum* [234]	**cytotoxic assay** (no activity) [234]
77	*Omphalia lapidescens* [16]	**cytotoxic assay** (GES-1, IC_{50} > 50 µM; HGC-27, IC_{50} 12.28 µM; MDA-MB-231, IC_{50} 11.33 µM) [16]
78	*Omphalia lapidescens* [16], *Pleurotus eryngii* [6]	**cytotoxic assay** (GES-1, IC_{50} 28.0 µM; HGC-27, IC_{50} > 50 µM; MDA-MB-231, IC_{50} 24.85 µM) [16], **NO production inhibition assay** (IC_{50} > 30 µM) [6]
79	*Ganoderma duripora* [237], *Ganoderma lucidum* [232,238], *Phellinus linteus* [198]	**cytotoxic assay** (HL-60, IC_{50} 12.7 µM; LLC, IC_{50} 45.2 µM; MCF-7, IC_{50} > 100 µM) [232], (A549, MCF-7, PC-3, IC_{50} > 50 µM) [238], **HNE inhibitory assay** (IC_{50} > 100 µM) [198]
80	*Lasiodiplodia pseudotheobromae* [11]	**AChE inhibitory assay** (no activity) [11], **α-glucosidase inhibition assay** (no activity) [11]
81	*Penicillium granulatum* [234]	**cytotoxic assay** (A549, IC_{50} 5.5 µM) [234]
82	*Penicillium granulatum* [234]	**cytotoxic assay** (A549, BEL-7402, SHG-44, IC_{50} > 20 µM; ECA-109, IC_{50} 9.2 µM; HepG2, IC_{50} 7.0 µM) [234]
83	*Omphalia lapidescens* [16]	**cytotoxic assay** (GES-1, HGC-27, MDA-MB-231, IC_{50} > 50 µM) [16]

Table 3. *Cont.*

Compound	Fungal Source [Ref.]	Assays (Activity) [Ref.]
84	*Fomes fomentarius* [208], *Omphalia lapidescens* [16]	**cytotoxic assay** (MDA-MB-231, IC_{50} 140.86 μM) [16], **NO production inhibition assay** (98.77% inhibitory activity at 50 μM) [208]
85	*Penicillium chrysogenum* [239], *Penicillium granulatum* [240]	**anti-fungal assay** (8 mm diameter at 20 μg/disk) [239], **cytotoxic assay** (HeLa, IC_{50} 15 μg/mL; NCI-H460, IC_{50} 40 μg/mL; SW1990, IC_{50} 31 μg/mL) [239], (HepG2, IC_{50} 8.2 μM) [240]
86	*Penicillium granulatum* [234]	**cytotoxic assay** (no activity) [234]
87	*Penicillium granulatum* [234]	**cytotoxic assay** (A549, IC_{50} 8.0 μM; BEL-7402, IC_{50} 8.5 μM; ECA-109, IC_{50} 8.3 μM; HepG2, IC_{50} 6.7 μM; SHG-44, IC_{50} 4.8 μM) [234]
88	*Penicillium granulatum* [234]	**cytotoxic assay** (no activity) [234]

Yoo et al. studied the HNE-inhibitory potency of ergostanes isolated from the mycelium of *Phellinus linteus* [198]. Methyl ether **61a** revealed the highest activity among all tested compounds with an IC_{50} 14.6 μM, which was comparable with the positive control (epigallocatechin gallate, IC_{50} 12.5 μM). The corresponding alcohol **60** was five times less active than **61a**.

Kim et al. studied the inhibitory activity of steroids isolated from *Hericium erinaceum* against tartrate-resistant acid phosphatase (TRAP) [223]. The latter has become a promising target for the development of new therapeutics for the treatment of osteoporosis and other bone-related diseases. Compounds **60, 61a, 61c, 62a** at a concentration of 10 μM reduced TRAP activity in osteoclasts differentiated from RAW 264.7 cells, from 322% in control cells to 28–139% in treated cells.

Compared to 5α,6-diols, other fungal polyols (Figure 10) have been relatively less studied. As mentioned above, many ergostane steroids are found in both mushrooms and plants. In particular, this applies to triol **73** found in various fungal species [101,103,105,235]. Among sixty-three compounds isolated from bamboo *Sinocalamus affinis* and studied as inhibitors of estrogen biosynthesis, triol **73** showed the highest activity with an IC_{50} value of 0.5 μM [241]. It reduced the level of expression of aromatase mRNA in granulosa-like cells of human ovaries without affecting the catalytic activity of aromatase. This discovery makes the steroid **73** an interesting lead compound in the development of new agents for the treatment of estrogen-dependent cancers.

Studying the cytotoxicity of compounds isolated from the fruiting bodies of a medicinal mushroom *Ganoderma lucidum*, Min et al. selected the 2β,3α,9α-triol **79** for a more detailed evaluation [232]. Treatment with **79** in a dose-dependent manner inhibited the growth of HL-60 human premyelocytic leukemia cells with the IC_{50} value of 12.7 μg/mL. The effect was attributed to the induction of the apoptotic process, including activation of DNA fragmentation and caspase-3 activity.

6. Hydroxyketones

This group of ergostanes in the present review is divided into compounds containing two (Figure 11), three (Figure 12), and four or more (Figure 13) functional groups in the cyclic part of the steroid molecule. It should be borne in mind that such a classification is rather arbitrary and does not cover all the aspects that are relevant to these steroids.

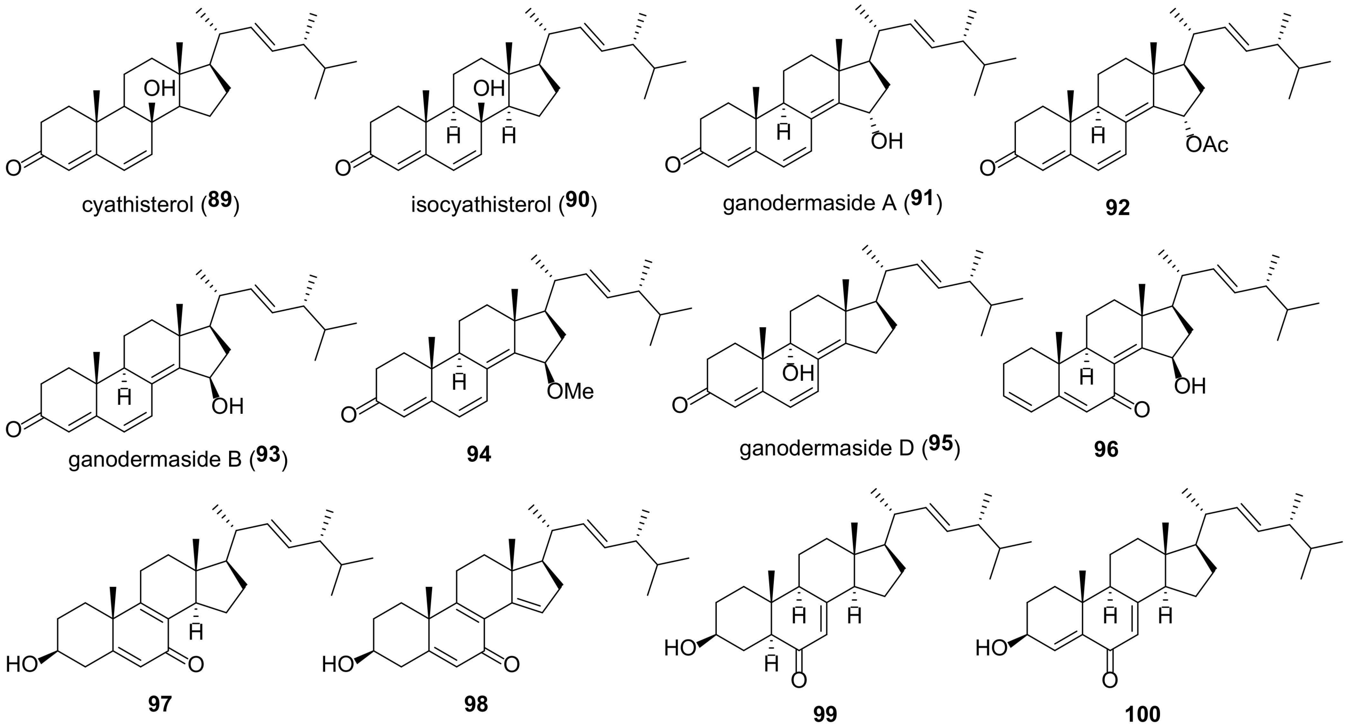

Figure 11. Structures of fungal hydroxyketones with two functional groups.

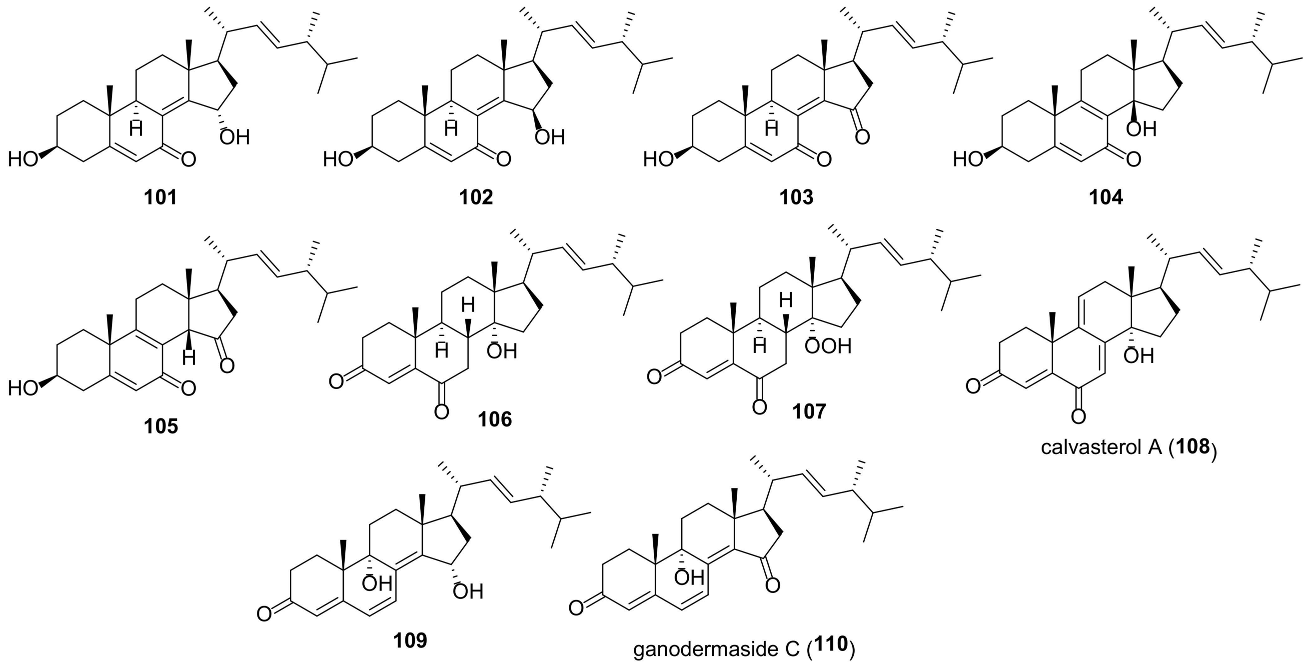

Figure 12. Structures of fungal hydroxyketones with three functional groups.

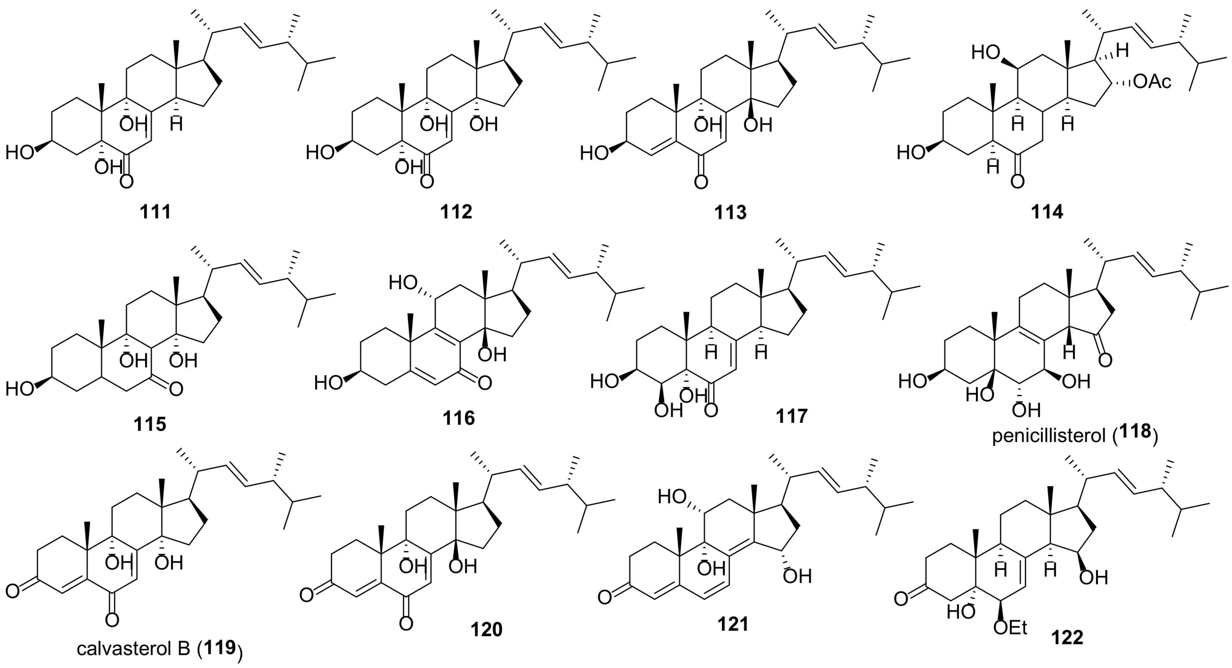

Figure 13. Structures of fungal hydroxyketones with four or more functional groups.

The first 8β-hydroxyergosta-3-one type of steroid, cyathisterol (**89**), was isolated from the fruiting body of *Caluatia cyathiformis* [242]. Later, Ji et al. isolated from an algicolous strain of *Aspergillus ustus* a very similar but not identical compound called isocyathisterol (**90**) [231]. A detailed NMR study allowed to determine the configuration of all stereocenters in **90**. The authors concluded that the difference between the compounds **89** and **90** was in the C-9 and/or C-14 configuration.

Li et al. reported theoretical and experimental results on the properties of isocyathisterol (**90**) as inhibitor of isocitrate dehydrogenase IDH1 [233]. Mutations in this enzyme are associated with certain brain tumors, that makes IDH1 inhibitors as potential anticancer therapeutics for glioma patients. Based on the results of molecular virtual screening, isocyathisterol (**90**) had a low equilibrium dissociation constant of 18.40 µM, which confirmed the strongest binding to the IDH1 mutant. Kinetic studies showed that **90** inhibited the mutant enzyme in a noncompetitive manner.

Qi et al. isolated from spores of a medicinal mushroom *Ganoderma lucidum* a number of steroids possessing a 4,6,8(14),22-tetraene-3-one unit [243,244]. The obtained compounds called as ganodermasides A-D **91, 93, 110, 95** were tested for their antiaging effect on the yeast replicative lifespan assay (Table 4). All of them increased the average lifespan compared to negative control and exhibited effect similar to the known anti-aging substance, resveratrol.

A number of ergosterol metabolites including hydroxyketones **91, 93, 109** were isolated from a non-pathogenic filamentous fungus *Talaromyces stipitatus* [204]. Compounds **91, 93, 109** showed remarkable cytotoxic activities against hepatoma cell lines with IC_{50} values ranging down to 5.26 µM.

Table 4. Sources and biological activity of fungal hydroxyketones.

Compound	Fungal Source [Ref.]	Assays (Activity) [Ref.]
89	*Calvatia cyathiformis* [242]	
90	*Aspergillus ustus* [231], *Calvatia nipponica* [126], *Ganoderma sinense* [233], *Stereum hirsutum* [17], *Tricholoma imbricatum* [245]	**antibacterial assay** (against *E. coli*, *S. aureus*, and *A. salina* with inhibitory zones of 6.7, 5.7, and 5.1 mm, respectively, at 30 µg/disk) [231], **cytotoxic assay** (A549, IC_{50} 12.3 µM; HL-60, IC_{50} 18.7 µM; K562, IC_{50} 27.2 µM; MCF-7, IC_{50} 23.8 µM; SMMC-7721, IC_{50} 15.7 µM; SW480, IC_{50} 19.1 µM) [245], (MCF-7, IC_{50} > 100 µM) [126], (A549, IC_{50} 19.1 µM; HL-60, IC_{50} 14.6 µM; MCF-7, IC_{50} 20.4 µM; SMMC-7721, IC_{50} 19.0 µM; SW480, IC_{50} 25.7 µM) [17]
91	*Ganoderma lucidum* [243,244], *Talaromyces stipitatus* [204]	**cytotoxic assay** (Hep3B, IC_{50} 9.67 µM; HepG2, IC_{50} 11.83 µM) [204], **lifespan assay** (number of divisions of K6001 yeast strain cells before death: 8.2 in control, 8.9 at 1 µM, 11.4 at 10 µM, 9.4 at 100 µM) [244]
92	*Polyporus ellisii* [184]	**cytotoxic assay** (A549, HL-60, MCF-7, SMMC-7721, SW480, IC_{50} > 40 µM; HL-60, IC_{50} 22.8 µM) [184]
93	*Ganoderma lucidum* [243,244], *Talaromyces stipitatus* [204]	**cytotoxic assay** (Hep3B, IC_{50} 12.59 µM; HepG2, IC_{50} 18.95 µM; Huh-7, IC_{50} 32.81 µM) [204], **lifespan assay** (number of divisions of K6001 yeast strain cells before death: 8.2 in control, 9.1 at 1 µM, 11.1 at 10 µM, 9.6 at 100 µM) [244]
94	*Polyporus ellisii* [184]	**cytotoxic assay** (A549, HL-60, MCF-7, SMMC-7721, SW480, IC_{50} > 40 µM; HL-60, IC_{50} 17.8 µM) [184]
95	*Ganoderma lucidum* [243], *Phomopsis* sp. [246]	**antifungal assay** (MIC 64 µg/mL against *Fusarium avenaceum*, MIC 128 µg/mL against *Hormodendrum compactum*) [246], **lifespan assay** (number of divisions of K6001 yeast strain cells before death: 7.5 in control, 10.0 at 3 µM, 10.7 at 10 µM, 9.2 at 30 µM) [243]
96	*Chaetomium globosum* [247]	**cytotoxic assay** (A549, MG-63, SMMC-7721, IC_{50} > 50 µg/mL) [247]
97	*Colletotrichum* sp. [206], *Penicillium brasilianum* [227], *Pleurotus eryngii* [6], *Tricholoma imbricatum* [245]	**cytotoxic assay** (A549, IC_{50} 21.7 µM; HL-60, IC_{50} 7.9 µM) [245], **NO production inhibition assay** (IC_{50} 12.4 µM) [6]
98	*Tricholoma imbricatum* [245]	**cytotoxic assay** (HL-60, IC_{50} 25.7 µM; SMMC-7721, IC_{50} 27.3 µM; SW480, IC_{50} 37.7 µM) [245]
99	*Fomes fomentarius* [208], *Grifola frondosa* [48], *Phellinus linteus* [198]	**β-hexosaminidase release assay** (no activity) [48], **HNE inhibitory assay** (IC_{50} > 100 µM) [198], **NO production inhibition assay** (IC_{50} 32.87 µM) [208]
100	*Hericium erinaceum* [187]	**TNF-α secretion assay** (24.6% inhibition at 10 µg/mL) [187]
101	*Tricholoma imbricatum* [245]	**cytotoxic assay** (A549, IC_{50} 12.4 µM; HL-60, IC_{50} 12.2 µM; K562, IC_{50} 13.8 µM; MCF-7, IC_{50} 17.8 µM; SMMC-7721, IC_{50} 27.6 µM; SW480, IC_{50} 19.7 µM) [245]
102	*Chaetomium globosum* [247], *Phomopsis* sp. [202], *Tricholoma imbricatum* [245]	**α-glucosidase inhibition assay** (IC_{50} > 100 µM) [202], **cytotoxic assay** (A549, IC_{50} 20.72 µg/mL; MG-63, IC_{50} 15.34 µg/mL; SMMC-7721, IC_{50} 19.20 µg/mL) [247], (A549, IC_{50} 27.3 µM; HL-60, IC_{50} 23.6 µM) [245]
103	*Tricholoma imbricatum* [245]	**cytotoxic assay** (A549, IC_{50} 36.7 µM; HL-60, IC_{50} 16.6 µM; K562, IC_{50} 19.9 µM; MCF-7, IC_{50} 21.3 µM; SMMC-7721, IC_{50} 23.5 µM) [245]
104	*Pleurotus eryngii* [248]	**NO production inhibition assay** (weak activity) [248]
105	*Tricholoma imbricatum* [245]	**cytotoxic assay** (A549, IC_{50} 12.7 µM; HL-60, IC_{50} 7.7 µM) [245]
106	*Stereum hirsutum* [17]	**cytotoxic assay** (A549, IC_{50} 11.0 µM; HL-60, IC_{50} 3.1 µM; MCF-7, IC_{50} 12.3 µM; SMMC-7721, IC_{50} 9.0 µM; SW480, IC_{50} 13.4 µM) [17]
107	*Stereum hirsutum* [17]	**cytotoxic assay** (A549, HL-60, MCF-7, SMMC-7721, SW480, IC_{50} > 40 µM) [17]
108	*Gymnoascus reessii* [249], *Polyporus ellisii* [198], *Phomopsis* sp. [246]	**antifungal assay** (MIC 64 µg/mL against *Fusarium avenaceum*, MIC 256 µg/mL against *Aspergillus niger* and *Trichophyton gypseum*) [246], **antimalarial assay** (IC_{50} 3.4 µg/mL against *Plasmodium falciparum*) [249], **cytotoxic assay** (KB, IC_{50} 3.8 µM; MCF-7, IC_{50} 7.9 µM; NCI-H187, IC_{50} 1.9 µM; Vero, IC_{50} 3.3 µM) [249], **HNE inhibitory assay** (IC_{50} 20.5 µM) [198],

Table 4. *Cont.*

Compound	Fungal Source [Ref.]	Assays (Activity) [Ref.]
89	*Calvatia cyathiformis* [242]	
109	*Ganoderma resinaceum* [103], *Omphalia lapidescens* [15], *Talaromyces stipitatus* [204]	**cytotoxic assay** (Hep3B, IC_{50} 5.26 µM; HepG2, IC_{50} 6.29 µM; Huh-7, IC_{50} 16.23 µM) [204], (HGC-27, IC_{50} 16.93 µM) [15]
110	*Ganoderma lucidum* [243]	**lifespan assay** (number of divisions of K6001 yeast strain cells before death: 7.5 in control, 8.8 at 3 µM, 10.8 at 10 µM, 9.4 at 30 µM) [243]
111	*Colletotrichum* sp. [206], *Ganoderma sinense* [196], *Pleurotus eryngii* [250], *Psathyrella candolleana* [251], *Volvariella volvacea* [123]	**cytotoxic assay** (HepG2, IC_{50} 5.90 µM; SGC-7901, IC_{50} 12.03 µM) [123], (A549, HL-60, MCF-7, SMMC-7721, SW480, IC_{50} > 40 µM) [251], (RAW264.7, IC_{50} > 100 µM) [250], **NO production inhibition assay** (IC_{50} 28.5 µM) [196], (IC_{50} 100 µM) [250]
112	*Volvariella volvacea* [123]	**cytotoxic assay** (HepG2, IC_{50} 20.27 µM) [123]
113	*Ganoderma resinaceum* [103]	**NO production inhibition assay** (IC_{50} 35.19 µM) [103]
114	*Gliomastix* sp. [252]	**antiviral assay** (EV-71 virus, IC_{50} 17.8 µM) [252], **cytotoxic assay** (HL-60, IC_{50} 1.75 µM; DU-145, IC_{50} 7.37 µM; HeLa, IC_{50} 12.1 µM; MOLT-4, IC_{50} 6.53 µM) [252]
115	*Ganoderma philippii* [253]	**AChE inhibitory assay** (35.8% inhibition at 50 µg/mL) [253]
116	*Ganoderma resinaceum* [103]	**NO production inhibition assay** (IC_{50} 32.87 µM) [103]
117	*Pleurotus eryngii* [6]	**NO production inhibition assay** (IC_{50} 18.1 µM) [6]
118	*Penicillium purpurogenum* [254]	**cytotoxic assay** (A549, HepG2, MCF-7, IC_{50} > 100 µM) [254]
119	*Gymnoascus reessii* [249], *Phomopsis* sp. [246], *Talaromyces* sp. [255]	**antifungal assay** (MIC 128 µg/mL against *Candida albicans*, MIC 256 µg/mL against *Aspergillus niger* and *Hormodendrum compactum*) [246], **antimalarial assay** (IC_{50} 3.4 µg/mL against *Plasmodium falciparum*) [249], **cytotoxic assay** (KB, IC_{50} 20.4 µM; MCF-7, IC_{50} > 50 µM; NCI-H187, IC_{50} 12.5 µM; Vero, IC_{50} 19.3 µM) [249]
120	*Stereum hirsutum* [17], *Phomopsis* sp. [246]	**antifungal assay** (MIC 64 µg/mL against *Candida albicans* and *Hormodendrum compactum*, MIC 128 µg/mL against *Aspergillus niger*) [246], **cytotoxic assay** (A549, IC_{50} 27.8 µM; HL-60, IC_{50} 14.4 µM; MCF-7, IC_{50} > 40 µM; SMMC-7721, IC_{50} 32.0 µM; SW480, IC_{50} > 40 µM) [17]
121	*Lasiodiplodia pseudotheobromae* [11]	**AChE inhibitory assay** (no activity) [11], **α-glucosidase inhibition assay** (no activity) [11]
122	*Phomopsis* sp. [246]	**antifungal assay** (MIC 128 µg/mL against *Candida albicans* and *Fusarium avenaceum*, MIC 256 µg/mL against *Hormodendrum compactum*) [246]

7. Ketones

Most compounds of this group of ergostane-type steroids contain keto functions at C-3 and C-6, as well as a number of double bonds (Figure 14). Ergone (**124**) is probably the best studied among them [256]. It is found in many fungal sources (Table 5), usually with a content of less than 10 µg/g of mushroom fruit bodies. *Polyporus umbellatus*, in comparison with other mushrooms, contains the highest amount of this compound, which, under optimized conditions, can reach 86.9 µg/g [257]. For practical purposes, ergone (**124**) can be easily obtained through a three-step chemical synthesis from ergosterol [258]. Ergone has been reported to possess various activities (Table 5), including cytotoxic, anti-bacterial [205], anti-inflammatory [228,259], anti-malarial [249], diuretic [260] abilities, and protective effects of early renal injury [261,262].

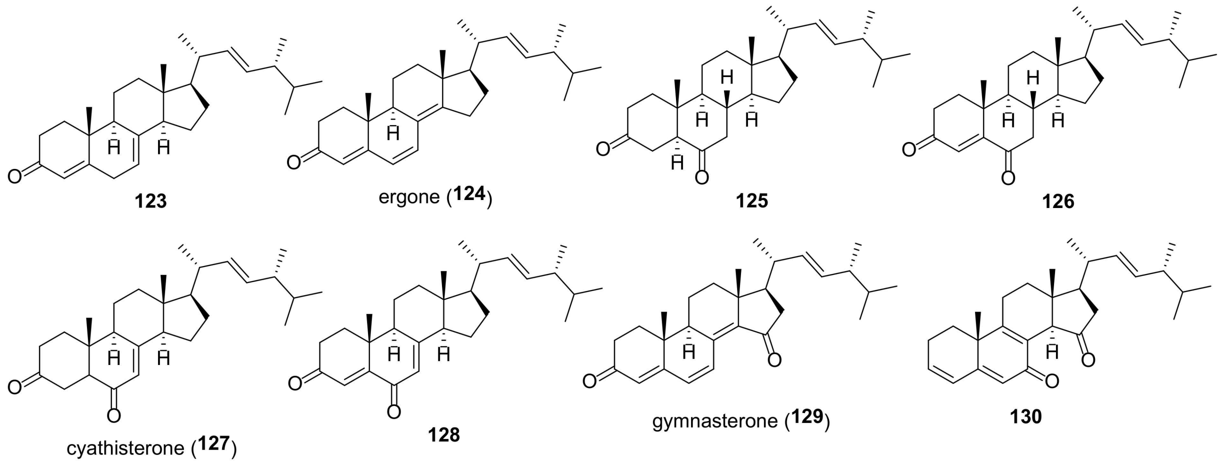

Figure 14. Structures of fungal ketones.

Table 5. Sources and biological activity of fungal ketones.

Compound	Fungal Source [Ref.]	Assays (Activity) [Ref.]
123	*Gymnoascus reessii* [249]	**antimalarial assay** (IC_{50} 3.3 µg/mL against *Plasmodium falciparum*) [249], **cytotoxic assay** (KB, IC_{50} 32.5 µM; MCF-7, IC_{50} > 50 µM; NCI-H187, IC_{50} 16.3 µM; Vero, IC_{50} 17.0 µM) [249]
124	*Antrodia cinnamomea* [263], *Aspergillus penicillioides* [205], *A. ustus* [231], *Colletotrichum* sp. [190], *Cortinarius xiphidipus* [85], *Fulviformes fastuosus* [264], *Ganoderma sinense* [220,233], *Gymnoascus reessii* [249], *Hygrophorus russula* [183], *Lentinus polychrous* [225], *Leucocalocybe mongolica* [210], *Mahonia fortune* [265], *Nigrospora sphaerica* [104], *Phellinus pini* [90], *Pleurotus tuber-regium* [228], *Polyporus umbellatus* [266,267], *Talaromyces* sp. [268], *Xylaria* sp. [259]	**antibacterial assay** (MIC 16 µg/mL against *Edwardsiella tarda* and *Micrococcus luteus*) [205], **antimalarial assay** (IC_{50} 4.5 µg/mL against *Plasmodium falciparum*) [249], **cytotoxic assay** (A549, IC_{50} 98.56 µM; HeLa, IC_{50} 53.19 µM; HepG2, IC_{50} 34.02 µM; MCF-7, IC_{50} 45.92 µM) [210], (HepG2, IC_{50} 68.32 µM; RD, IC_{50} 1.49 µM) [264], (LNCap, IC_{50} 34.7 µM; MCF-7, IC_{50} 57.5 µM; N2A, IC_{50} 20.8 µM; Saos-2, IC_{50} 27.8 µM) [85], (KB, IC_{50} 48.1 µM; NCI-H187, IC_{50} 58.8 µM) [269], (HL60, IC_{50} 30 µM; K562, IC_{50} 350 µM) [104], (KB, IC_{50} 40.9 µM; MCF-7, IC_{50} > 50 µM; NCI-H187, IC_{50} 47.9 µM; Vero, IC_{50} 49.2 µM) [249], (MDA-MB-231, IC_{50} 33 µM) [268], (A549, IC_{50} 18.8 µg/mL; XF498, IC_{50} 24.6 µg/mL) [183], (AGS, IC_{50} 56.1 µM; Hela229, IC_{50} 67 µM; Hep3B, IC_{50} 12.7 µM; HT-29, IC_{50} 18.4 µM;) [267], (HepG2, IC_{50} 10 µM) [270], (LU-1, IC_{50} 10.21 µg/mL) [271], **NO production inhibition assay** (IC_{50} 28.96 µM) [259], (IC_{50} 29.7 µM) [90]
125	*Stereum hirsutum* [17]	**cytotoxic assay** (A549, MCF-7, SMMC-7721, SW480, IC_{50} > 40 µM; HL-60, IC_{50} 34.3 µM) [17]
126	*Stereum hirsutum* [17], *Xerula furfuracea* [10]	**cytotoxic assay** (A549, HL-60, MCF-7, SMMC-7721, SW480, IC_{50} > 40 µM) [17]
127	*Apiospora montagnei* [269], *Gymnoascus reessii* [249]	**cytotoxic assay** (NCI-H187, IC_{50} 14.8 µM) [269], (KB, MCF-7, NCI-H187, Vero, IC_{50} > 50 µM) [249]
128	*Polyporus ellisii* [198]	**HNE inhibitory assay** (IC_{50} 55.2 µM) [198]
129	*Phomopsis* sp. [202], *Polyporus ellisii* [184], *Talaromyces stipitatus* [204]	**α-glucosidase inhibition assay** (IC_{50} > 100 µM) [202], **cytotoxic assay** (Hep3B, IC_{50} 36.27 µM; HepG2, IC_{50} 36.51 µM) [204]
130	*Tricholoma imbricatum* [245]	**cytotoxic assay** (A549, IC_{50} 22.8 µM; SMMC-7721, IC_{50} 19.5 µM) [245]

Attempts were made to study the mechanism of its action. A strong anticancer effect of **124** to HepG2 cells was associated with the induction of G2/M cell cycle arrest and apoptosis in a caspase-dependent manner [270].

Wang et al. studied the effect of ergone (**124**) on lipopolysaccharide-induced acute lung injury [272]. Pretreatment of mice with **124** was found to reduce neutrophil recruitment, regulate the release of inflammatory cytokines, reduce pulmonary edema, and correct pulmonary insufficiency. The observed effects were associated with inhibition of the NLRP3 signaling pathway.

Ergone (**124**) was found to inhibit signaling pathways STAT3 and Src in head and neck cancer-initiating cells [263] that results in the reduction of their stemness properties and tumorigenicity and is of interest for the treatment of head and neck squamous cell carcinoma.

The variety of pharmacological activities prompted scientists to study pharmacokinetic properties of ergone. Fan et al. investigated the interactions between ergone and human serum albumin [273]. The latter is a carrier protein for many endogenous and exogenous molecules in blood and greatly affects the pharmacokinetics of drugs. Fluorescence spectroscopy revealed the binding of ergone to albumin, in which hydrogen bonds and hydrophobic interactions play a dominant role.

The following pharmacokinetic parameters were measured after a single oral administration (20 mg/kg) of ergone to rats: the area under the plasma concentration versus time curve from time 0 h to indefinite time ($AUC_{0-\infty}$) was 19.6 μg h mL^{-1}, peak plasma concentration (C_{max}) was 1.5 μg/mL, the elimination half-life ($t_{1/2}$) was 5.90 h, and time to C_{max} (T_{max}) was 3.8 h [266].

To improve the therapeutic effect of ergone, several drug delivery systems has been proposed [274,275]. The folate receptor is known to be overexpressed in a wide variety of cancers, which is the basis for the development of tumor-targeted drug delivery systems. One of them uses the most abundant protein in plasma, albumin. Folate-modified ergone bovine serum albumin nanoparticles showed increased cellular uptake, targeting ability and cytotoxicity toward KB cells [274]. An in vivo experiment showed a higher antitumor effect and less toxicity of ergone nanoparticles compared to free ergone. Another delivery system was based on the encapsulation of ergone in PEGylated liposomes [275]. Pharmacokinetic studies have shown that encapsulation provides a longer residence time of ergone in the blood, which leads to a more effective in vivo antitumor effect.

8. Fungal Steroids with a Transformed Side Chain

The metabolic transformations of the ergosterol side chain are not as diverse as those of the tetracyclic skeleton. As a rule, they include hydrogenation of the Δ^{22}-double bond, its epoxidation, and hydroxylation of the terminal fragment (in most cases at C-25), as well as subsequent secondary transformations of the introduced functional groups.

Many steroids of this class of ergostanes are 25-hydroxy derivatives (Figure 15). Compounds **131–140** were tested in inflammatory, cytotoxic, and antibacterial assays, but showed no particular activity (Table 6).

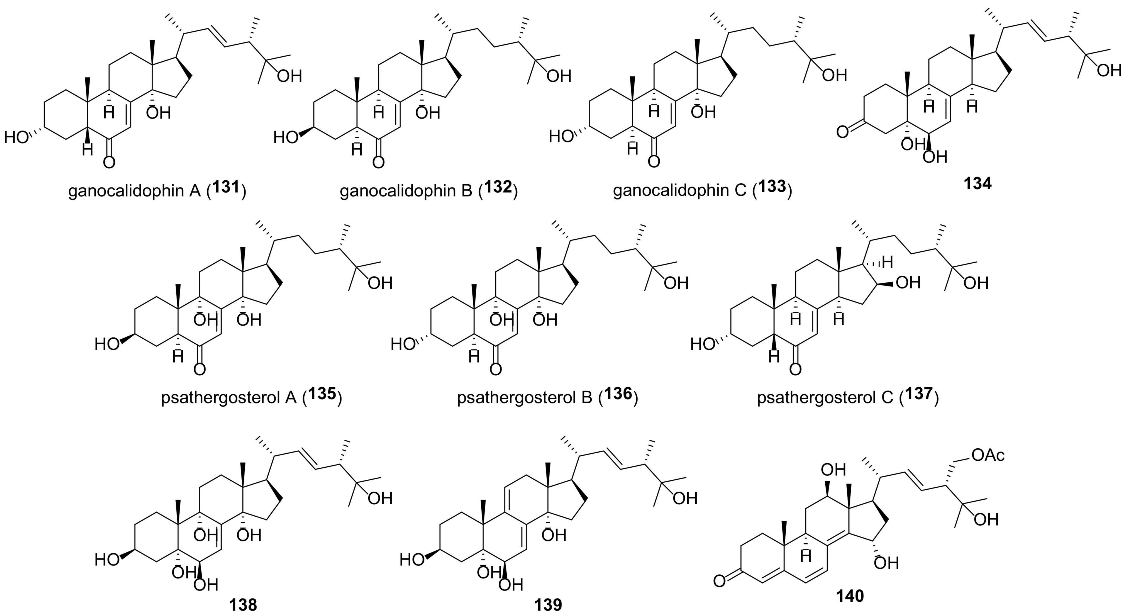

Figure 15. Structures of fungal 25-hydroxy steroids.

The epoxide **143** (Figure 16) was isolated from a halotolerant fungus *Aspergillus flocculosus* PT05-1 cultured in a hypersaline medium [13]. It exhibited a moderate antibacterial and antifungal activity and a weak cytotoxicity against HL-60 and BEL-7402 cell lines.

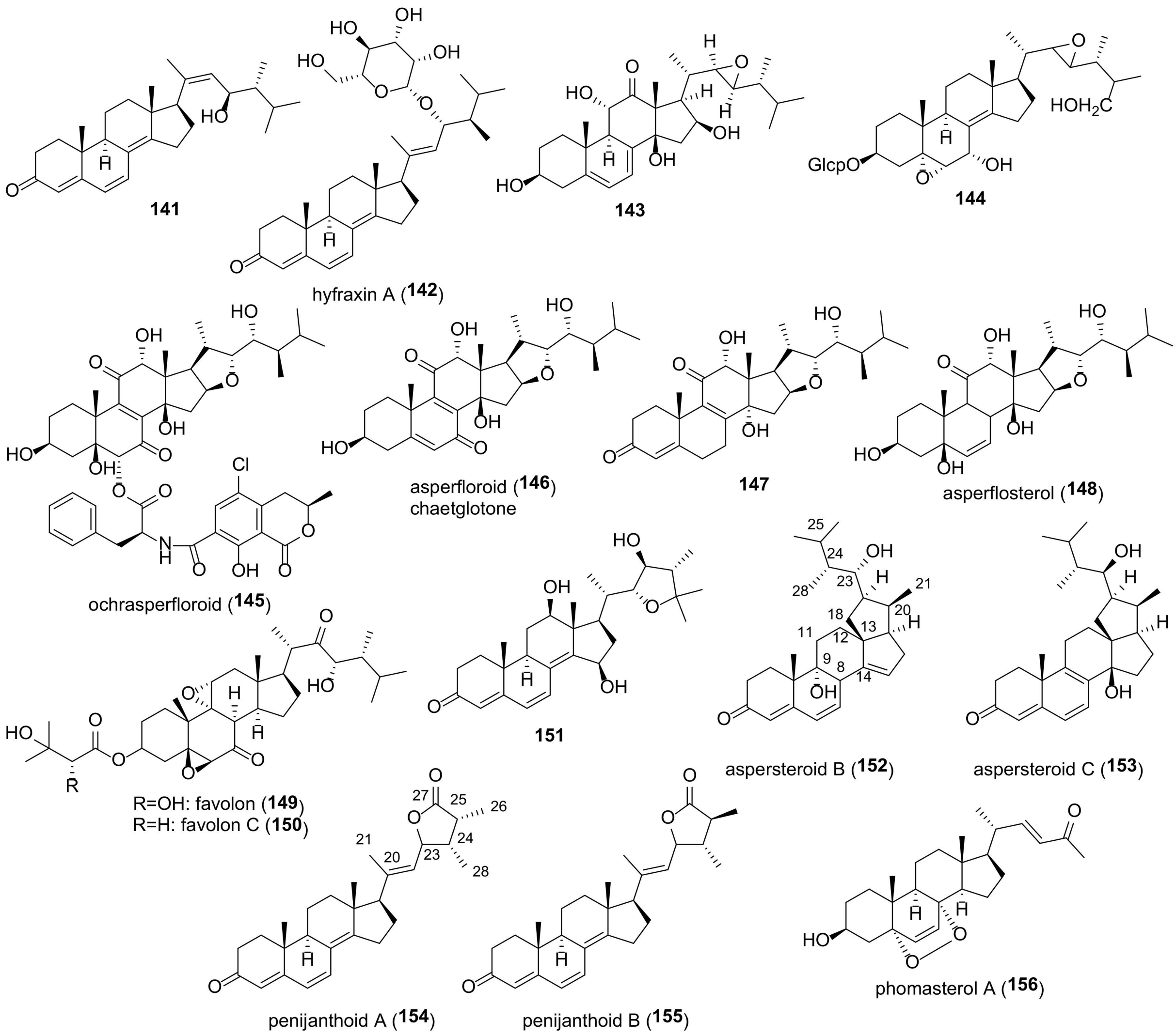

Figure 16. Structures of steroids with a transformed side chain.

An ochratoxin-ergosteroid heterodimer, ochrasperfloroid (**145**), was isolated from the sponge-derived fungus *Aspergillus flocculosus* 16D-1 [276]. It showed potent inhibitory effects on IL-6 production in LPS-induced cells and NO production in LPS-activated macrophages (Table 6). Fungi of *Aspergillus* genus have been the source of three more steroids with the same side chain, including asperfloroid (**146**) [277], asperflosterol (**148**) [278], and compound **147** [279]. Anti-inflammatory properties were identified for asperfloroid (**146**) and asperflosterol (**148**) (Table 6).

Three 18,22-cyclosterols, including aspersteroid B (**152**) and aspersteroid C (**153**), were isolated from the culture extract of *Aspergillus ustus* NRRL 275 [280]. Both compounds exhibited no cytotoxicity against MCF-7, HeLa, A549, and HT-29 cells. When analyzing the immunosuppressive effect on the proliferation of T- and B-lymphocytes in vitro, they showed activity from moderate to weak.

Two bis-epoxides, favolon (**149**) and favolon C (**150**), were isolated from the cultures of basidiomycete *Favolaschia calocera* BCC 36684 [281]. They were evaluated for a number of activities such as antimalarial, antitubercular, cytotoxic, but a positive result was obtained only in the antifungal assay.

A pair of steroidal epimers, penijanthoids A and B (**154** and **155**), were isolated from the marine-derived fungus *Penicillium janthinellum* [246]. Both compounds showed weak anti-*Vibrio* activity against three pathogenic *Vibrio* spp.

Table 6. Sources and biological activity of fungal steroids with a transformed side chain.

Compound	Fungal Source [Ref.]	Assays (Activity) [Ref.]
131	*Ganoderma sinense* [196]	**NO production inhibition assay** (IC_{50} 17.7 µM) [196]
132	*Ganoderma sinense* [196]	**NO production inhibition assay** (IC_{50} 32.4 µM) [196]
133	*Ganoderma sinense* [196]	**NO production inhibition assay** (IC_{50} 19.8 µM) [196]
134	*Fusarium chlamydosporum* [218]	**lipoxygenase inhibitory assay** (IC_{50} 7.23 µM) [218]
136	*Psathyrella candolleana* [251]	**cytotoxic assay** (A549, HL-60, MCF-7, SMMC-7721, SW480, IC_{50} > 40 µM) [251]
136	*Psathyrella candolleana* [251]	**cytotoxic assay** (A549, IC_{50} 23.4 µM; HL-60, IC_{50} 32.3 µM; MCF-7, IC_{50} 28.3 µM) [251]
137	*Psathyrella candolleana* [251]	**cytotoxic assay** (MCF-7, IC_{50} 22.3 µM; SMMC-7721, IC_{50} 29.3 µM) [251]
138	*Conocybe siliginea* [282]	**NO production inhibition assay** (IC_{50} > 40 µM) [282]
139	*Conocybe siliginea* [282]	**NO production inhibition assay** (IC_{50} > 40 µM) [282]
140	*Aspergillus alabamensis* [283]	**antimicrobial assay** (MIC 32 µg/mL against *Edwardsiella ictaluri*, MIC 64 µg/mL against *Vibrio alginolyticus*) [283]
141	*Mahonia fortune* [265]	**antibacterial assay** (MIC 100 µg/mL against *Staphylococcus aureus*) [265]
142	*Hymenoscyphus fraxineus* [284]	**antibacterial assay** (MIC 16.7 µg/mL against *Bacillus subtilis*, *Micrococcus luteus* and *Staphylococcus aureus*) [284], **cytotoxic assay** (L929, IC_{50} 24 µg/mL) [284]
143	*Aspergillus flocculosus* [13]	**antibacterial assay** (MIC 3.3 µg/mL against *Candida albicans*, 3.3 µg/mL against *Pseudomonas aeruginosa*, 1.6 µg/mL against *Enterobacter aerogenes*) [13]
144	*Trichoderma* sp. [230]	**HIV-inhibitory assay** (IC_{50} 41.6 µM) [230], **NO production inhibition assay** (10% inhibition at 10 µM) [230]
145	*Aspergillus flocculosus* [276]	**cytotoxic assay** (A549, IC_{50} 55.0 µM; HepG2, IC_{50} 23.6 µM) [276], **IL-6 immune-suppressive activity assay** (IC_{50} 2.02 µM) [276], **NO inhibitory activity assay** (IC_{50} 1.11 µM) [276]
146	*Aspergillus flocculosus* [277], *Chaetomium globosum* [285]	**cytotoxic assay** (A549, HepG2, THP-1, IC_{50} > 80 µM) [277], **IL-6 immune-suppressive activity assay** (IC_{50} 22 µM) [277]
147	*Aspergillus* sp. [279]	**antiviral assay** (no activity against H3N2 and EV71 viruses) [279]
148	*Aspergillus flocculosus* [278]	**cytotoxic assay** (A549, HepG2, THP-1, IC_{50} > 80 µM) [278], **IL-6 immune-suppressive activity assay** (IC_{50} 24 µM), **TNF-α secretion assay** (IC_{50} 28 µM) [278]
149	*Favolaschia calocera* [281]	**antifungal assay** (active in the agar diffusion test) [281]
150	*Favolaschia calocera* [281]	**antifungal assay** (active in the agar diffusion test) [281]
151	*Albatrellus confluens* [286]	**cytotoxic assay** (HL-60, PANC-1, A549, SK-BR-3, SMMC-7721, no activity) [286]
152	*Aspergillus ustus* [280]	**immunosuppressive assay** (ConA-induced T-cell proliferation, IC_{50} 22.49 µM; LPS-induced B-cell proliferation, IC_{50} 22.49 µM) [280]
153	*Aspergillus ustus* [280]	**immunosuppressive assay** (ConA-induced T-cell proliferation, IC_{50} 69.68 µM; LPS-induced B-cell proliferation, IC_{50} 69.68 µM) [280]
154	*Penicillium janthinellum* [246]	**antibacterial assay** (MICs 25.0–50.0 µM against three pathogenic *Vibrio* spp.) [246]
155	*Penicillium janthinellum* [246]	**antibacterial assay** (MICs 25.0–50.0 µM against three pathogenic *Vibrio* spp.) [246]
156	*Phoma* sp. [287]	**PTP inhibitory activity assay** (PTP1B, IC_{50} 25 µM each) [287]

9. Ergostanes with a Rearranged Tetracyclic Skeleton

Due to their intriguing structural complexity and promising biological activities, ergostanes with a rearranged tetracyclic carbon skeleton have become very attractive targets for chemists and biologists. A recent review [23] has covered this area quite thoroughly, but for consistency and completeness some results will be briefly discussed here.

Most ergostanes with a modified skeleton are highly functionalized compounds bearing three and more functional groups. A certain exception are aromatic 1(10→6)abeo-ergostane-type steroids **157–160** (Figure 17). Two of them, **157** and **158**, exhibited significant cytotoxicity toward murine colorectal CT26 and human leukemia K562 cancer cell lines (Table 7). Citreoanthrasteroid B (**158**) was also tested for the neuroprotective effects on PC12 cells injured by glutamate (15 mM) [288]. Compound **158** showed potential neuroprotective activities by inhibiting the death of injured PC12 cells with EC_{50} value of 24.2 μM.

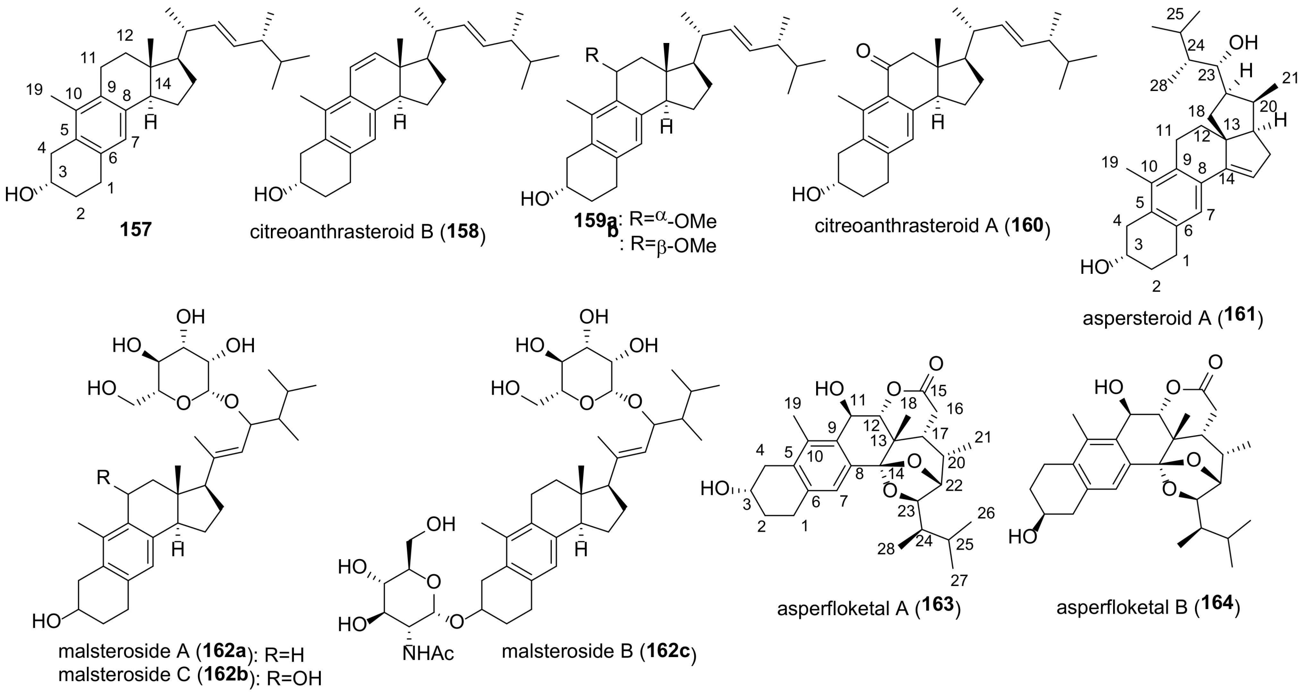

Figure 17. Structures of 1(10→6)abeo-ergostane-type steroids.

Another 1(10→6)abeo-steroid, aspersteroid A (**161**), was isolated from the culture extract of *Aspergillus ustus* [280]. It exhibited moderate cytotoxicity on four cancer cell lines, antimicrobial activity against Gram-negative and Gram-positive bacteria and immunosuppressive activities against the proliferation of T and B lymphocyte cells in vitro (Table 7).

Three anthrasteroid glycosides, malsterosides A-C (**162a–c**), were isolated from the fungus *Malbranchea filamentosa* [289]. The sugar moiety in the side chain of all glycosides was found to be D-mannose and the glycoside **162c** contained N-acetyl-D-glucosamine at the C-3 position. Cytotoxicity studies were performed with the A549 and Hela cancer cell lines. A moderate cytotoxicity in both lines was noted for malsteroside A (**162a**).

Two 1(10→6)-abeo-14,15-secosteroids, asperfloketals A (**163**) and B (**164**), were found in the sponge-associated fungus *Aspergillus f locculosus* 16D-1 [290]. They exhibited no cytotoxicity against three tested cancer cell lines. Promising results were obtained in anti-inflammatory assays. Compounds **163** and **164** displayed stronger activity in the $CuSO_4$-induced transgenic fluorescent zebrafish than ibuprofen used as a positive control.

A-nor-B-homo steroid **165** (Figure 18) containing a 10(5→4)-abeo-ergostane fragment was isolated from culture of basidiomycete *Polyporus ellisii* [184] and from the mangrove-derived fungus *Phomopsis* sp. MGF222 [202]. Compound **165** exhibited inhibitory activities against four out of five human cancer cell lines tested except A549 [184] (Table 7). It was also tested for the antibacterial activities against seven pathogenic bacteria and for the inhibitory activities against α-glucosidase, but no effect was observed [202].

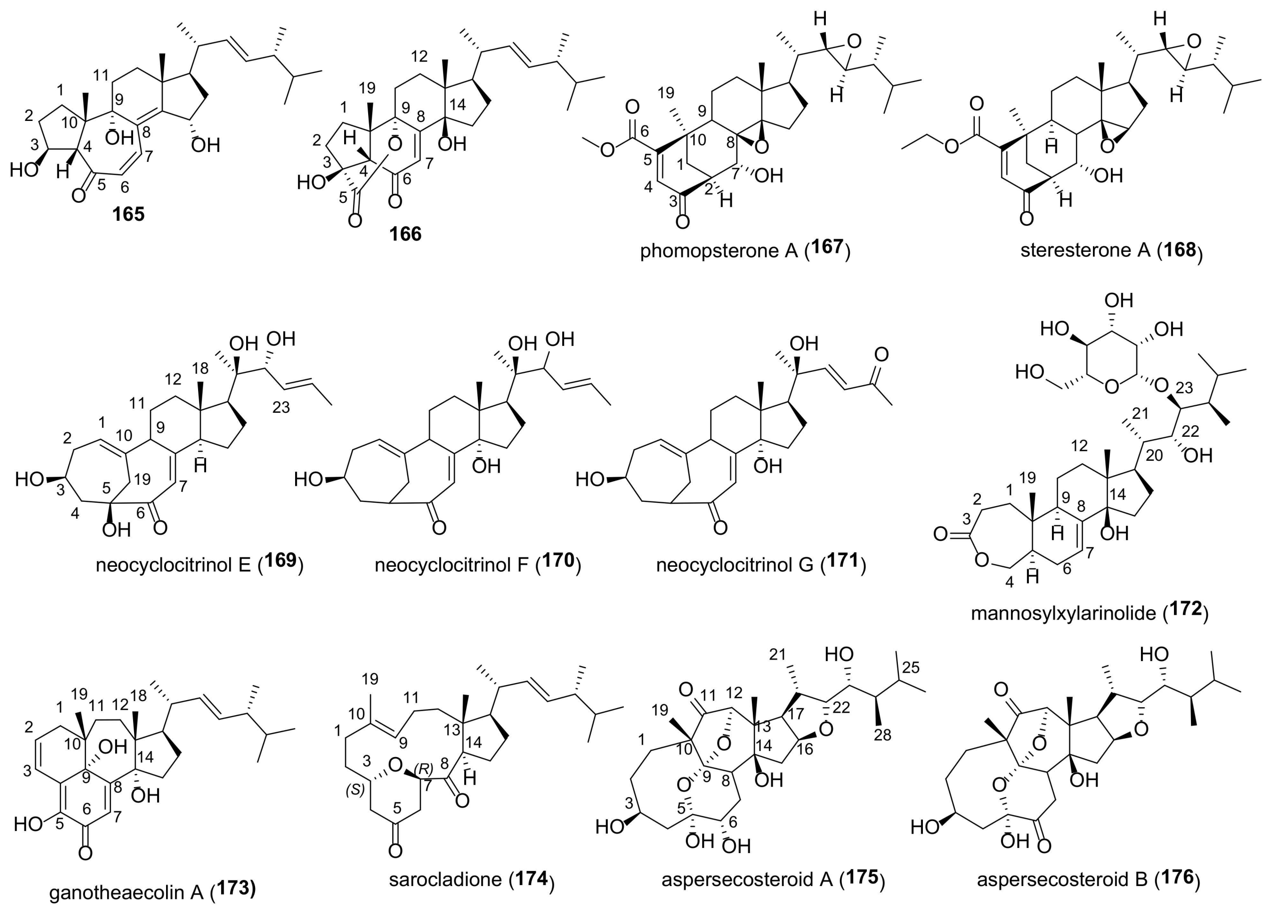

Figure 18. Structures of ergostanes with a rearranged A-ring.

Another A-nor steroid **166** was isolated from the fungus of *Lasiodiplodia pseudotheobromae* [11]. A distinguished structural feature of this compound is an additional δ-lactone ring between C-3 and C-9.

Two nearly identical steroids **167** and **168** featured a bicyclo[3.3.1]nonane motif were discovered in the fungi *Phomopsis* sp. TJ507A [7] and *Stereum hirsutum* [17]. The only difference in their structures is the presence of a methoxy group in phomopsterone A (**167**) instead of an ethoxy one in steresterone A (**168**). Compound **167** was tested for NO inhibitory activity. Steresterone A (**168**) was evaluated for the cytotoxicity against five human cancer cell lines. Both compounds showed no activity in the respective tests.

Three C25 steroids, neocyclocitrinols E-G (**169–171**) were isolated from endophytic fungus *Chaetomium* sp. M453 [189]. All compounds were tested for AChE inhibitory activities and cytotoxicity, however, no effect was found.

Cheng et al. isolated from *Ganoderma theaecolum* ganotheaecolin A (**173**), having a naphtho[1,8-ef]azulene ring system steroid [291]. At a concentration of 10 μM, it showed activity to promote neurite growth in PC12 cells, comparable to that of nerve growth factor used as control.

A new steroid sarocladione (**174**) bearing a 5,10:8,9-diseco moiety was isolated from the deep-sea-derived fungus *Sarocladium kiliense* [292]. The initially proposed configuration at C-3 and C-7 proved to be incorrect and was revised to 3*S*,7*R* through the chemical synthesis [293]. Cytotoxic studies of compound **174** revealed no apparent cellular toxicities.

Lin et al. isolated from the sponge-derived fungus *Aspergillus flocculosus* 16D-1 two 11(9→10)-*abeo*-5,10-secosteroids, aspersecosteroids A (**175**) and B (**176**) [278], a characteristic structural feature of which was the presence of a dioxatetraheterocyclic ring system. Both compounds were non-cytotoxic at the concentrations up to 40 μM and showed a strong inhibitory effect on the production of TNF-α and IL-6.

Spiroseoflosterol (**177**) (Figure 19), having a unique spiro[4.5]decan-6-one moiety, was isolated from the fruiting bodies of *Butyriboletus roseoflavus* [294]. It showed a strong cytotoxic effect on HepG2 cell line (IC_{50} 9.1 μM), which was comparable to that of sorafenib (IC_{50} 5.5 μM) used as a positive control. Moreover, spiroseoflosterol (**177**) was active against sorafenib-resistant Huh7/S cells with an IC_{50} value of 6.2 μM, that makes it a promising candidate for antihepatoma drug development.

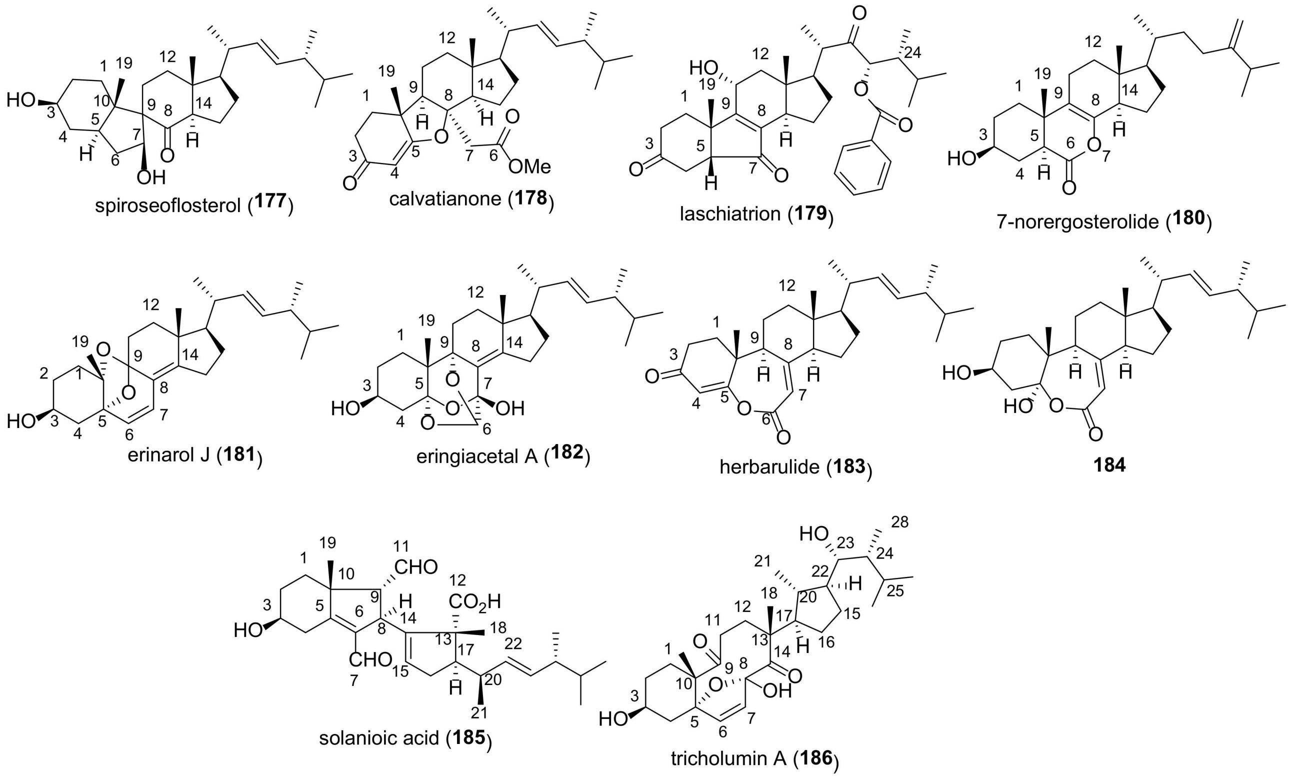

Figure 19. Structures of ergostanes with a rearranged B-ring.

Calvatianone (**178**), featuring a contracted tetrahydrofuran B-ring, was found in a rare mushroom *Calvatia nipponica* [126]. It showed a weak cytotoxicity against MCF-7 with IC_{50} > 100 μM (Table 7).

Another compound with a five-membered B ring, laschiatrion (**179**), was isolated from fermentations of *Favolaschia* sp. [281,295]. It was not active in antibacterial and cytotoxic assays, but exhibited antifungal activity in the agar diffusion test [281].

7-Nor-ergosterolide (**180**), featuring a pentalactone B-ring system, was found in the culture extract of an endophytic fungus *Aspergillus ochraceus* EN-31 [296] and a halotolerant fungus *Aspergillus flocculosus* PT05-1 [13]. Compound **180** showed pronounced cytotoxic and antibacterial properties.

A characteristic structural feature of erinarol J (**181**), isolated from the dried fruiting bodies of *Hericium erinaceum*, is the presence of 6,8-dioxabicyclo[3.2.1]oct-2-ene moiety [187]. Biotests have shown potent anti-inflammatory activity of **181** due to the inhibition of TNF-α secretion and NO production.

The first natural 5,6-secosteroid, eringiacetal A (**182**), was isolated from the fruiting bodies of mushroom *Pleurotus eryngii* [250]. Biological assays showed its modest cytotoxicity and ability to inhibit NO production.

Herbarulide (**183**) was first isolated from the endophytic fungus *Pleospora herbarum* as a compound having a campestane side chain [297]. Later the same structure was assigned to one of the constituents of the Taiwanese fungus *Antrodia camphorate* [298]. The correct structure of herbarulide (**183**) was proposed by Chen and Liu who isolated it from the fungus *Stereum hirsutum* [17]. The assignment was based rather on the assumption that the C-24 stereocenter of the starting ergosterol will remain unchanged during the transformations in the cyclic part. Finally, the correct structure of **183** was confirmed by its chemical synthesis [299]. Compound **184**, structurally very close to herbarulide (**183**), was isolated from the fruiting bodies of *Ganoderma resinaceum* [103].

Solanioic acid (**185**) is a degraded and rearranged steroid isolated from laboratory cultures of the fungus *Rhizoctonia solani* [300]. An important feature of its biological activity is antibacterial effect against methicillin-resistant *Staphylococcus aureus*. The latter is a cause of infection that is difficult to treat due to resistance to many antibiotics.

Tricholumin A (**186**) was isolated from the alga-endophytic fungus *Trichoderma asperellum* [301]. The only structural element of the parent ergosterol that remained after a number of metabolic stages of its biosynthesis is cycle A. The rest of the molecule, including a fragment of the side chain, has undergone deep transformations. Inhibitory properties of **186** against harmful microalgae and weak antibacterial activity against five aquatic pathogens were found.

Dankasterone A (**187**) (Figure 20) was first isolated from a fungal strain of *Gymnascella dankaliensis* derived from the sponge *Halichondria japonica* [302]. The initial erroneous assignment of stereochemistry at C-24 was corrected from *S* to *R* in a follow-up work by these authors [303]. Subsequently, compound **187** was repeatedly isolated from fungal sources as one of the ergostane constituents (Table 7). The only structural difference between **187** and dankasterone B (**188**) is the saturated ring A. From the endophytic fungus *Phomopsis* sp. TJ507A was also isolated phomopsterone B (**190**) differing from **187** by the presence of a methyl group at C-23 [7]. Dankasterone A (**187**) showed promising anticancer activities with IC_{50} down to 2.3 μM on a range of cancer cell lines (Table 7). Structure activity relationship studies of dankasterones A and B showed that the Δ^4-double bond is essential for high cytotoxicity against the cancer cell lines tested. Carbonyl groups in dankasterone B (**188**) were other structural elements important for the high biological activity, because products of its $NaBH_4$ reduction were not cytotoxic [17]. Phomopsterone B (**190**) was tested for inflammatory activity and showed promising results in iNOS inhibitory and NO production inhibition assays [7].

At first glance, the carbon skeleton of periconiastone A (**189**) [304] looks completely different from that of dankasterone B (**188**). In fact, compound **189** is available from **188** in one step via the intramolecular aldol reaction [305], which is also evidently realized in the course of its biosynthesis. So far, periconiastone A (**189**) has been tested for anti-inflammatory and antibacterial activities. Positive results were obtained in an antibacterial assay against Gram-positive bacteria [304].

An 8,14-seco-steroid, childinasterone A (**191**), was isolated from fruiting bodies of the ascomycete *Daldinia childiae* [306]. It showed no activity in cytotoxic studies and exhibited strong inhibition of NO production (IC_{50} value of 21.2 μM versus 41.5 μM for L-NMMA used as a positive control).

9,11-Secosteroids are quite common in sea sponges [22], but rather rare in fungal sources. The first such an ergostane **192** was isolated from king trumpet mushroom *Pleurotus eryngii* [6]. Compound **192** exhibited NO inhibitory activity similar to that of L-NMMA and revealed no cytotoxicity. Another 9,11-secoergostane (**193**), found in the fruiting bodies of *Pleurotus eryngii*, displayed similar profile of biological activity [6].

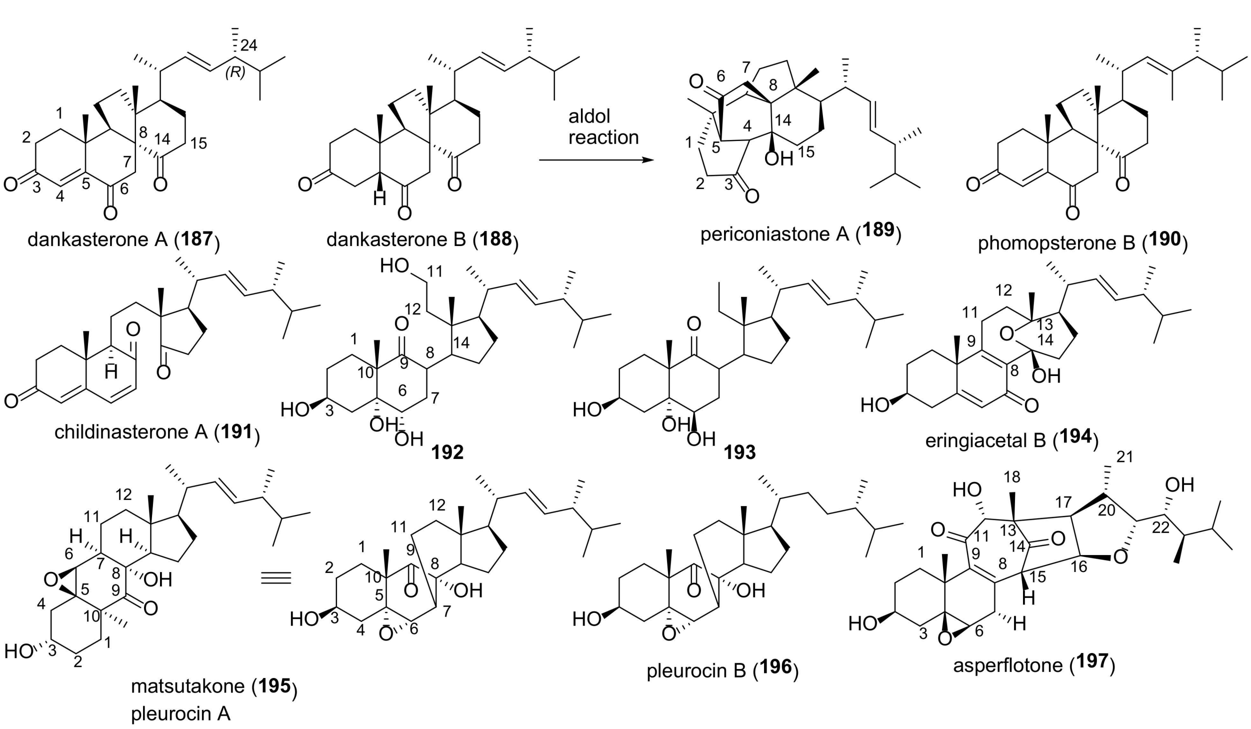

Figure 20. Structures of ergostanes with a rearranged C-ring.

Three steroids with a rearranged ring B, eringiacetal B (**194**), matsutakone (**195**), and pleurocin B (**196**), were isolated from the fruiting bodies of *Pleurotus eryngii* by Tanaka et al. [248]. All three compounds revealed inhibitory activity on production of NO which was stronger than that of L-NMMA. The 13,14-seco-13,14-epoxysteroid, eringiacetal B (**194**), was most active with an IC_{50} of 13.0 μM compared to 23.9 μM for the L-NMMA positive control.

An 8(14→15)-abeo-steroid, asperflotone (**197**), was obtained from the solid culture of *Aspergillus flocculosus* 16D-1 [277]. Its characteristic structural feature is a rearranged bicyclo[4.2.1]non-2-ene ring system. Compound **197** was tested on three cancer cell lines with no cytotoxic effects. In immune-suppressive activity assay, asperflotone (**197**) exhibited inhibitory effects on IL-6 secretion.

The 15(14→22)abeo-steroid framework is common for ergostanes **198–203** (Figure 21), collectively referred to as strophasterols. It took some effort to establish the correct structures of these structurally related compounds. Strophasterols A–D (**198–201**) were first isolated from the mushroom *Stropharia rugosoannulata* [307]. The structure of strophasterin A (**198**) was established by X-ray crystallographic analysis. Comparison of the NMR data made it possible to assign the structure of **199** as the C-22 isomer of strophasterol A that was later confirmed by X-ray analysis [193]. Structure of strophasterol C (**200**) was proposed based on NOE correlations by Aung et al., who isolated it from the basidiomycete *Cortinarius glaucopus* together with glaucoposterol A (**203**) [195]. Additional evidence for the structure of **200** was obtained by its chemical synthesis [308]. Two more steroids with a strophastane skeleton, strophasterol E (**202**) and strophasterol F (**203**), were isolated from the fruiting bodies of *Pleurotus eryngii* [201]. Their structures were determined by X-ray analysis of the corresponding tris-p-bromobenzoate derivatives. Structural elucidation of strophasterol D (**201**) was done by comparing it with a synthetically prepared sample [309]. This work also showed that glaucoposterol A and strophasterol F are the same compound (**203**).

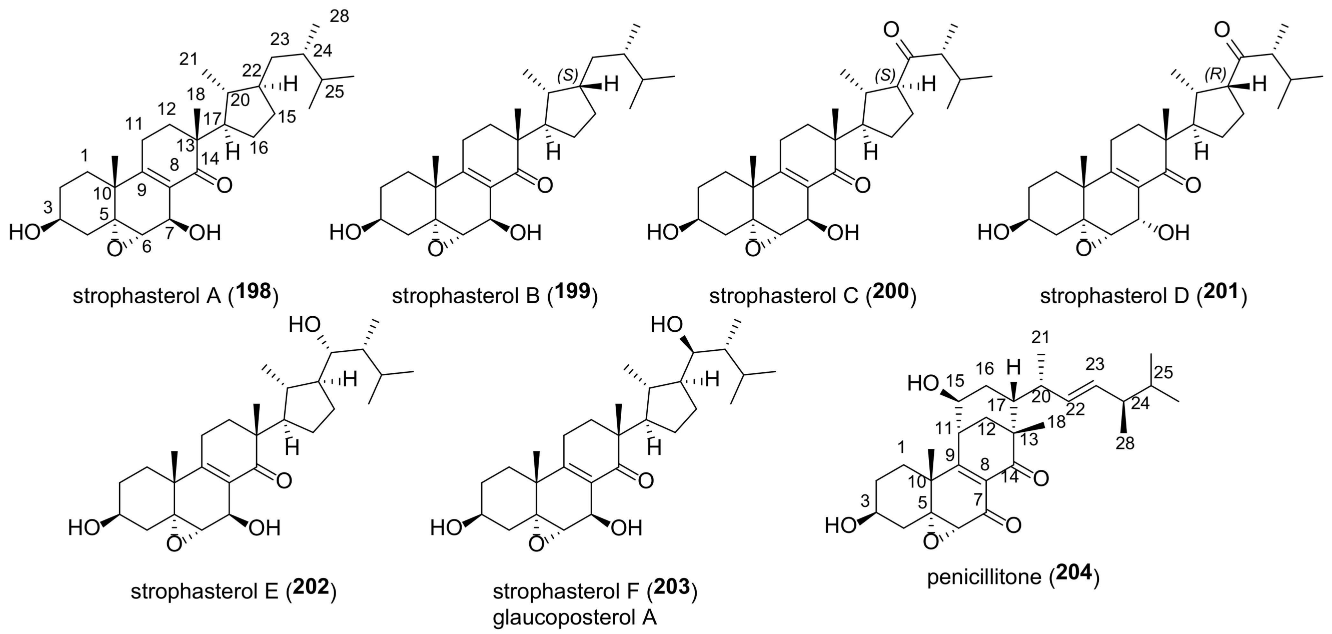

Figure 21. Structures of ergostanes with a rearranged D-ring.

So far, the biological activity of strophasterols has been studied only marginally. Strophasterol A (**198**) showed a dose-dependent inhibitory effect on the toxicity of thapsigargin. The latter is known to disrupt the balance of the Ca^{2+} concentration in the endoplasmic reticulum that is especially harmful to neuronal cells. Under the action of strophasterol A (**198**), an increase in cell viability by 10.3% compared with the control was noted [307]. Strophasterols E and F were tested for anti-inflammatory activity, but showed no promising results [201].

A 15(14→11)-abeo-ergostane, penicillitone (**204**), was isolated from the culture of the fungus *Penicillium purpurogenum* SC0070 [254]. It was evaluated for cytotoxicity against three cancer lines and showed good potency with IC_{50} ranging from 4.44 to 5.98 μM. In addition, compound **204** was active in the inflammatory assay on the production of TNF-α and IL-6. At the concentration of 5 μM it reduced their secretion by 70.7% and 96.6%, respectively. For comparison, inhibition rates of the positive control dexamethasone at 100 μM were 87.3% and 96.7%, respectively. This makes promising further in-depth study of penicillitone (**204**) as an anti-inflammatory or antitumor agent.

Table 7. Sources and biological activity of fungal steroids with a rearranged tetracyclic carbon skeleton.

Compound	Fungal Source [Ref.]	Assays (Activity) [Ref.]
157	*Antrodia camphorata* [310], *Aspergillus ustus* [231], *Gibberella zeae* [311]	**cytotoxic assay** (CT26, IC_{50} 15.3 μM; K562, IC_{50} 19.9 μM) [310]
158	*Antrodia camphorata* [310], *Penicillium citreo-viride* [312], *Phyllosticta capitalensis* [288]	**cytotoxic assay** (CT26, IC_{50} 18.2 μM; K562, IC_{50} 12.5 μM) [310], **neuroprotective activity assay** (EC_{50} 24.2 μM) [288]
159a	*Aspergillus ustus* [231]	
159b	*Aspergillus ustus* [231]	
160	*Penicillium citreo-viride* [312]	
161	*Aspergillus ustus* [280]	**antimicrobial assay** (*Candida albicans*, MIC_{50} 17.24 μg/mL; *Escherichia coli*, MIC_{50} 17.24 μg/mL; *Staphylococcus aureus*, MIC_{50} 15.51 μg/mL) [280], **cytotoxic assay** (A549, IC_{50} 40.32 μM; Hela, IC_{50} 26.09 μM; HT-29, IC_{50} 43.58 μM; MCF-7, IC_{50} 32.03 μM) [280], **immunosuppressive assay** (ConA-induced T-cell proliferation, IC_{50} 23.61 μM; LPS-induced B-cell proliferation, IC_{50} 23.61 μM) [280]
162a	*Malbranchea filamentosa* [289]	**cytotoxic assay** (A549, IC_{50} 38.6 μM; Hela, IC_{50} 28.1 μM) [289]
162b	*Malbranchea filamentosa* [289]	**cytotoxic assay (A549, Hela, no activity) [289]**
162c	*Malbranchea filamentosa* [289]	**cytotoxic assay (Hela, IC50 76.9 μM) [289]**
163	*Aspergillus flocculosus* [290]	**anti-inflammatory assay [290]**
164	*Aspergillus flocculosus* [290]	**anti-inflammatory assay** [290]
165	*Phomopsis* sp. [202], *Polyporus ellisii* [184]	**α-glucosidase inhibition assay** (IC_{50} > 100 μM) [202], **cytotoxic assay** (A549, IC_{50} > 40 μM; HL-60, IC_{50} 17.1 μM; MCF-7, IC_{50} 23.3 μM; SMMC-7721, IC_{50} 21.3 μM; SW480, IC_{50} 16.3 μM) [184]
166	*Lasiodiplodia pseudotheobromae* [11]	
167	*Phomopsis* sp. [7]	**NO production inhibition assay** (IC_{50} > 25 μM) [7]
168	*Stereum hirsutum* [17]	**cytotoxic assay** (A549, HL-60, MCF-7, SMMC-7721, SW480, IC_{50} > 40 μM) [17]
169	*Chaetomium* sp. [189]	**cytotoxic assay** (A549, HL-60, MCF-7, SMMC-7721, SW480, IC_{50} > 40 μM) [189]
170	*Chaetomium* sp. [189]	**cytotoxic assay** (A549, HL-60, MCF-7, SMMC-7721, SW480, IC_{50} > 40 μM) [189]
171	*Chaetomium* sp. [189]	**cytotoxic assay** (A549, HL-60, MCF-7, SMMC-7721, SW480, IC_{50} > 40 μM) [189]
172	*Xylaria* sp. [313]	
173	*Ganoderma theaecolum* [291]	**neurite outgrowth-promoting assay in PC12 cells** (stimulated cell differentiation with a maximum effect at 10 μM) [291]
174	*Sarocladium kiliense* [292]	**cytotoxic assay** (Bel-7402, ECA-109, HeLa, PANC-1, SHG-44, no activity) [292]
175	*Aspergillus flocculosus* [278]	**cytotoxic assay** (A549, HepG2, THP-1, IC_{50} > 80 μM) [278], **IL-6 immune-suppressive activity assay** (IC_{50} 21 μM), **TNF-α secretion assay** (IC_{50} 28 μM) [278]
176	*Aspergillus flocculosus* [278]	**cytotoxic assay** (A549, HepG2, THP-1, IC_{50} > 80 μM) [278], **IL-6 immune-suppressive activity assay** (IC_{50} 26 μM), **TNF-α secretion assay** (IC_{50} 31 μM) [278]
177	*Butyriboletus roseoflavus* [294]	**cytotoxic assay** (HepG2, IC_{50} 9.1 μM; Huh7/S, IC_{50} 6.2 μM; L02, IC_{50} 22.8 μM) [294]
178	*Calvatia nipponica* [126]	**cytotoxic assay** (MCF-7, IC_{50} > 100 μM) [126]
179	*Favolaschia calocera* [281], *Favolaschia* sp. [295]	**antifungal assay** (activity against *Candida albicans*, *Cryptococcus neoformans*, etc. at concentrations of 10–50 μg/mL) [295]
180	*Aspergillus flocculosus* [13], *Aspergillus ochraceus* [296]	**antibacterial assay** (MIC 1.9 μg/mL against *Candida albicans*, 7.5 μg/mL against *Pseudomonas aeruginosa* and *Enterobacter aerogenes*) [13], **cytotoxic assay** (BEL-7402, IC_{50} 17.7 μM; HL-60, IC_{50} 12.4 μM) [13], (NCI-H460, IC_{50} 5.0 μg/mL; SMMC-7721, IC_{50} 7.0 μg/mL; SW1990, IC_{50} 28.0 μg/mL) [296]

Table 7. *Cont.*

Compound	Fungal Source [Ref.]	Assays (Activity) [Ref.]
181	*Hericium erinaceum* [187]	**NO production inhibition assay** (38.4% inhibition at 10 µg/mL) [187], **TNF-α secretion assay** (43.3% inhibition at 10 µg/mL) [187]
182	*Pleurotus eryngii* [250]	**cytotoxic assay** (RAW264.7, IC_{50} 25.6 µM) [250], **NO production inhibition assay** (IC_{50} 19.9 µM) [250]
183	*Antrodia camphorate* [298], *Gymnoascus reessii* [249], *Stereum hirsutum* [17]	**cytotoxic assay** (A549, HL-60, MCF-7, SMMC-7721, SW480, IC_{50} > 40 µM) [17], (KB, MCF-7, IC_{50} > 50 µM; NCI-H187, IC_{50} 22.6 µM; Vero, IC_{50} 43.8 µM) [249]
184	*Ganoderma resinaceum* [103]	**NO production inhibition assay** (56.37% inhibition at 50 µM) [103]
185	*Rhizoctonia solani* [300]	**antibacterial assay** (MIC 1 µg/mL against the Gram-positive bacteria *Bacillus subtilis*, *Staphylococcus aureus*, and MRSA; MIC 16 µg/mL against the yeast *Candida albicans*; MIC 64 µg/mL against the Gram-negative bacteria *Escherichia coli* and *Pseudomonas aeruginosa*) [300]
186	*Trichoderma asperellum* [301]	**antibacterial assay** (against *V. harveyi*, *V. splendidus*, and *P. citrea* with inhibitory zones of 10, 7.5, and 8.0 mm, respectively, at 50 µg/disk) [301], **antifungal assay** (MIC 12 µg/mL against *Glomerella cingulate*) [301]
187	*Antrodia camphorate* [310], *Arthrinium* sp. [314], *Aspergillus penicillioides* [205], *Colletotrichum* sp. [206], *Conocybe siliginea* [315], *Gymnascella dankaliensis* [303], *Neosartorya fennelliae, N. tsunodae* [316], *Pestalotiopsis* sp. [139], *Phomopsis* sp. [7], *Pleosporales* sp. [317], *Stereum hirsutum* [17], *Talaromyces purpurogenus* [318], *Talaromyces* sp. [255]	**cytotoxic assay** (P388, ED_{50} 2.2 µg/mL) [303], (A549, IC_{50} 4.4 µM; HL-60, IC_{50} 2.3 µM; MCF-7, IC_{50} 2.7 µM; SMMC-7721, IC_{50} 3.3 µM; SW480, IC_{50} 3.5 µM) [17], (K562, IC_{50} > 20 µM; ST26, IC_{50} 6.7 µM) [310], (A549, IC_{50} 21.3 µM; HL-60, IC_{50} 7.9 µM; MCF-7, IC_{50} 23.8 µM; SMMC-7721, IC_{50} > 40 µM; SW480, IC_{50} 14.2 µM) [318], **iNOS inhibitory assay** (IC_{50} 6.58 µM) [7], **NO production inhibition assay** (IC_{50} 13.04 µM) [7]
188	*Antrodia camphorate* [310], *Calvatia nipponica* [126], *Gymnascella dankaliensis* [303], *Stereum hirsutum* [17]	**cytotoxic assay** (P388, ED_{50} 2.8 µg/mL) [303], (MCF-7, IC_{50} > 100 µM) [126], (A549, IC_{50} 16.6 µM; HL-60, IC_{50} 15.6 µM; MCF-7, IC_{50} 17.2 µM; SMMC-7721, IC_{50} 16.3 µM; SW480, IC_{50} 17.3 µM) [17], (K562, IC_{50} 23.1 µM; ST26, IC_{50} 8.4 µM) [310]
189	*Periconia* sp. [304]	**antibacterial assay** (MIC 4 µg/mL against *Staphylococcus aureus*, MIC 32 µg/mL against *Enterococcus faecalis*; MIC > 100 µg/mL against all four Gram-negative bacteria tested) [304], **NO production inhibition assay** (IC_{50} > 40 µM) [304]
190	*Phomopsis* sp. [7]	**iNOS inhibitory assay** (IC_{50} 1.49 µM) [7], **NO production inhibition assay** (IC_{50} 4.65 µM) [7]
191	*Daldinia childiae* [306]	**cytotoxic assay** (MCF-7, SMMC-7721, SW480, IC_{50} > 40 µM) [306], **NO production inhibition assay** (IC_{50} 21.2 µM) [306]
192	*Pleurotus eryngii* [6]	**NO production inhibition assay** (IC_{50} 10.3 µM) [6]
193	*Pleurotus eryngii* [201]	**NO production inhibition assay** (NO produced 57.8% at 30 µM) [201]
194	*Pleurotus eryngii* [248]	**NO production inhibition assay** (IC_{50} 13.0 µM) [248]
195	*Tricholoma matsutake* [319], *Pleurotus eryngii* [248]	**AChE inhibitory assay** (62.8% inhibition at 50 µg/mL) [319], **NO production inhibition assay** (IC_{50} 25 µM) [248]
196	*Pleurotus eryngii* [248]	**NO production inhibition assay** (IC_{50} 23.6 µM) [248]
197	*Aspergillus flocculosus* [277]	**cytotoxic assay** (A549, HepG2, THP-1, IC_{50} > 80 µM) [277], **IL-6 immune-suppressive activity assay** (IC_{50} 22 µM) [277]
198	*Stropharia rugosoannulata* [307]	
199	*Stropharia rugosoannulata* [307]	
200	*Stropharia rugosoannulata* [307]	
201	*Cortinarius glaucopus* [195], *Stropharia rugosoannulata* [307]	
202	*Pleurotus eryngii* [201]	**cytotoxic assay** (RAW 264.7, IC_{50} > 30 µM) [201]
203	*Pleurotus eryngii* [201]	**cytotoxic assay** (RAW 264.7, IC_{50} > 30 µM) [201]
204	*Penicillium purpurogenum* [254]	**cytotoxic assay** (A549, IC_{50} 5.57 µM; HepG2, IC_{50} 4.44 µM; MCF-7, IC_{50} 5.98 µM) [254], **IL-6 immune-suppressive activity assay** (96.7% inhibition at 5 µg/mL) [254], **NO production inhibition assay** (70.7% inhibition at 5 µg/mL) [254]

10. Degraded Sterols

The progressive degradation of ergostane-type steroids through 5,6- and 9,10-oxidative cleavages leads to the loss of ring A and the formation of highly degraded sterols (Figure 22). The most common and best studied among them is demethylincisterol A_3 (**206**). It demonstrated a potent activity against many cancer lines (Table 8). Cytotoxicity-guided investigation of Chinese mangrove *Rhizophora mucronata* endophytic *Pestalotiopsis* sp. yielded **206** as the most active compound with IC_{50} values reaching nanomolar order [139].

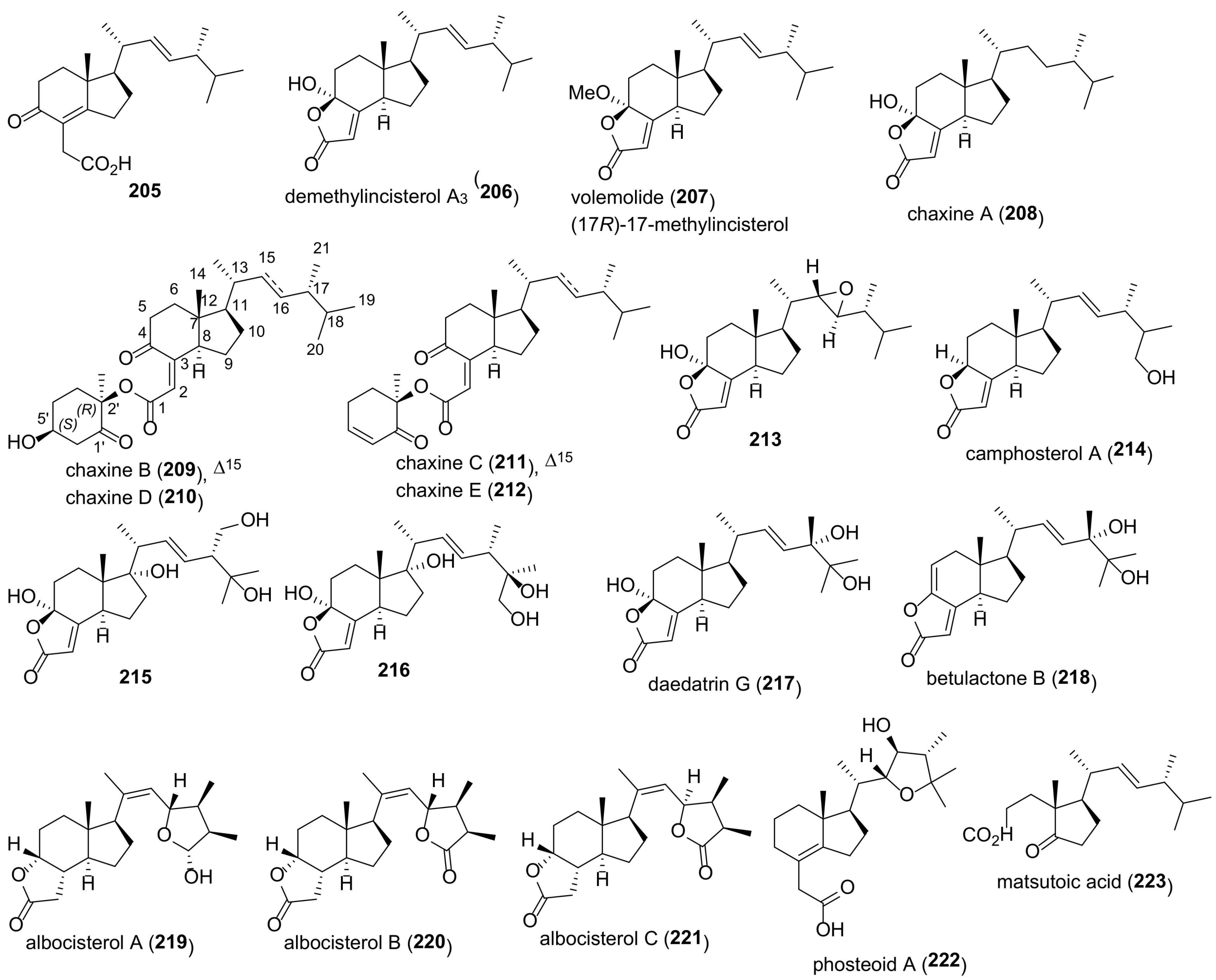

Figure 22. Structures of degraded sterols.

Luo et al. examined a collection of secondary metabolites of endophytic fungi in search for inhibitors of SH2 containing protein tyrosine phosphatase-2 (SHP2) [320]. The latter is an oncogenic phosphatase participating in many signaling cascades and identified as a potential therapeutic target for cancer. It was found that demethylincisterol A_3 (**206**) inhibited the protein tyrosine phosphatase activity of SHP2 with an IC_{50} of 6.75 μg/mL. In comparison, sodium orthovanadate used as a positive control showed an IC_{50} value of 114 μg/mL.

Demethylincisterol A_3 (**206**) revealed significant antibacterial activities against a number of pathogenic bacteria with MICs values ranging from 3.13 to 12.5 μM (MICs of the positive control ciprofloxacin varied from 0.78 to 1.56 μM) [321].

Agrocybe chaxingu extract was shown to have a very strong osteoclast suppression effect, useful in the prevention and control of osteoporosis. In search of the active components of this mushroom, Kawagishi et al. isolated a number of degraded sterols **208–212**, collectively called as chaxines [322,323]. The initially assigned 2′*S*,5′*S* stereochemistry of the A ring of chaxine B (**209**) was erroneous and was subsequently revised to 2′*R*,5′*S* [324,325]. Chaxines A-C were evaluated in the osteoclast-forming assay and were shown to suppress the rate of osteoclast formation with no cytotoxicity [322,323].

Chaxine C (**211**) was also isolated from traditional Chinese medicinal mushroom *Cordyceps jiangxiensis* under the name jiangxienone and showed promising results in inhibiting cancer cells [326]. Its IC_{50} values against A549 and SGC-7901 cells were six-fold lower than that of cisplatin.

Albocisterols A-C (**219–221**) isolated from cultures of *Antrodiella albocinnamomea* were tested for inhibitory activities against protein tyrosine phosphatase [327]. A mixture of compounds **220** and **221** exhibited significant activity with IC_{50} value of 1.1 µg/mL (IC_{50} 1.2 µg/mL for ursolic acid used as a positive control). The corresponding C-27 alcohol, albocisterol A (**219**), was inactive at 50 µg/mL.

Table 8. Sources and biological activity of fungal degraded sterols.

Compound	Fungal Source [Ref.]	Assays (Activity) [Ref.]
205	*Fusarium solani* [328]	**cytotoxic assay** (A549, HL-60, MCF-7, SMMC-7721, SW480, IC_{50} > 40 µM) [328], **COX-2 inhibitory assay** (IC_{50} > 20 µM) [328]
206	*Agrocybe chaxingu* [322], *Amauroderma amoiensis* [82], *Aspergillus* sp. [321], *Colletotrichum* sp. [206], *Gymnascella dankaliensis* [329], *Omphalia lapidescens* [16], *Pestalotiopsis* sp.[139,320], *Pleosporales* sp. [317], *Termitomyces microcarpus* [132], *Tricholoma imbricatum* [245], *Xylaria allantoidea* [330]	**AChE inhibitory assay** (<10% inhibition at 50 µg/mL) [82], **antibacterial assay** (MIC 12.5 µM against *S. aureus*, 3.13 µM against *S. epidermidis*, 3.13 µM against *B. cereus*) [321], **cytotoxic assay** (A549, IC_{50} 11.14 nM; Hela, IC_{50} 0.17 nM; HepG2, IC_{50} 14.16 nM) [139],(A549, IC_{50} 27.2 µM; HL-60, IC_{50} 18.1 µM; K562, IC_{50} 13.6 µM; MCF-7, IC_{50} 10.9 µM; SMMC-7721, IC_{50} 21.7 µM; SW480, IC_{50} 19.2 µM) [245], (GES-1, IC_{50} 7.81 µM; HGC-27, IC_{50} 51.16 µM; MDA-MB-231, IC_{50} 16.48 µM) [16], (HeLa, IC_{50} 2.24 µg/mL; HCT-116, IC_{50} 2.51 µg/mL; HT-29, IC_{50} 3.50 µg/mL; MCF-7, IC_{50} 3.77 µg/mL; Vero, IC_{50} 3.65 µg/mL) [330], (P388, ED_{50} 1.0 µg/mL) [329], **osteoclast differentiation assay** (at 4.8 µM suppressed the rate of osteoclast formation to 55%) [322], **protein tyrosine phosphatase assay** (IC_{50} 6.75 µg/mL) [320]
207	*Amauroderma amoiensis* [82], *Armillariella tabescens* [170], *Aspergillus aculeatinus* [331], *Aspergillus* sp. [332], *Pyropolyporus fomentarius* [333], *Tricholoma imbricatum* [245]	**AChE inhibitory assay** (46.3% inhibition at 50 µg/mL) [82], **cytotoxic assay** (A549, IC_{50} 7.1 µM; HL-60, IC_{50} 22.1 µM; K562, IC_{50} 17.1 µM; MCF-7, IC_{50} 18.9 µM; SMMC-7721, IC_{50} 19.3 µM; SW480, IC_{50} 16.7 µM) [245], (A549, IC_{50} 18.2 µM; HL-60, IC_{50} 23.9 µM; K562, IC_{50} > 40 µM; MCF-7, IC_{50} 16.9 µM; SMMC-7721, IC_{50} 27.3 µM; SW480, IC_{50} >40 µM) [333], **NO production inhibition assay** (IC_{50} 36.48 µM) [170]
208	*Agrocybe chaxingu* [322]	**osteoclast differentiation assay** (at 4.8 µM suppressed the rate of osteoclast formation to 6.7%) [322]
209	*Agrocybe chaxingu* [323]	**osteoclast differentiation assay** (at 3.1 µg/mL suppressed the rate of osteoclast formation to 66%) [323]
210	*Agrocybe chaxingu* [323]	
211	*Agrocybe chaxingu* [323], *Cordyceps jiangxiensis* [326], *Tricholoma imbricatum* [245], *Xylaria allantoidea* [330]	**cytotoxic assay** (A549, IC_{50} 7.9 µM; MCF-7, IC_{50} 10.2 µM) [245], (HeLa, IC_{50} 50.17 µg/mL; Vero, IC_{50} 76.57 µg/mL) [330], (A549, IC_{50} 2.93 µM; SGC-7901, IC_{50} 1.38 µM) [326], **osteoclast differentiation assay** (at 3.1 µg/mL suppressed the rate of osteoclast formation to 0%) [323]
212	*Agrocybe chaxingu* [323]	
213	*Hericium alpestre* [334]	**cytotoxic assay** (A549, IC_{50} 71.1 µM; HeLa, IC_{50} 69.6 µM; HT-29, IC_{50} 54.8 µM) [334]
214	*Antrodia camphorate* [335]	**cytotoxic assay** (A-2058, IC_{50} 31.1 µM; B16F10, IC_{50} 26.69 µM; Huh-7, IC_{50} 43.03 µM; MCF-7, IC_{50} 77.59 µM) [335]
215	*Ganoderma capense* [8]	**cytotoxic assay** (BGC823, Daoy, HCT116, HepG2, NCI-H1650, IC_{50} > 50 µM) [8]
216	*Ganoderma sinense* [220]	**cytotoxic assay** (SW1990, Vero, IC_{50} > 100 µM) [220]
217	*Daedaleopsis tricolor* [336]	**cytotoxic assay** (A-549, HL-60, MCF-7, SMMC-7721, SW480, IC_{50} > 40 µM) [336]
218	*Lenzites betulinus* [337]	**PTP1B inhibitory activity assay** (IC_{50} 21.5 µg/mL) [337]

Table 8. *Cont.*

Compound	Fungal Source [Ref.]	Assays (Activity) [Ref.]
219	*Antrodiella albocinnamomea* [327]	**PTP1B inhibitory activity assay** (no activity against DPP-IV and PTP1B at 50 µg/mL) [327]
220	*Antrodiella albocinnamomea* [327]	**PTP1B inhibitory activity assay** (IC_{50} 1.1 µg/mL in a mixture with **10–46**) [327]
221	*Antrodiella albocinnamomea* [327]	**PTP1B inhibitory activity assay** (IC_{50} 1.1 µg/mL in a mixture with **10–45**) [327]
222	*Phomopsis tersa* [338]	**cytotoxic assay** (A549, HepG2, MCF-7, SF-268, IC_{50} > 100 µM) [338]
223	*Tricholoma matsutake* [319]	**AChE inhibitory assay** (40.3% inhibition at 50 µg/mL) [319]

11. Conclusions

Fungi have been a traditional object of human practical interest throughout history. At first this was due to the nutritional value of mushrooms. Currently, fungi are attracting special attention as a source of a large number of biologically active compounds belonging to different classes: polyketides, terpenoids, peptides, alkaloids, etc., [339]. A wide variety of fungi secondary metabolites, their low content in natural material and the complexity of structural identification have led to the rapid development of research in this area only in the last two–three decades through the use of highly efficient methods of instrumental analysis and separation of complex natural compositions. A special place among fungi constituents is occupied by the metabolic products of ergosterol, the most important fungal sterol. Many of them are discussed in this review and some appear promising as leads for new medicines. At the same time, it is obvious that the described results not only characterize the achieved high level of research in this area, but also indicate directions for further scientific search, which is necessary for a better understanding of the content of the fungal metabolome and will allow revealing more fully the possibilities of practical use of its components in human healthcare.

Author Contributions: V.N.Z., P.D., and V.A.K. contributed equally. All authors have read and agreed to the published version of the manuscript.

Funding: The financial support by the Belarusian Foundation for Fundamental Research (projects X22ChI-025 and X22MC-004) is greatly appreciated.

Institutional Review Board Statement: Not applicable.

Informed Consent Statement: Not applicable.

Data Availability Statement: Not applicable.

Acknowledgments: We would like to acknowledge the *Molecules* journal for providing the APC waiver.

Conflicts of Interest: The authors declare no conflict of interest.

Abbreviations

AChE	acetylcholinesterase
bw	body weight
ConA	concanavalin A
COX	cyclooxygenase
DHEP	9,11-dehydroergosterol peroxide
DPP-IV	dipeptidyl peptidase IV
DPPH	2,2-diphenyl-1-picrylhydrazyl radical
ED_{50}	median effective dose
EP	ergosterol peroxide
GIRK	G protein-coupled inwardly-rectifying potassium channel
Galp	galactopyranosyl
Glcp	glucopyranosyl

HNE	human neutrophil elastase
IC_{50}	half maximal inhibitory concentration
IDH	isocitrate dehydrogenase
IL	interleukin
iNOS	inducible nitric oxide synthase
LDL-C	low density lipoprotein cholesterol
L-NMMA	N^G-methyl-L-arginine acetate salt
LPS	lipopolysaccharide
MDM2	mouse double minute 2 homolog
MIC	minimum inhibitory concentration
MRSA	methicillin resistant *Staphylococcus aureus*
NF-κB	nuclear factor kappa-light-chain-enhancer of activated B cells
NO	nitric oxide
NOE	nuclear Overhauser effect
ORAC	Oxygen Radical Antioxidant Capacity
PCSK9	proprotein convertase subtilisin/kexin type 9
PEG	poly(ethylene glycol)
PGE_2	prostaglandin E_2
PTP	protein tyrosine phosphatase
PTP1B	protein tyrosine phosphatase 1B
ROS	reactive oxygen species
PPAR	peroxisome proliferator-activated receptor
SHP2	SH2-containing protein tyrosine phosphatase-2
TE	Trolox equivalent
TNF-α	tumor necrosis factor alpha
TRAP	tartrate-resistant acid phosphatase

References

1. Öztürk, M.; Tel-Çayan, G.; Muhammad, A.; Terzioğlu, P.; Duru, M.E. Mushrooms: A Source of Exciting Bioactive Compounds. In *Studies in Natural Products Chemistry*; Atta-ur, R., Ed.; Elsevier: Amsterdam, The Netherlands, 2015; Volume 45, pp. 363–456. [CrossRef]
2. Lindequist, U.; Niedermeyer, T.H.J.; Jülich, W.D. The pharmacological potential of mushrooms. *eCAM* **2005**, *2*, 285–299. [CrossRef] [PubMed]
3. Sanjai, S.; Manmohan, C.; Inder Pal, S. Fungal bioactive compounds in pharmaceutical research and development. *Curr. Bioact. Compd.* **2019**, *15*, 211–231. [CrossRef]
4. Rodrigues, M.L. The multifunctional fungal ergosterol. *mBio* **2018**, *9*, e01755-18. [CrossRef] [PubMed]
5. Zhang, B.-B.; Han, X.-L.; Jiang, Q.; Liao, Z.-X.; Wang, H.-S. Cytotoxic cholestane-type and ergostane-type steroids from the aerial parts of *Euphorbia altotibetic*. *Steroids* **2013**, *78*, 38–43. [CrossRef] [PubMed]
6. Kikuchi, T.; Maekawa, Y.; Tomio, A.; Masumoto, Y.; Yamamoto, T.; In, Y.; Yamada, T.; Tanaka, R. Six new ergostane-type steroids from king trumpet mushroom (*Pleurotus eryngii*) and their inhibitory effects on nitric oxide production. *Steroids* **2016**, *115*, 9–17. [CrossRef]
7. Hu, Z.; Wu, Y.; Xie, S.; Sun, W.; Guo, Y.; Li, X.-N.; Liu, J.; Li, H.; Wang, J.; Luo, Z.; et al. Phomopsterones A and B, two functionalized ergostane-type steroids from the endophytic fungus *Phomopsis* sp. TJ507A. *Org. Lett.* **2017**, *19*, 258–261. [CrossRef]
8. Tan, Z.; Zhao, J.L.; Liu, J.M.; Zhang, M.; Chen, R.D.; Xie, K.B.; Chen, D.W.; Dai, J.G. Lanostane triterpenoids and ergostane-type steroids from the cultured mycelia of *Ganoderma capense*. *J. Asian Nat. Prod. Res.* **2018**, *20*, 844–851. [CrossRef]
9. Happi, G.M.; Wouamba, S.C.N.; Ismail, M.; Kouam, S.F.; Frese, M.; Lenta, B.N.; Sewald, N. Ergostane-type steroids from the Cameroonian 'white tiama' *Entandrophragma angolense*. *Steroids* **2020**, *156*, 108584. [CrossRef]
10. Lee, S.R.; Choi, J.H.; Ryoo, R.; Kim, J.-C.; Pang, C.; Kim, S.-H.; Kim, K.H. Ergostane-type steroids from Korean wild mushroom *Xerula furfuracea* that control adipocyte and osteoblast differentiation. *J. Microbiol. Biotechnol.* **2020**, *30*, 1769–1776. [CrossRef]
11. Liang, Y.; Zhang, M.; Yu, M.; Wang, J.; Zhu, H.; Chen, C.; Zhang, Y. Four new ergostane-type steroids from *Lasiodiplodia pseudotheobromae*. *Tetrahedron Lett.* **2020**, *61*, 151737. [CrossRef]
12. Yu, J.H.; Yu, S.J.; Liu, K.L.; Wang, C.; Liu, C.; Sun, J.Y.; Zhang, H. Cytotoxic ergostane-type steroids from *Ganoderma lingzhi*. *Steroids* **2021**, *165*, 108767. [CrossRef] [PubMed]
13. Zheng, J.; Wang, Y.; Wang, J.; Liu, P.; Li, J.; Zhu, W. Antimicrobial ergosteroids and pyrrole derivatives from halotolerant *Aspergillus flocculosus* PT05-1 cultured in a hypersaline medium. *Extremophiles* **2013**, *17*, 963–971. [CrossRef] [PubMed]
14. Han, J.-J.; Bao, L.; Tao, Q.-Q.; Yao, Y.-J.; Liu, X.-Z.; Yin, W.-B.; Liu, H.-W. Gloeophyllins A–J, cytotoxic ergosteroids with various skeletons from a Chinese Tibet fungus *Gloeophyllum abietinum*. *Org. Lett.* **2015**, *17*, 2538–2541. [CrossRef] [PubMed]

15. Wang, Y.; Dai, O.; Peng, C.; Su, H.G.; Miao, L.L.; Liu, L.S.; Xiong, L. Polyoxygenated ergosteroids from the macrofungus *Omphalia lapidescens* and the structure-cytotoxicity relationship in a human gastric cancer cell line. *Phytochem. Lett.* **2018**, *25*, 99–104. [CrossRef]
16. Liu, F.; Chen, J.-F.; Wang, Y.; Guo, L.; Zhou, Q.-M.; Peng, C.; Xiong, L. Cytotoxicity of lanostane-type triterpenoids and ergosteroids isolated from *Omphalia lapidescens* on MDA-MB-231 and HGC-27 cells. *Biomed. Pharmacother.* **2019**, *118*, 109273. [CrossRef]
17. Zhao, Z.-Z.; Han, K.-Y.; Li, Z.-H.; Feng, T.; Chen, H.-P.; Liu, J.-K. Cytotoxic ergosteroids from the fungus *Stereum hirsutum*. *Phytochem. Lett.* **2019**, *30*, 143–149. [CrossRef]
18. Lardy, H.; Partridge, B.; Kneer, N.; Wei, Y. Ergosteroids: Induction of thermogenic enzymes in liver of rats treated with steroids derived from dehydroepiandrosterone. *Proc. Natl. Acad. Sci. USA* **1995**, *92*, 6617–6619. [CrossRef]
19. Glotter, E. Withanolides and related ergostane-type steroids. *Nat. Prod. Rep.* **1991**, *8*, 415–440. [CrossRef]
20. Chen, L.X.; He, H.; Qiu, F. Natural withanolides: An overview. *Nat. Prod. Rep.* **2011**, *28*, 705–740. [CrossRef]
21. Xu, Q.Q.; Wang, K.W. Natural bioactive new withanolides. *Mini Rev. Med. Chem.* **2020**, *20*, 1101–1117. [CrossRef]
22. Aiello, A.; Fattorusso, E.; Menna, M. Steroids from sponges: Recent reports. *Steroids* **1999**, *64*, 687–714. [CrossRef] [PubMed]
23. Duecker, F.L.; Reuß, F.; Heretsch, P. Rearranged ergostane-type natural products: Chemistry, biology, and medicinal aspects. *Org. Biomol. Chem.* **2019**, *17*, 1624–1633. [CrossRef] [PubMed]
24. Merdivan, S.; Lindequist, U. Ergosterol peroxide: A mushroom-derived compound with promising biological activities-a review. *Int. J. Med. Mushrooms* **2017**, *19*, 93–105. [CrossRef] [PubMed]
25. Choi, J.-H. Biologically functional molecules from mushroom-forming fungi. *Biosci. Biotechnol. Biochem.* **2018**, *82*, 372–382. [CrossRef]
26. Clericuzio, M.; Mellerio, G.G.; Finzi, P.V.; Vidari, G. Secondary metabolites isolated from *Tricholoma* species (Basidiomycota, Tricholomatacee): A review. *Nat. Prod. Commun.* **2018**, *13*, 1213–1224. [CrossRef]
27. Vil, V.A.; Gloriozova, T.A.; Poroikov, V.V.; Terent'ev, A.O.; Savidov, N.; Dembitsky, V.M. Peroxy steroids derived from plant and fungi and their biological activities. *Appl. Microbiol. Biotechnol.* **2018**, *102*, 7657–7667. [CrossRef]
28. Vil, V.A.; Terent'ev, A.O.; Savidov, N.; Gloriozova, T.A.; Poroikov, V.V.; Pounina, T.A.; Dembitsky, V.M. Hydroperoxy steroids and triterpenoids derived from plant and fungi: Origin, structures and biological activities. *J. Steroid Biochem. Mol. Biol.* **2019**, *190*, 76–87. [CrossRef]
29. Dai, Z.B.; Wang, X.; Li, G.H. Secondary metabolites and their bioactivities produced by *Paecilomyces*. *Molecules* **2020**, *25*, 5077. [CrossRef]
30. Xiao, J.; Gao, M.; Fei, B.; Huang, G.; Diao, Q. Nature-derived anticancer steroids outside cardica glycosides. *Fitoterapia* **2020**, *147*, 104757. [CrossRef]
31. Ha, J.W.; Kim, J.; Kim, H.; Jang, W.; Kim, K.H. Mushrooms: An important source of natural bioactive compounds. *Nat. Prod. Sci.* **2020**, *26*, 118–131. [CrossRef]
32. Savidov, N.; Gloriozova, T.A.; Poroikov, V.V.; Dembitsky, V.M. Highly oxygenated isoprenoid lipids derived from fungi and fungal endophytes: Origin and biological activities. *Steroids* **2018**, *140*, 114–124. [CrossRef]
33. Loria-Kohen, V.; Lourenco-Nogueira, T.; Espinosa-Salinas, I.; Marin, F.R.; Soler-Rivas, C.; Ramirez de Molina, A. Nutritional and functional properties of edible mushrooms: A food with promising health claims. *J. Pharm. Nutr. Sci.* **2014**, *4*, 187. [CrossRef]
34. Nowak, R.; Nowacka-Jechalke, N.; Pietrzak, W.; Gawlik-Dziki, U. A new look at edible and medicinal mushrooms as a source of ergosterol and ergosterol peroxide—UHPLC-MS/MS analysis. *Food Chem.* **2022**, *369*, 130927. [CrossRef]
35. Shao, S.; Hernandez, M.; Kramer, J.K.; Rinker, D.L.; Tsao, R. Ergosterol profiles, fatty acid composition, and antioxidant activities of button mushrooms as affected by tissue part and developmental stage. *J. Agric. Food Chem.* **2010**, *58*, 11616–11625. [CrossRef] [PubMed]
36. Schneider, I.; Kressel, G.; Meyer, A.; Krings, U.; Berger, R.G.; Hahn, A. Lipid lowering effects of oyster mushroom (*Pleurotus ostreatus*) in humans. *J. Funct. Foods* **2011**, *3*, 17–24. [CrossRef]
37. Gil-Ramirez, A.; Ruiz-Rodriguez, A.; Marin, F.R.; Reglero, G.; Soler-Rivas, C. Effect of ergosterol-enriched extracts obtained from *Agaricus bisporus* on cholesterol absorption using an in vitro digestion model. *J. Funct. Foods* **2014**, *11*, 589–597. [CrossRef]
38. Morales, D.; Tejedor-Calvo, E.; Jurado-Chivato, N.; Polo, G.; Tabernero, M.; Ruiz-Rodriguez, A.; Largo, C.; Soler-Rivas, C. In vitro and in vivo testing of the hypocholesterolemic activity of ergosterol- and β-glucan-enriched extracts obtained from shiitake mushrooms (*Lentinula edodes*). *Food Funct.* **2019**, *10*, 7325–7332. [CrossRef] [PubMed]
39. Wu, M.; Huang, T.; Wang, J.; Chen, P.; Mi, W.; Ying, Y.; Wang, H.; Zhao, D.; Huang, S. Antilung cancer effect of ergosterol and cisplatin-loaded liposomes modified with cyclic arginine-glycine-aspartic acid and octa-arginine peptides. *Medicine* **2018**, *97*, e11916. [CrossRef]
40. Lin, Y.-C.; Lee, B.-H.; Alagie, J.; Su, C.-H. Combination treatment of ergosterol followed by amphotericin B induces necrotic cell death in human hepatocellular carcinoma cells. *Oncotarget* **2017**, *8*, 72727–72738. [CrossRef]
41. Sankaran, M.; Isabella, S.; Amaranth, K. Anti proliferative potential of ergosterol: A unique plant sterol on Hep2 cell line. *Int. J. Pharma Res. Health Sci.* **2017**, *5*, 1736–1742. [CrossRef]
42. Li, X.; Wu, Q.; Xie, Y.; Ding, Y.; Du, W.W.; Sdiri, M.; Yang, B.B. Ergosterol purified from medicinal mushroom *Amauroderma rude* inhibits cancer growth in vitro and in vivo by up-regulating multiple tumor suppressors. *Oncotarget* **2015**, *6*, 17832–17846. [CrossRef] [PubMed]

43. Hu, X.; Jiang, D.; Li, F.; Wu, Z.; Huang, Y.; Song, S.; Wang, Z. Ergosterol reverses multidrug resistance in SGC7901/Adr cells. *Pharmazie* **2014**, *69*, 396–400. [CrossRef] [PubMed]
44. Munoz-Fonseca, M.B.; Vidal-Limon, A.; Fernandez-Pomares, C.; Rojas-Duran, F.; Hernandez-Aguilar, M.E.; Espinoza, C.; Trigos, A.; Suarez-Medellin, J. Ergosterol exerts a differential effect on AR-dependent LNCaP and AR-independent DU-145 cancer cells. *Nat. Prod. Res.* **2021**, *35*, 4857–4860. [CrossRef] [PubMed]
45. Yazawa, Y.; Ikarashi, N.; Hoshino, M.; Kikkawa, H.; Sakuma, F.; Sugiyama, K. Inhibitory effect of ergosterol on bladder carcinogenesis is due to androgen signaling inhibition by brassicasterol, a metabolite of ergosterol. *J. Nat. Med.* **2020**, *74*, 680–688. [CrossRef]
46. Kuo, C.-F.; Hsieh, C.-H.; Lin, W.-Y. Proteomic response of LAP-activated RAW 264.7 macrophages to the anti-inflammatory property of fungal ergosterol. *Food Chem.* **2011**, *126*, 207–212. [CrossRef]
47. Kageyama-Yahara, N.; Wang, P.; Wang, X.; Yamamoto, T.; Kadowaki, M. The inhibitory effect of ergosterol, a bioactive constituent of a traditional Japanese herbal medicine saireito on the activity of mucosal-type mast cells. *Biol. Pharm. Bull.* **2010**, *33*, 142–145. [CrossRef]
48. Kawai, J.; Higuchi, Y.; Hirota, M.; Hirasawa, N.; Mori, K. Ergosterol and its derivatives from *Grifola frondosa* inhibit antigen-induced degranulation of RBL-2H3 cells by suppressing the aggregation of high affinity IgE receptors. *Biosci. Biotechnol. Biochem.* **2018**, *82*, 1803–1811. [CrossRef]
49. Zhang, S.-Y.; Xu, L.-T.; Li, A.-X.; Wang, S.-M. Effects of ergosterol, isolated from *Scleroderma polyrhizum* Pers., on lipopolysaccharide-induced inflammatory responses in acute lung injury. *Inflammation* **2015**, *38*, 1979–1985. [CrossRef]
50. Wang, H.; Zhang, T.; Li, Y.; Wang, S. Effects of ergosterol on COPD in mice via JAK3/STAT3/NF-κB pathway. *Inflammation* **2017**, *40*, 884–893. [CrossRef]
51. Sun, X.; Feng, X.; Zheng, D.; Li, A.; Li, C.; Li, S.; Zhao, Z. Ergosterol attenuates cigarette smoke extract-induced COPD by modulating inflammation, oxidative stress and apoptosis in vitro and in vivo. *Clin. Sci.* **2019**, *133*, 1523–1536. [CrossRef]
52. Xu, J.; Lin, C.; Wang, T.; Zhang, P.; Liu, Z.; Lu, C. Ergosterol attenuates LPS-induced myocardial injury by modulating oxidative stress and apoptosis in rats. *Cell. Physiol. Biochem.* **2018**, *48*, 583–592. [CrossRef] [PubMed]
53. Xie, Q.; Li, S.; Gao, Y.; Jin, L.; Dai, C.; Song, J. Ergosterol attenuates isoproterenol-induced myocardial cardiotoxicity. *Cardiovasc. Toxicol.* **2020**, *20*, 500–506. [CrossRef] [PubMed]
54. Cai, D.; Yan, H.; Liu, J.; Chen, S.; Jiang, L.; Wang, X.; Qin, J. Ergosterol limits osteoarthritis development and progression through activation of Nrf2 signaling. *Exp. Ther. Med.* **2021**, *21*, 194. [CrossRef]
55. Dong, Z.; Sun, Y.; Wei, G.; Li, S.; Zhao, Z. Ergosterol ameliorates diabetic nephropathy by attenuating mesangial cell proliferation and extracellular matrix deposition via the TGF-β1/Smad2 signaling pathway. *Nutrients* **2019**, *11*, 483. [CrossRef]
56. Liu, C.; Zhao, S.; Zhu, C.; Gao, Q.; Bai, J.; Si, J.; Chen, Y. Ergosterol ameliorates renal inflammatory responses in mice model of diabetic nephropathy. *Biomed. Pharmacother.* **2020**, *128*, 110252. [CrossRef]
57. Xiong, M.; Huang, Y.; Liu, Y.; Huang, M.; Song, G.; Ming, Q.; Ma, X.; Yang, J.; Deng, S.; Wen, Y.; et al. Antidiabetic activity of ergosterol from *Pleurotus ostreatus* in KK-A^y mice with spontaneous type 2 diabetes mellitus. *Mol. Nutr. Food Res.* **2018**, *62*, 1700444. [CrossRef]
58. Tai, C.-J.; Choong, C.-Y.; Lin, Y.-C.; Shi, Y.-C.; Tai, C.-J. The anti-hepatic fibrosis activity of ergosterol depended on upregulation of PPARgamma in HSC-T6 cells. *Food Funct.* **2016**, *7*, 1915–1923. [CrossRef]
59. Kikuchi, T.; Motoyashiki, N.; Yamada, T.; Shibatani, K.; Ninomiya, K.; Morikawa, T.; Tanaka, R. Ergostane-type sterols from king trumpet mushroom (*Pleurotus eryngii*) and their inhibitory effects on aromatase. *Int. J. Mol. Sci.* **2017**, *18*, 2479.
60. Medina, M.E.; Galano, A.; Trigos, A. Scavenging ability of homogentisic acid and ergosterol toward free radicals derived from ethanol consumption. *J. Phys. Chem. B* **2018**, *122*, 7514–7521. [CrossRef]
61. Zhao, Y.-Y.; Cheng, X.-L.; Liu, R.; Ho, C.C.; Wei, F.; Yan, S.-H.; Lin, R.-C.; Zhang, Y.; Sun, W.-J. Pharmacokinetics of ergosterol in rats using rapid resolution liquid chromatography-atmospheric pressure chemical ionization multi-stage tandem mass spectrometry and rapid resolution liquid chromatography/tandem mass spectrometry. *J. Chromatogr. B Anal. Technol. Biomed. Life Sci.* **2011**, *879*, 1945–1953. [CrossRef]
62. Zhang, H.-Y.; Firempong, C.K.; Wang, Y.-W.; Xu, W.-Q.; Wang, M.-M.; Cao, X.; Zhu, Y.; Tong, S.-S.; Yu, J.-N.; Xu, X.-M. Ergosterol-loaded poly(lactide-*co*-glycolide) nanoparticles with enhanced in vitro antitumor activity and oral bioavailability. *Acta Pharmacol. Sin.* **2016**, *37*, 834–844. [CrossRef] [PubMed]
63. Dong, Z.; Iqbal, S.; Zhao, Z. Preparation of ergosterol-loaded nanostructured lipid carriers for enhancing oral bioavailability and antidiabetic nephropathy effects. *AAPS PharmSciTech* **2020**, *21*, 64. [CrossRef] [PubMed]
64. Cheng, J.; Zhao, H.; Yao, L.; Li, Y.; Qi, B.; Wang, J.; Yang, X. Simple and multifunctional natural self-assembled sterols with anticancer activity-mediated supramolecular photosensitizers for enhanced antitumor photodynamic therapy. *ACS Appl. Mater. Interfaces* **2019**, *11*, 29498–29511. [CrossRef] [PubMed]
65. Yi, C.; Fu, M.; Cao, X.; Tong, S.; Zheng, Q.; Firempong, C.K.; Jiang, X.; Xu, X.; Yu, J. Enhanced oral bioavailability and tissue distribution of a new potential anticancer agent, *Flammulina velutipes* sterols, through liposomal encapsulation. *J. Agric. Food Chem.* **2013**, *61*, 5961–5971. [CrossRef]
66. He, W.-S.; Yin, J.; Xu, H.-S.; Qian, Q.-Y.; Jia, C.-S.; Ma, H.-L.; Feng, B. Efficient synthesis and characterization of ergosterol laurate in a solvent-free system. *J. Agric. Food Chem.* **2014**, *62*, 11748–11755. [CrossRef]

67. Park, S.H.; Kim, H.K. Antibacterial activity of emulsions containing unsaturated fatty acid ergosterol esters synthesized by lipase-mediated transesterification. *Enzyme Microb. Technol.* **2020**, *139*, 109581. [CrossRef]
68. He, W.S.; Li, L.; Zhao, J.; Xu, H.; Rui, J.; Cui, D.; Li, H.; Zhang, H.; Liu, X. *Candida* sp. 99-125 lipase-catalyzed synthesis of ergosterol linolenate and its characterization. *Food Chem.* **2019**, *280*, 286–293. [CrossRef]
69. Park, H.G.; Lee, T.H.; Chang, F.; Kwon, H.J.; Kim, J.; Kim, H. Synthesis of ergosterol and 5,6-dihydroergosterol glycosides and their inhibitory activities on lipopolysaccharide-induced nitric oxide production. *Bull. Korean Chem. Soc.* **2013**, *34*, 1339–1344. [CrossRef]
70. Dissanayake, A.A.; Zhang, C.-R.; Mills, G.L.; Nair, M.G. Cultivated maitake mushroom demonstrated functional food quality as determined by in vitro bioassays. *J. Funct. Foods* **2018**, *44*, 79–85. [CrossRef]
71. Aziz, S.; Elfahmi; Soemardji, A.A. Molecular docking, synthesis and biological evaluation of ergosteryl-ferulate as a HMG-Coa reductase inhibitor. *Pak. J. Pharm. Sci.* **2020**, *33*, 997–1003.
72. Lin, M.; Li, H.; Zhao, Y.; Cai, E.; Zhu, H.; Gao, Y.; Liu, S.; Yang, H.; Zhang, L.; Tang, G. 2-Naphthoic acid ergosterol ester, an ergosterol derivative, exhibits anti-tumor activity by promoting apoptosis and inhibiting angiogenesis. *Steroids* **2017**, *122*, 9–15. [CrossRef] [PubMed]
73. Lin, M.; Li, H.; Zhao, Y.; Cai, E.; Zhu, H.; Gao, Y.; Liu, S.; Yang, H.; Zhang, L.; Tang, G.; et al. Ergosteryl 2-naphthoate, an ergosterol derivative, exhibits antidepressant effects mediated by the modification of GABA ergic and glutamatergic systems. *Molecules* **2017**, *22*, 565. [CrossRef]
74. Karatavuk, A.O.; Karabulut, H.R.F. Synthesis of novel dimers containing cholesterol and ergosterol using click reaction and their anti-proliferative effects. *Mon. Chem.* **2020**, *151*, 837–844. [CrossRef]
75. Weete, J.D. Structure and Function of Sterols in Fungi. In *Advances in Lipid Research*; Paoletti, R., Kritchevsky, D., Eds.; Elsevier: Amsterdam, The Netherlands, 1989; Volume 23, pp. 115–167. [CrossRef]
76. Weete, J.D.; Abril, M.; Blackwell, M. Phylogenetic distribution of fungal sterols. *PLoS ONE* **2010**, *5*, e10899. [CrossRef]
77. Lee, H.S.; Hwang, I.H.; Kim, J.A.; Choi, J.Y.; Jang, T.-S.; Osada, H.; Ahn, J.S.; Na, M.; Lee, S.H. Isolation of protein tyrosine phosphatase 1B inhibitory constituents from the sclerotia of *Polyporus umbellatus* fries. *Bull. Korean Chem. Soc.* **2011**, *32*, 697–700. [CrossRef]
78. Xiao, J.-H.; Sun, Z.-H.; Pan, W.-D.; Zhong, J.-J. Secondary metabolite steroids isolated from medicinal entomogenous mushroom *Cordyceps jiangxiensis* mycelium. *Nat. Prod. Indian J.* **2011**, *7*, 118–123.
79. Tian, M.-Q.; Wu, Q.-L.; Wang, X.; Zhang, K.-Q.; Li, G.-H. A new compound from *Stereum insigne* CGMCC5.57. *Nat. Prod. Res.* **2017**, *31*, 932–937. [CrossRef]
80. Qiao, M.-F.; Yi, Y.-W.; Deng, J. Steroids from an endophytic *Eurotium rubrum* strain. *Chem. Nat. Compd.* **2017**, *53*, 678–681. [CrossRef]
81. Wu, J.; Fushimi, K.; Tokuyama, S.; Ohno, M.; Miwa, T.; Koyama, T.; Yazawa, K.; Nagai, K.; Matsumoto, T.; Hirai, H.; et al. Functional-food constituents in the fruiting bodies of *Stropharia rugosoannulata*. *Biosci. Biotechnol. Biochem.* **2011**, *75*, 1631–1634. [CrossRef]
82. Zhang, S.S.; Ma, Q.Y.; Zou, X.S.; Dai, H.F.; Huang, S.Z.; Luo, Y.; Yu, Z.F.; Luo, H.R.; Zhao, Y.X. Chemical constituents from the fungus *Amauroderma amoiensis* and their in vitro acetylcholinesterase inhibitory activities. *Planta Med.* **2013**, *79*, 87–91. [CrossRef]
83. Wang, Q.; Wang, Y.G.; Ma, Q.Y.; Huang, S.Z.; Kong, F.D.; Zhou, L.M.; Dai, H.F.; Zhao, Y.X. Chemical constituents from the fruiting bodies of *Amauroderma subresinosum*. *J. Asian Nat. Prod. Res.* **2016**, *18*, 1030–1035. [CrossRef] [PubMed]
84. Gao, J.; Wang, L.W.; Zheng, H.C.; Damirin, A.; Ma, C.M. Cytotoxic constituents of *Lasiosphaera fenzlii* on different cell lines and the synergistic effects with paclitaxel. *Nat. Prod. Res.* **2016**, *30*, 1862–1865. [CrossRef] [PubMed]
85. Torres, S.; Cajas, D.; Palfner, G.; Astuya, A.; Aballay, A.; Pérez, C.; Hernández, V.; Becerra, J. Steroidal composition and cytotoxic activity from fruiting body of *Cortinarius xiphidipus*. *Nat. Prod. Res.* **2017**, *31*, 473–476. [CrossRef]
86. Borlagdan, M.S.; De Castro, M.E.G.; van Altena, I.A.; Ragasa, C.Y. Sterols from *Trametes versicolor*. *Res. J. Pharm. Biol. Chem. Sci.* **2017**, *8*, 740–744.
87. Giroux, S.; Corey, E.J. An efficient, stereocontrolled synthesis of the 25-(*R*)-diastereomer of dafachronic acid A from β-ergosterol. *Org. Lett.* **2008**, *10*, 801–802. [CrossRef] [PubMed]
88. Pereira, D.M.; Correia-da-Silva, G.; Valentao, P.; Teixeira, N.; Andrade, P.B. Anti-inflammatory effect of unsaturated fatty acids and ergosta-7,22-dien-3-ol from *Marthasterias glacialis*: Prevention of CHOP-mediated ER-stress and NF-κB activation. *PLoS ONE* **2014**, *9*, e88341. [CrossRef]
89. Pereira, D.M.; Correia-da-Silva, G.; Valentao, P.; Teixeira, N.; Andrade, P.B. Palmitic acid and ergosta-7,22-dien-3-ol contribute to the apoptotic effect and cell cycle arrest of an extract from *Marthasterias glacialis* L. in neuroblastoma cells. *Mar. Drugs* **2014**, *12*, 54. [CrossRef]
90. Hong, Y.J.; Jang, A.R.; Jang, H.J.; Yang, K.S. Inhibition of nitric oxide production, iNOS and COX-2 expression of ergosterol derivatives from *Phellinus pini*. *Nat. Prod. Sci.* **2012**, *18*, 147–152.
91. Sárközy, A.; Béni, Z.; Dékány, M.; Zomborszki, Z.P.; Rudolf, K.; Papp, V.; Hohmann, J.; Ványolós, A. Cerebrosides and steroids from the edible mushroom *Meripilus giganteus* with antioxidant potential. *Molecules* **2020**, *25*, 1395. [CrossRef]
92. Budipramana, K.; Junaidin, J.; Wirasutisna, K.R.; Pramana, Y.B.; Sukrasno, S. An integrated in silico and in vitro assays of dipeptidyl peptidase-4 and α-glucosidase inhibition by stellasterol from *Ganoderma austral*. *Sci. Pharm.* **2019**, *87*, 21. [CrossRef]
93. Joseph, S.; Janardhanan, K.K.; George, V.; Baby, S. A new epoxidic ganoderic acid and other phytoconstituents from *Ganoderma lucidum*. *Phytochem. Lett.* **2011**, *4*, 386–388. [CrossRef]

94. Jung, M.; Lee, T.H.; Oh, H.J.; Kim, H.; Son, Y.; Lee, E.H.; Kim, J. Inhibitory effect of 5,6-dihydroergosteol-glucoside on atopic dermatitis-like skin lesions via suppression of NF-κB and STAT activation. *J. Dermatol. Sci.* **2015**, *79*, 252–261. [CrossRef] [PubMed]
95. Kim, T.K.; Cho, Y.K.; Park, H.; Lee, T.H.; Kim, H. Comparison of the inhibitory activities of 5,6-dihydroergosterol glycoside α- and β-anomers on skin inflammation. *Molecules* **2019**, *24*, 371. [CrossRef]
96. Park, Y.S.; Moon, H.J.; Ahn, K.H.; Lee, T.H.; Kim, H. Comparative study of the effect of 5,6-dihydroergosterol and 3-*epi*-5,6-dihydroergosterol on chemokine expression in human keratinocytes. *Molecules* **2020**, *25*, 522. [CrossRef]
97. Moon, H.; Ko, M.; Park, Y.; Kim, J.; Yoon, D.; Lee, E.; Lee, T.; Kim, H. $\Delta^{8(14)}$-Ergostenol glycoside derivatives inhibit the expression of inflammatory mediators and matrix metalloproteinase. *Molecules* **2021**, *26*, 4547. [CrossRef] [PubMed]
98. Kuo, Y.H.; Lin, C.H.; Shih, C.C. Ergostatrien-3β-ol from *Antrodia camphorata* inhibits diabetes and hyperlipidemia in high-fat-diet treated mice via regulation of hepatic related genes, glucose transporter 4, and AMP-activated protein kinase phosphorylation. *J. Agric. Food Chem.* **2015**, *63*, 2479–2489. [CrossRef] [PubMed]
99. Chang, Y.Y.; Liu, Y.C.; Kuo, Y.H.; Lin, Y.L.; Wu, Y.S.; Chen, J.W.; Chen, Y.C. Effects of antrosterol from *Antrodia camphorata* submerged whole broth on lipid homeostasis, antioxidation, alcohol clearance, and anti-inflammation in livers of chronic-alcohol fed mice. *J. Ethnopharmacol.* **2017**, *202*, 200–207. [CrossRef]
100. Kuo, Y.H.; Lin, T.Y.; You, Y.J.; Wen, K.C.; Sung, P.J.; Chiang, H.M. Antiinflammatory and antiphotodamaging effects of ergostatrien-3β-ol, isolated from *Antrodia camphorata*, on hairless mouse skin. *Molecules* **2016**, *21*, 1213. [CrossRef]
101. Ma, Q.-Y.; Yang, S.; Huang, S.-Z.; Kong, F.-D.; Xie, Q.-Y.; Dai, H.-F.; Yu, Z.-F.; Zhao, Y.-X. Ergostane steroids from *Coprinus setulosus*. *Chem. Nat. Compd.* **2018**, *54*, 710–713. [CrossRef]
102. Hsieh, W.T.; Hsu, M.H.; Lin, W.J.; Xiao, Y.C.; Lyu, P.C.; Liu, Y.C.; Lin, W.Y.; Kuo, Y.H.; Chung, J.G. Ergosta-7,9 (11),22-trien-3β-ol interferes with LPS docking to LBP, CD14, and TLR4/MD-2 co-receptors to attenuate the NF-κB inflammatory pathway in vitro and *Drosophila*. *Int. J. Mol. Sci.* **2021**, *22*, 6511. [CrossRef]
103. Shi, Q.; Huang, Y.; Su, H.; Gao, Y.; Peng, X.; Zhou, L.; Li, X.; Qiu, M. C_{28} steroids from the fruiting bodies of *Ganoderma resinaceum* with potential anti-inflammatory activity. *Phytochemistry* **2019**, *168*, 112109. [CrossRef] [PubMed]
104. Metwaly, A.M.; Kadry, H.A.; El-Hela, A.A.; Mohammad, A.-E.I.; Ma, G.; Cutler, S.J.; Ross, S.A. Nigrosphaerin A a new isochromene derivative from the endophytic fungus *Nigrospora sphaerica*. *Phytochem. Lett.* **2014**, *7*, 1–5. [CrossRef] [PubMed]
105. Xiong, J.; Huang, Y.; Wu, X.-Y.; Liu, X.-H.; Fan, H.; Wang, W.; Zhao, Y.; Yang, G.-X.; Zhang, H.-Y.; Hu, J.-F. Chemical constituents from the fermented mycelia of the medicinal fungus *Xylaria nigripes*. *Helv. Chim. Acta* **2016**, *99*, 83–89. [CrossRef]
106. Kao, S.-T.; Kuo, Y.-H.; Wang, S.-D.; Hong, H.-J.; Lin, L.-J. Analogous corticosteroids, 9A and EK100, derived from solid-state-cultured mycelium of *Antrodia camphorata* inhibit proinflammatory cytokine expression in macrophages. *Cytokine* **2018**, *108*, 136–144. [CrossRef] [PubMed]
107. Huang, G.-J.; Huang, S.-S.; Lin, S.-S.; Shao, Y.-Y.; Chen, C.-C.; Hou, W.-C.; Kuo, Y.-H. Analgesic effects and the mechanisms of anti-inflammation of ergostatrien-3β-ol from *Antrodia camphorata* submerged whole broth in mice. *J. Agric. Food Chem.* **2010**, *58*, 7445–7452. [CrossRef]
108. Tsai, T.-C.; Tung, Y.-T.; Kuo, Y.-H.; Liao, J.-W.; Tsai, H.-C.; Chong, K.-Y.; Chen, H.-L.; Chen, C.-M. Anti-inflammatory effects of *Antrodia camphorata*, a herbal medicine, in a mouse skin ischemia model. *J. Ethnopharmacol.* **2015**, *159*, 113–121. [CrossRef]
109. Chao, T.Y.; Hsieh, C.C.; Hsu, S.M.; Wan, C.H.; Lian, G.T.; Tseng, Y.H.; Kuo, Y.H.; Hsieh, S.C. Ergostatrien-3β-ol (EK100) from *Antrodia camphorata* attenuates oxidative stress, inflammation, and liver injury in vitro and in vivo. *Prev. Nutr. Food Sci.* **2021**, *26*, 58–66. [CrossRef]
110. Wang, Y.H.; Chern, C.M.; Liou, K.T.; Kuo, Y.H.; Shen, Y.C. Ergostatrien-7,9(11),22-trien-3β-ol from *Antrodia camphorata* ameliorates ischemic stroke brain injury via downregulation of p65NF-κ-B and caspase 3, and activation of Akt/GSK3/catenin-associated neurogenesis. *Food Funct.* **2019**, *10*, 4725–4738. [CrossRef]
111. Hsueh, P.J.; Wang, M.H.; Hsiao, C.J.; Chen, C.K.; Lin, F.L.; Huang, S.H.; Yen, J.L.; Tsai, P.H.; Kuo, Y.H.; Hsiao, G. Ergosta-7,9(11),22-trien-3β-ol alleviates intracerebral hemorrhage-induced brain injury and bv-2 microglial activation. *Molecules* **2021**, *26*, 2970. [CrossRef]
112. Chen, Y.M.; Sung, H.C.; Kuo, Y.H.; Hsu, Y.J.; Huang, C.C.; Liang, H.L. The effects of ergosta-7,9(11),22-trien-3β-ol from *Antrodia camphorata* on the biochemical profile and exercise performance of mice. *Molecules* **2019**, *24*, 1225. [CrossRef]
113. Robalo, J.R.; do Canto, A.M.T.M.; Carvalho, A.J.P.; Ramalho, J.P.P.; Loura, L.M.S. Behavior of fluorescent cholesterol analogues dehydroergosterol and cholestatrienol in lipid bilayers: A molecular dynamics study. *J. Phys. Chem. B* **2013**, *117*, 5806–5819. [CrossRef] [PubMed]
114. Pourmousa, M.; Rog, T.; Mikkeli, R.; Vattulainen, l.; Solanko, L.M.; Wustner, D.; List, N.H.; Kongsted, J.; Karttunen, M. Dehydroergosterol as an analogue for cholesterol: Why it mimics cholesterol so well-or does it? *J. Phys. Chem. B* **2014**, *118*, 7345–7357. [CrossRef] [PubMed]
115. Chattopadhyay, A.; Biswas, S.C.; Rukmini, R.; Saha, S.; Samanta, A. Lack of environmental sensitivity of a naturally occurring fluorescent analog of cholesterol. *J. Fluoresc.* **2021**, *31*, 1401–1407. [CrossRef] [PubMed]
116. Ano, Y.; Kutsukake, T.; Hoshi, A.; Yoshida, A.; Nakayama, H. Identification of a novel dehydroergosterol enhancing microglial anti-inflammatory activity in a dairy product fermented with *Penicillium candidum*. *PLoS ONE* **2015**, *10*, e0116598. [CrossRef]
117. Ano, Y.; Ikado, K.; Shindo, K.; Koizumi, H.; Fujiwara, D. Identification of 14-dehydroergosterol as a novel anti-inflammatory compound inducing tolerogenic dendritic cells. *Sci. Rep.* **2017**, *7*, 13903. [CrossRef]

118. Liu, Z.; Dong, Z.; Qiu, P.; Wang, Q.; Yan, J.; Lu, Y.; Wasu, P.-A.; Hong, K.; She, Z. Two new bioactive steroids from a mangrove-derived fungus *Aspergillus* sp. *Steroids* **2018**, *140*, 32–38. [CrossRef]
119. Liangsakul, J.; Srisurichan, S.; Pornpakakul, S. Anthraquinone-steroids, evanthrasterol A and B, and a meroterpenoid, emericellic acid, from endophytic fungus, Emericella variecolor. *Steroids* **2016**, *106*, 78–85. [CrossRef]
120. Elsebai, M.F.; Ghabbour, H.A.; Mehiri, M. Unusual nitrogenous phenalenone derivatives from the marine-derived fungus *Coniothyrium cereale*. *Molecules* **2016**, *21*, 178. [CrossRef]
121. Hou, G.M.; Xu, X.M.; Wang, Q.; Li, D.Y.; Li, Z.L. Hybrid of dehydroergosterol and nitrogenous alternariol derivative from the fungus *Pestalotiopsis uvicola*. *Steroids* **2018**, *138*, 43–46. [CrossRef]
122. El-Sherif, N.F.; Ahmed, S.A.; Ibrahim, A.K.; Habib, E.S.; El-Fallal, A.A.; El-Sayed, A.K.; Wahba, A.E. Ergosterol peroxide from the egyptian red lingzhi or reishi mushroom, *Ganoderma resinaceum* (Agaricomycetes), showed preferred inhibition of MCF-7 over MDA-MB-231 breast cancer cell lines. *Int. J. Med. Mushrooms* **2020**, *22*, 389–396. [CrossRef]
123. Chen, P.; Qin, H.-J.; Li, Y.-W.; Ma, G.-X.; Yang, J.-S.; Wang, Q. Study on chemical constituents of an edible mushroom *Volvariella volvacea* and their antitumor activity in vitro. *Nat. Prod. Res.* **2020**, *34*, 1417–1422. [CrossRef] [PubMed]
124. Govindharaj, M.; Arumugam, S.; Nirmala, G.; Bharadwaj, M.; Murugiyan, K. Effect of marine basidiomycetes *Fulvifomes* sp.-derived ergosterol peroxide on cytotoxicity and apoptosis induction in MCF-7 cell line. *J. Fungi* **2019**, *5*, 16.
125. Wu, H.-Y.; Yang, F.-L.; Li, L.-H.; Rao, Y.K.; Ju, T.-C.; Wong, W.-T.; Hsieh, C.-Y.; Pivkin, M.V.; Hua, K.-F.; Wu, S.-H. Ergosterol peroxide from marine fungus *Phoma* sp. induces ROS-dependent apoptosis and autophagy in human lung adenocarcinoma cells. *Sci. Rep.* **2018**, *8*, 17956. [CrossRef] [PubMed]
126. Lee, S.; Lee, D.; Ryoo, R.; Kim, J.-C.; Park, H.B.; Kang, K.S.; Kim, K.H. Calvatianone, a sterol possessing a 6/5/6/5-fused ring system with a contracted tetrahydrofuran B-ring, from the fruiting bodies of *Calvatia nipponica*. *J. Nat. Prod.* **2020**, *83*, 2737–2742. [CrossRef]
127. Chen, Y.K.; Kuo, Y.H.; Chiang, B.H.; Lo, J.M.; Sheen, L.Y. Cytotoxic activities of 9,11-dehydroergosterol peroxide and ergosterol peroxide from the fermentation mycelia of *Ganoderma lucidum* cultivated in the medium containing leguminous plants on Hep 3B cells. *J. Agric. Food Chem.* **2009**, *57*, 5713–5719. [CrossRef]
128. Lee, C.; Kim, S.; Li, W.; Bang, S.; Lee, H.; Lee, H.-J.; Noh, E.-Y.; Park, J.-E.; Bang, W.Y.; Shim, S.H. Bioactive secondary metabolites produced by an endophytic fungus *Gaeumannomyces* sp. JS0464 from a maritime halophyte *Phragmites communis*. *J. Antibiot.* **2017**, *70*, 737–742. [CrossRef]
129. Kobori, M.; Yoshida, M.; Ohnishi-Kameyama, M.; Takei, T.; Shinmoto, H. 5α,8α-Epidioxy-22E-ergosta-6,9(11),22-trien-3β-ol from an edible mushroom suppresses growth of HL60 leukemia and HT29 colon adenocarcinoma cells. *Biol. Pharm. Bull.* **2006**, *29*, 755–759. [CrossRef]
130. Cui, Y.J.; Guan, S.H.; Feng, L.X.; Song, X.Y.; Ma, C.; Cheng, C.R.; Wang, W.B.; Wu, W.Y.; Yue, Q.X.; Liu, X.; et al. Cytotoxicity of 9,11-dehydroergosterol peroxide isolated from *Ganoderma lucidum* and its target-related proteins. *Nat. Prod. Commun.* **2010**, *5*, 1183–1186.
131. Zheng, L.; Wong, Y.S.; Shao, M.; Huang, S.; Wang, F.; Chen, J. Apoptosis induced by 9,11-dehydroergosterol peroxide from *Ganoderma Lucidum* mycelium in human malignant melanoma cells is Mcl-1 dependent. *Mol. Med. Rep.* **2018**, *18*, 938–944. [CrossRef]
132. Njue, A.W.; Omolo, J.O.; Cheplogoi, P.K.; Langat, M.K.; Mulholland, D.A. Cytotoxic ergostane derivatives from the edible mushroom *Termitomyces microcarpus* (Lyophyllaceae). *Biochem. Syst. Ecol.* **2018**, *76*, 12–14. [CrossRef]
133. Chen, Z.; Bishop, K.S.; Tanambell, H.; Buchanan, P.; Smith, C.; Quek, S.Y. Characterization of the bioactivities of an ethanol extract and some of its constituents from the New Zealand native mushroom *Hericium novae-zealandiae*. *Food Funct.* **2019**, *10*, 6633–6643. [CrossRef] [PubMed]
134. He, L.; Shi, W.; Liu, X.; Zhao, X.; Zhang, Z. Anticancer action and mechanism of ergosterol peroxide from *Paecilomyces cicadae* fermentation broth. *Int. J. Mol. Sci.* **2018**, *19*, 3935. [CrossRef]
135. Tan, W.; Pan, M.; Liu, H.; Tian, H.; Ye, Q.; Liu, H. Ergosterol peroxide inhibits ovarian cancer cell growth through multiple pathways. *OncoTargets Ther.* **2017**, *10*, 3467–3474. [CrossRef] [PubMed]
136. Shin, M.-K.; Sasaki, F.; Ki, D.-W.; Win, N.N.; Morita, H.; Hayakawa, Y. Anti-metastatic effects of ergosterol peroxide from the entomopathogenic fungus *Ophiocordyceps gracilioides* on 4T1 breast cancer cells. *J. Nat. Med.* **2021**, *75*, 824–832. [CrossRef] [PubMed]
137. Yang, Y.; Luo, X.; Yasheng, M.; Zhao, J.; Li, J.; Li, J. Ergosterol peroxide from *Pleurotus ferulae* inhibits gastrointestinal tumor cell growth through induction of apoptosis via reactive oxygen species and endoplasmic reticulum stress. *Food Funct.* **2020**, *11*, 4171–4184. [CrossRef] [PubMed]
138. Zhao, F.; Xia, G.; Chen, L.; Zhao, J.; Xie, Z.; Qiu, F.; Han, G. Chemical constituents from *Inonotus obliquus* and their antitumor activities. *J. Nat. Med.* **2016**, *70*, 721–730. [CrossRef] [PubMed]
139. Zhou, J.; Li, G.; Deng, Q.; Zheng, D.; Yang, X.; Xu, J. Cytotoxic constituents from the mangrove endophytic *Pestalotiopsis* sp. induce G(0)/G(1) cell cycle arrest and apoptosis in human cancer cells. *Nat. Prod. Res.* **2018**, *32*, 2968–2972. [CrossRef]
140. Xiao, L.-G.; Zhang, Y.; Zhang, H.-L.; Li, D.; Gu, Q.; Tang, G.-H.; Yu, Q.; An, L.-K. Spiroconyone A, a new phytosterol with a spiro [5,6] ring system from *Conyza japonica*. *Org. Biomol. Chem.* **2020**, *18*, 5130–5136. [CrossRef]

141. Shaker, S.; Sun, T.-T.; Wang, L.-Y.; Ma, W.-Z.; Wu, D.-L.; Guo, Y.-W.; Dong, J.; Chen, Y.-X.; Zhu, L.-P.; Yang, D.-P.; et al. Reactive oxygen species altering the metabolite profile of the marine-derived fungus *Dichotomomyces cejpii* F31-1. *Nat. Prod. Res.* **2021**, *35*, 41–48. [CrossRef]
142. Le, B.V.; Nguyen, T.M.N.; Yang, S.Y.; Kim, J.H.; Le, T.V.; Huong, P.T.T.; Nguyen, V.T.; Nguyen, X.C.; Nguyen, H.N.; Chau, V.M.; et al. A new rearranged abietane diterpene from *Clerodendrum inerme* with antioxidant and cytotoxic activities. *Nat. Prod. Res.* **2018**, *32*, 2001–2007. [CrossRef]
143. Nguyen, T.T.; Nguyen, D.H.; Zhao, B.T.; Le, D.D.; Min, B.S.; Kim, Y.H.; Woo, M.H. Triterpenoids and sterols from the grains of Echinochloa utilis Ohwi & Yabuno and their cytotoxic activity. *Biomed. Pharmacother.* **2017**, *93*, 202–207. [CrossRef] [PubMed]
144. Hung, D.X.; Kuo, P.-C.; Tuan, N.N.; Van Trung, H.; Tan Thanh, N.; Thi Ha, N.; Long Giang, B.; Quang Trung, N.; Thi Ngan, N.; Hai, H.V.; et al. Triterpenoids and steroids from the fruiting bodies of Hexagonia tenuis and their cytotoxicity. *Nat. Prod. Res.* **2021**, *35*, 251–256. [CrossRef] [PubMed]
145. Bu, M.; Li, H.; Wang, H.; Wang, J.; Lin, Y.; Ma, Y. Synthesis of ergosterol peroxide conjugates as mitochondria targeting probes for enhanced anticancer activity. *Molecules* **2019**, *24*, 3307. [CrossRef]
146. Bu, M.; Cao, T.; Li, H.; Guo, M.; Yang, B.B.; Zeng, C.; Hu, L. Synthesis of 5α,8α-ergosterol peroxide 3-carbamate derivatives and a fluorescent mitochondria-targeting conjugate for enhanced anticancer activities. *ChemMedChem* **2017**, *12*, 466–474. [CrossRef]
147. Chen, S.; Yong, T.; Zhang, Y.; Su, J.; Jiao, C.; Xie, Y. Anti-tumor and anti-angiogenic ergosterols from *Ganoderma lucidum*. *Front. Chem.* **2017**, *5*, 85. [CrossRef] [PubMed]
148. Nowak, R.; Drozd, M.; Mendyk, E.; Lemieszek, M.; Krakowiak, O.; Kisiel, W.; Rzeski, W.; Szewczyk, K. A new method for the isolation of ergosterol and peroxyergosterol as active compounds of *Hygrophoropsis aurantiaca* and in vitro antiproliferative activity of isolated ergosterol peroxide. *Molecules* **2016**, *21*, 946. [CrossRef]
149. Ling, T.; Lang, W.H.; Martinez-Montemayor, M.M.; Rivas, F. Development of ergosterol peroxide probes for cellular localisation studies. *Org. Biomol. Chem.* **2019**, *17*, 5223–5229. [CrossRef] [PubMed]
150. Martínez-Montemayor, M.M.; Ling, T.; Suárez-Arroyo, I.J.; Ortiz-Soto, G.; Santiago-Negrón, C.L.; Lacourt-Ventura, M.Y.; Valentín-Acevedo, A.; Lang, W.H.; Rivas, F. Identification of biologically active *Ganoderma lucidum* compounds and synthesis of improved derivatives that confer anti-cancer activities in vitro. *Front. Pharm.* **2019**, *10*, 115. [CrossRef]
151. Kim, K.H.; Choi, S.U.; Noh, H.J.; Zee, O.; Lee, K.R. Cytotoxic ergosterol derivatives from the mushroom *Naematoloma fasciculare*. *Nat. Prod. Sci.* **2014**, *20*, 76–79.
152. Shi, X.-W.; Li, X.-J.; Gao, J.-M.; Zhang, X.-C. Fasciculols H and I, two lanostane derivatives from chinese mushroom *Naematoloma fasciculare*. *Chem. Biodivers.* **2011**, *8*, 1864–1870. [CrossRef]
153. Ibrahim, S.R.M.; Mohamed, G.A.; Haari, R.A.A.; Abd-Elmoneim, A.; El-Kholy, S.; Asfour, H.Z.; Zayed, M.F. Fusaristerol A: A new cytotoxic and antifungal ergosterol fatty acid ester from the endophytic fungus *Fusarium* sp. associated with *Mentha longifolia* roots. *Pharmacogn. Mag.* **2018**, *14*, 308–313. [CrossRef]
154. Chen, S.; Yong, T.; Xiao, C.; Su, J.; Zhang, Y.; Jiao, C.; Xie, Y. Pyrrole alkaloids and ergosterols from *Grifola frondosa* exert anti-α-glucosidase and anti-proliferative activities. *J. Funct. Foods* **2018**, *43*, 196–205. [CrossRef]
155. Lee, S.; Lee, S.; Roh, H.-S.; Song, S.-S.; Ryoo, R.; Pang, C.; Baek, K.-H.; Kim, K.H. Cytotoxic constituents from the sclerotia of *Poria cocos* against human lung adenocarcinoma cells by inducing mitochondrial apoptosis. *Cells* **2018**, *7*, 116. [CrossRef]
156. Su, Z.; Wang, P.; Yuan, W.; Li, S. Chemical constituents from the fruit body of *Chlorophyllum molybdites*. *Nat. Prod. Commun.* **2013**, *8*, 1227–1228. [CrossRef]
157. Shimizu, T.; Kawai, J.; Ouchi, K.; Kikuchi, H.; Osima, Y.; Hidemi, R. Agarol, an ergosterol derivative from *Agaricus blazei*, induces caspase-independent apoptosis in human cancer cells. *Int. J. Oncol.* **2016**, *48*, 1670–1678. [CrossRef]
158. Meza-Menchaca, T.; Poblete-Naredo, I.; Albores-Medina, A.; Pedraza-Chaverri, J.; Quiroz-Figueroa, F.R.; Cruz-Gregorio, A.; Zepeda, R.C.; Melgar-Lalanne, G.; Lagunes, I.; Trigos, Á. Ergosterol peroxide isolated from oyster medicinal mushroom, *Pleurotus ostreatus* (Agaricomycetes), potentially induces radiosensitivity in cervical cancer. *Int. J. Med. Mushrooms* **2020**, *22*, 1109–1119. [CrossRef]
159. Cayan, F.; Tel-Cayan, G.; Deveci, E.; Duru, M.E.; Tuerk, M. A detailed study on multifaceted bioactivities of the extracts and isolated compounds from truffle *Reddellomyces parvulosporus*. *Int. J. Food Sci. Technol.* **2022**, *57*, 1411–1419. [CrossRef]
160. Li, F.; Guo, S.; Zhang, S.; Peng, S.; Cao, W.; Ho, C.-T.; Bai, N. Bioactive constituents of *F. esculentum* bee pollen and quantitative analysis of samples collected from seven areas by HPLC. *Molecules* **2019**, *24*, 2705. [CrossRef]
161. Wu, S.-J.; Tung, Y.-J.; Ng, L.-T. Anti-diabetic effects of *Grifola frondosa* bioactive compound and its related molecular signaling pathways in palmitate-induced C2C12 cells. *J. Ethnopharmacol.* **2020**, *260*, 112962. [CrossRef]
162. Wonkam, A.K.N.; Ngansop, C.A.N.; Tchuenmogne, M.A.T.; Tchegnitegni, B.T.; Bitchagno, G.T.M.; Awantu, A.F.; Bankeu, J.J.K.; Boyom, F.F.; Sewald, N.; Lenta, B.N. Chemical constituents from *Baphia leptobotrys* Harms (Fabaceae) and their chemophenetic significance. *Biochem. Syst. Ecol.* **2021**, *96*, 104260. [CrossRef]
163. Meza-Menchaca, T.; Ramos-Ligonio, A.; Lopez-Monteon, A.; Limon, A.V.; Kaluzhskiy, L.A.; Shkel, T.V.; Strushkevich, N.V.; Jimenez-Garcia, L.F.; Moreno, L.T.A.; Gallegos-Garcia, V.; et al. Insights into ergosterol peroxide's trypanocidal activity. *Biomolecules* **2019**, *9*, 484. [CrossRef]
164. Zhou, B.; Liang, X.; Feng, Q.; Li, J.; Pan, X.; Xie, P.; Jiang, Z.; Yang, Z. Ergosterol peroxide suppresses influenza A virus-induced pro-inflammatory response and apoptosis by blocking RIG-I signaling. *Eur. J. Pharmacol.* **2019**, *860*, 172543. [CrossRef] [PubMed]

165. Duan, C.; Wang, J.; Liu, Y.; Zhang, J.; Si, J.; Hao, Z.; Wang, J. Antiviral effects of ergosterol peroxide in a pig model of porcine deltacoronavirus (PDCoV) infection involves modulation of apoptosis and tight junction in the small intestine. *Vet. Res.* **2021**, *52*, 86. [CrossRef] [PubMed]
166. Duan, C.; Liu, Y.; Hao, Z.; Wang, J. Ergosterol peroxide suppresses porcine deltacoronavirus (PDCoV)-induced autophagy to inhibit virus replication via p38 signaling pathway. *Vet. Microbiol.* **2021**, *257*, 109068. [CrossRef] [PubMed]
167. Duan, C.; Ge, X.; Wang, J.; Wei, Z.; Feng, W.-h.; Wang, J. Ergosterol peroxide exhibits antiviral and immunomodulatory abilities against porcine deltacoronavirus (PDCoV) via suppression of NF-κB and p38/MAPK signaling pathways in vitro. *Int. Immunopharmacol.* **2021**, *93*, 107317. [CrossRef] [PubMed]
168. Jin, M.; Zhou, W.; Jin, C.; Jiang, Z.; Diao, S.; Jin, Z.; Li, G. Anti-inflammatory activities of the chemical constituents isolated from *Trametes versicolor*. *Nat. Prod. Res.* **2019**, *33*, 2422–2425. [CrossRef]
169. Lee, S.; Lee, D.; Jang, T.S.; Kang, K.S.; Nam, J.-W.; Lee, H.-J.; Kim, K.H. Anti-inflammatory phenolic metabolites from the edible fungus *Phellinus baumii* in LPS-stimulated RAW264.7 cells. *Molecules* **2017**, *22*, 1583. [CrossRef]
170. Lee, S.; Lee, D.; Park, J.Y.; Seok, S.; Jang, T.S.; Park, H.B.; Shim, S.H.; Kang, K.S.; Kim, K.H. Antigastritis effects of *Armillariella tabescens* (Scop.) Sing. and the identification of its anti-inflammatory metabolites. *J. Pharm. Pharmacol.* **2018**, *70*, 404–412. [CrossRef]
171. Lee, S.; Choi, E.; Yang, S.-M.; Ryoo, R.; Moon, E.; Kim, S.-H.; Kim, K.H. Bioactive compounds from sclerotia extract of *Poria cocos* that control adipocyte and osteoblast differentiation. *Bioorg. Chem.* **2018**, *81*, 27–34. [CrossRef]
172. Jeong, Y.-U.; Park, Y.-J. Ergosterol peroxide from the medicinal mushroom *Ganoderma lucidum* inhibits differentiation and lipid accumulation of 3T3-L1 adipocytes. *Int. J. Mol. Sci.* **2020**, *21*, 460. [CrossRef]
173. Cateni, F.; Doljak, B.; Zacchigna, M.; Anderluh, M.; Piltaver, A.; Scialino, G.; Banfi, E. New biologically active epidioxysterols from *Stereum hirsutum*. *Bioorg. Med. Chem. Lett.* **2007**, *17*, 6330–6334. [CrossRef]
174. Zhai, M.M.; Qi, F.M.; Li, J.; Jiang, C.X.; Hou, Y.; Shi, Y.P.; Di, D.L.; Zhang, J.W.; Wu, Q.X. Isolation of secondary metabolites from the soil-derived fungus *Clonostachys rosea* YRS-06, a biological control agent, and evaluation of antibacterial activity. *J. Agric. Food Chem.* **2016**, *64*, 2298–2306. [CrossRef] [PubMed]
175. Sadorn, K.; Saepua, S.; Boonyuen, N.; Laksanacharoen, P.; Rachtawee, P.; Prabpai, S.; Kongsaeree, P.; Pittayakhajonwut, P. Allahabadolactones A and B from the endophytic fungus, *Aspergillus allahabadii* BCC45335. *Tetrahedron* **2016**, *72*, 489–495. [CrossRef]
176. Kornsakulkarn, J.; Saepua, S.; Laksanacharoen, P.; Rachtawee, P.; Thongpanchang, C. Chaetone G, a new dibenzo[b,e]oxepinone from the insect pathogenic fungus *Aschersonia luteola* BCC 31749. *Tetrahedron Lett.* **2016**, *57*, 305–307. [CrossRef]
177. Wang, A.; Li, P.; Han, P.; Gu, G.; Shan, T.; Lai, D.; Zhou, L. New nitrogen-containing metabolites from cultures of rice false smut pathogen *Villosiclava virens*. *Nat. Prod. Res.* **2021**, *35*, 272–281. [CrossRef] [PubMed]
178. Uc-Cachon, A.; Gamboa-Angulo, M.M.; Borges-Argaez, R.; Reyes-Estebanez, M.; Said-Fernandez, S.; Molina-Salinas, G. Antitubercular activity of the fungus *Gliocladium* sp. MR41 strain. *Iran. J. Pharm. Res.* **2019**, *18*, 860–866. [CrossRef]
179. Miao, F.-P.; Li, X.-D.; Liu, X.-H.; Cichewicz, R.H.; Ji, N.-Y. Secondary metabolites from an algicolous *Aspergillus versicolor* strain. *Mar. Drugs* **2012**, *10*, 131–139. [CrossRef] [PubMed]
180. Tian, N.-N.; Li, C.; Tian, N.; Zhou, Q.-X.; Hou, Y.-J.; Zhang, B.-W.; Wang, X.-S. Syntheses of 7-dehydrocholesterol peroxides and their improved anticancer activity and selectivity over ergosterol peroxide. *New J. Chem.* **2017**, *41*, 14843–14846. [CrossRef]
181. Bu, M.; Cao, T.; Li, H.; Guo, M.; Yang, B.B.; Zhou, Y.; Zhang, N.; Zeng, C.; Hu, L. Synthesis and biological evaluation of novel steroidal 5α,8α-endoperoxide derivatives with aliphatic side-chain as potential anticancer agents. *Steroids* **2017**, *124*, 46–53. [CrossRef]
182. Wu, J.; Choi, J.-H.; Yoshida, M.; Hirai, H.; Harada, E.; Masuda, K.; Koyama, T.; Yazawa, K.; Noguchi, K.; Nagasawa, K.; et al. Osteoclast-forming suppressing compounds, gargalols A, B, and C, from the edible mushroom *Grifola gargal*. *Tetrahedron* **2011**, *67*, 6576–6581. [CrossRef]
183. Lee, I.-S.; Kim, J.-P.; Na, M.-K.; Jung, H.-J.; Min, B.-S.; Bae, K.-H. Cytotoxicity of ergosterol derivatives from the fruiting bodies of *Hygrophorus russula*. *Nat. Prod. Sci.* **2011**, *17*, 85–89.
184. Wang, S.; Zhang, L.; Liu, L.-Y.; Dong, Z.-J.; Li, Z.-H.; Liu, J.-K. Six novel steroids from culture of basidiomycete *Polyporus ellisii*. *Nat. Prod. Bioprospect.* **2012**, *2*, 240–244. [CrossRef]
185. Froufe, H.J.C.; Abreu, R.M.V.; Ferreira, I.C.F.R. Virtual screening of low molecular weight mushrooms compounds as potential Mdm2 inhibitors. *J. Enzyme Inhib. Med. Chem.* **2013**, *28*, 569–575. [CrossRef] [PubMed]
186. Bang, S.; Chae, H.-S.; Lee, C.; Choi, H.G.; Ryu, J.; Li, W.; Lee, H.; Jeong, G.-S.; Chin, Y.-W.; Shim, S.H. New aromatic compounds from the fruiting body of *Sparassis crispa* (Wulf.) and their inhibitory activities on proprotein convertase subtilisin/kexin type 9 mRNA expression. *J. Agric. Food Chem.* **2017**, *65*, 6152–6157. [CrossRef] [PubMed]
187. Li, W.; Zhou, W.; Cha, J.Y.; Kwon, S.U.; Baek, K.-H.; Shim, S.H.; Lee, Y.M.; Kim, Y.H. Sterols from *Hericium erinaceum* and their inhibition of TNF-α and NO production in lipopolysaccharide-induced RAW 264.7 cells. *Phytochemistry* **2015**, *115*, 231–238. [CrossRef]
188. Li, W.; Bang, S.H.; Lee, C.; Ma, J.Y.; Shim, S.H.; Kim, Y.H. Sterols, aromatic compounds, and cerebrosides from the *Hericium erinaceus* fruiting body. *Biochem. Syst. Ecol.* **2017**, *70*, 254–259. [CrossRef]
189. Yu, F.-X.; Li, Z.; Chen, Y.; Yang, Y.-H.; Li, G.-H.; Zhao, P.-J. Four new steroids from the endophytic fungus *Chaetomium* sp. M453 derived of Chinese herbal medicine *Huperzia serrata*. *Fitoterapia* **2017**, *117*, 41–46. [CrossRef]

190. Li, Z.; Ma, N.; Zhao, P.-J. Acetylcholinesterase inhibitory active metabolites from the endophytic fungus *Colletotrichum* sp. YMF432. *Nat. Prod. Res.* **2019**, *33*, 1794–1797. [CrossRef]
191. Bok, J.W.; Lermer, L.; Chilton, J.; Klingeman, H.G.; Towers, G.H. Antitumor sterols from the mycelia of *Cordyceps sinensis*. *Phytochemistry* **1999**, *51*, 891–898. [CrossRef]
192. Yan, B.-F.; Fang, S.-T.; Li, W.-Z.; Liu, S.-J.; Wang, J.-H.; Xia, C.-H. A new minor diketopiperazine from the sponge-derived fungus *Simplicillium* sp. YZ-11. *Nat. Prod. Res.* **2015**, *29*, 2013–2017. [CrossRef]
193. Wu, J.; Kobori, H.; Kawaide, M.; Suzuki, T.; Choi, J.H.; Yasuda, N.; Noguchi, K.; Matsumoto, T.; Hirai, H.; Kawagishi, H. Isolation of bioactive steroids from the *Stropharia rugosoannulata* mushroom and absolute configuration of strophasterol B. *Biosci. Biotechnol. Biochem.* **2013**, *77*, 1779–1781. [CrossRef] [PubMed]
194. Zhang, Y.M.; Li, H.Y.; Hu, C.; Sheng, H.F.; Zhang, Y.; Lin, B.R.; Zhou, G.X. Ergosterols from the culture broth of marine *Streptomyces anandii* H41-59. *Mar. Drugs* **2016**, *14*, 84. [CrossRef]
195. Aung, H.T.; Porta, A.; Clericuzio, M.; Takaya, Y.; Vidari, G. Two new ergosterol derivatives from the basidiomycete *Cortinarius glaucopus*. *Chem. Biodivers.* **2017**, *14*, e1600421. [CrossRef]
196. Mei, R.-Q.; Zuo, F.-J.; Duan, X.-Y.; Wang, Y.-N.; Li, J.-R.; Qian, C.-Z.; Xiao, J.-P. Ergosterols from *Ganoderma sinense* and their anti-inflammatory activities by inhibiting NO production. *Phytochem. Lett.* **2019**, *32*, 177–180. [CrossRef]
197. Li, X.-J.; Gao, J.-M.; Chen, H.; Zhang, A.-L.; Tang, M. Toxins from a symbiotic fungus, *Leptographium qinlingensis* associated with *Dendroctonus armandi* and their in vitro toxicities to *Pinus armandi* seedlings. *Eur. J. Plant Pathol.* **2012**, *134*, 239–247. [CrossRef]
198. Lee, I.-S.; Bae, K.; Yoo, J.K.; Ryoo, I.-J.; Kim, B.Y.; Ahn, J.S.; Yoo, I.-D. Inhibition of human neutrophil elastase by ergosterol derivatives from the mycelium of *Phellinus linteus*. *J. Antibiot.* **2012**, *65*, 437–440. [CrossRef]
199. Bang, S.; Lee, C.; Ryu, J.; Li, W.; Koh, Y.-S.; Jeon, J.-H.; Lee, J.; Shim, S.H. Simultaneous determination of the bioactive compounds from *Sparassis crispa* (Wulf.) by HPLC-DAD and their inhibitory effects on LPS-stimulated cytokine production in bone marrow-derived dendritic cell. *Arch. Pharm. Res.* **2018**, *41*, 823–829. [CrossRef]
200. Li, W.; Zhou, W.; Song, S.B.; Shim, S.H.; Kim, Y.H. Sterol fatty acid esters from the mushroom *Hericium erinaceum* and their ppar transactivational effects. *J. Nat. Prod.* **2014**, *77*, 2611–2618. [CrossRef]
201. Kikuchi, T.; Isobe, M.; Uno, S.; In, Y.; Zhang, J.; Yamada, T. Strophasterols E and F: Rearranged ergostane-type sterols from *Pleurotus eryngii*. *Bioorg. Chem.* **2019**, *89*, 103011. [CrossRef]
202. Zhu, X.-C.; Huang, G.-L.; Mei, R.-Q.; Wang, B.; Sun, X.-P.; Luo, Y.-P.; Xu, J.; Zheng, C.-J. One new α,β-unsaturated 7-ketone sterol from the mangrove-derived fungus *Phomopsis* sp.MGF222. *Nat. Prod. Res.* **2020**, *35*, 3970–3976. [CrossRef]
203. Gao, H.; Hong, K.; Chen, G.-D.; Wang, C.-X.; Tang, J.-S.; Yu, Y.; Jiang, M.-M.; Li, M.-M.; Wang, N.-L.; Yao, X.-S. New oxidized sterols from *Aspergillus awamori* and the endo-boat conformation adopted by the cyclohexene oxide system. *Magn. Reson. Chem.* **2010**, *48*, 38–43. [CrossRef] [PubMed]
204. Zhang, M.; Deng, Y.; Liu, F.; Zheng, M.; Liang, Y.; Sun, W.; Li, Q.; Li, X.N.; Qi, C.; Liu, J.; et al. Five undescribed steroids from *Talaromyces stipitatus* and their cytotoxic activities against hepatoma cell lines. *Phytochemistry* **2021**, *189*, 112816. [CrossRef] [PubMed]
205. Chi, L.-P.; Yang, S.-Q.; Li, X.-M.; Li, X.-D.; Wang, B.-G.; Li, X. A new steroid with 7β,8β-epoxidation from the deep sea-derived fungus *Aspergillus penicillioides* SD-311. *J. Asian Nat. Prod. Res.* **2021**, *23*, 884–891. [CrossRef] [PubMed]
206. Lei, H.-M.; Ma, N.; Wang, T.; Zhao, P.-J. Metabolites from the endophytic fungus *Colletotrichum* sp. F168. *Nat. Prod. Res.* **2021**, *35*, 1077–1083. [CrossRef] [PubMed]
207. Lee, J.S.; Ma, C.M.; Park, D.K.; Yoshimi, Y.; Hatanaka, M.; Hattori, M. Transformation of ergosterol peroxide to cytotoxic substances by rat intestinal bacteria. *Biol. Pharm. Bull.* **2008**, *31*, 949–954. [CrossRef]
208. Zang, Y.; Xiong, J.; Zhai, W.-Z.; Cao, L.; Zhang, S.-P.; Tang, Y.; Wang, J.; Su, J.-J.; Yang, G.-X.; Zhao, Y.; et al. Fomentarols A-D, sterols from the polypore macrofungus *Fomes fomentarius*. *Phytochemistry* **2013**, *92*, 137–145. [CrossRef]
209. Ibrahim, S.R.M.; Elkhayat, E.S.; Mohamed, G.A.A.; Fat'hi, S.M.; Ross, S.A. Fusarithioamide A, a new antimicrobial and cytotoxic benzamide derivative from the endophytic fungus *Fusarium chlamydosporium*. *Biochem. Biophys. Res. Commun.* **2016**, *479*, 211–216. [CrossRef]
210. Wang, X.; Bao, H.; Bau, T. Investigation of the possible mechanism of two kinds of sterols extracted from *Leucocalocybe mongolica* in inducing HepG2 cell apoptosis and exerting anti-tumor effects in H22 tumor-bearing mice. *Steroids* **2020**, *163*, 108692. [CrossRef]
211. Zhao, Y.Y.; Chao, X.; Zhang, Y.; Lin, R.C.; Sun, W.J. Cytotoxic steroids from *Polyporus umbellatus*. *Planta Med.* **2010**, *76*, 1755–1758. [CrossRef]
212. Appiah, T.; Agyare, C.; Luo, Y.; Boamah, E.V.; Boakye, D.Y. Antimicrobial and resistance modifying activities of cerevisterol isolated from *Trametes species*. *Curr. Bioact. Compd.* **2020**, *16*, 115–123. [CrossRef]
213. Zhou, F.; Zhang, H.; Liu, R.; Zhang, D. Isolation and biological evaluation of secondary metabolites of the endophytic fungus *Aspergillus fumigatus* from *Astragalus membranaceus*. *Chem. Nat. Compd.* **2013**, *49*, 568–570. [CrossRef]
214. Yazdani, M.; Beni, Z.; Dekany, M.; Papp, V.; Lazar, A.; Burian, K.; Hohmann, J.; Vanyolos, A. Isolation and characterization of chemical constituents from the mushroom *Clitocybe nebularis*. *J. Res. Pharm.* **2020**, *24*, 908–913. [CrossRef]
215. Guo, K.; Fang, H.; Gui, F.; Wang, Y.; Xu, Q.; Deng, X. Two new ring A-cleaved lanostane-type triterpenoids and four known steroids isolated from endophytic fungus *Glomerella* sp. F00244. *Helv. Chim. Acta* **2016**, *99*, 601–607. [CrossRef]
216. Alam, B.M.; Chowdhury, N.S.; Sohrab, H.M.; Rana, S.M.; Hasan, C.M.; Lee, S.-H. Cerevisterol alleviates inflammation via suppression of MAPK/NF-κB/AP-1 and activation of the Nrf2/HO-1 signaling cascade. *Biomolecules* **2020**, *10*, 199. [CrossRef]

217. Pang, X.; Lin, X.; Wang, J.; Liang, R.; Tian, Y.; Salendra, L.; Luo, X.; Zhou, X.; Yang, B.; Tu, Z.; et al. Three new highly oxygenated sterols and one new dihydroisocoumarin from the marine sponge-derived fungus *Cladosporium* sp. SCSIO41007. *Steroids* **2018**, *129*, 41–46. [CrossRef]
218. Al-Rabia, M.W.; Mohamed, G.A.; Ibrahim, S.R.M.; Asfour, H.Z. Anti-inflammatory ergosterol derivatives from the endophytic fungus *Fusarium chlamydosporum*. *Nat. Prod. Res.* **2021**, *35*, 5011–5020. [CrossRef]
219. Wang, H.; Liu, T.; Xin, Z. A new glucitol from an endophytic fungus *Fusarium equiseti* Salicorn 8. *Eur. Food Res. Technol.* **2014**, *239*, 365–376. [CrossRef]
220. Bao, F.; Yang, K.; Wu, C.; Gao, S.; Wang, P.; Chen, L.; Li, H. New natural inhibitors of hexokinase 2 (HK2): Steroids from *Ganoderma sinense*. *Fitoterapia* **2018**, *125*, 123–129. [CrossRef]
221. Makropoulou, M.; Aligiannis, N.; Gonou-Zagou, Z.; Pratsinis, H.; Skaltsounis, A.-L.; Fokialakis, N. Antioxidant and cytotoxic activity of the wild edible mushroom *Gomphus clavatus*. *J. Med. Food* **2012**, *15*, 216–221. [CrossRef]
222. Lu, Q.-Q.; Tian, J.-M.; Wei, J.; Gao, J.-M. Bioactive metabolites from the mycelia of the basidiomycete *Hericium erinaceum*. *Nat. Prod. Res.* **2014**, *28*, 1288–1292. [CrossRef]
223. Li, W.; Lee, S.H.; Jang, H.D.; Ma, J.Y.; Kim, Y.H. Antioxidant and anti-osteoporotic activities of aromatic compounds and sterols from *Hericium erinaceum*. *Molecules* **2017**, *22*, 108. [CrossRef]
224. Vanyolos, A.; Orvos, P.; Chuluunbaatar, B.; Talosi, L.; Hohmann, J. GIRK channel activity of Hungarian mushrooms: From screening to biologically active metabolites. *Fitoterapia* **2019**, *137*, 104272. [CrossRef] [PubMed]
225. Fangkrathok, N.; Sripanidkulchai, B.; Umehara, K.; Noguchi, H. Bioactive ergostanoids and a new polyhydroxyoctane from *Lentinus polychrous* mycelia and their inhibitory effects on E2-enhanced cell proliferation of T47D cells. *Nat. Prod. Res.* **2013**, *27*, 1611–1619. [CrossRef] [PubMed]
226. Kim, J.-A.; Lau, E.; Tay, D.; Carcache De Blanco, E.J. Antioxidant and NF-κB inhibitory constituents isolated from *Morchella esculenta*. *Nat. Prod. Res.* **2011**, *25*, 1412–1417. [CrossRef] [PubMed]
227. Tang, H.-Y.; Zhang, Q.; Li, H.; Gao, J.-M. Antimicrobial and allelopathic metabolites produced by *Penicillium brasilianum*. *Nat. Prod. Res.* **2015**, *29*, 345–348. [CrossRef] [PubMed]
228. Liu, Y.-W.; Mei, H.-C.; Su, Y.-W.; Fan, H.-T.; Chen, C.-C.; Tsai, Y.-C. Inhibitory effects of *Pleurotus tuber-regium* mycelia and bioactive constituents on LPS-treated RAW 264.7 cells. *J. Funct. Foods* **2014**, *7*, 662–670. [CrossRef]
229. Kovacs, B.; Beni, Z.; Dekany, M.; Orban-Gyapai, O.; Sinka, I.; Zupko, I.; Hohmann, J.; Vanyolos, A. Chemical analysis of the edible mushroom *Tricholoma populinum*: Steroids and sulfinyladenosine compounds. *Nat. Prod. Commun.* **2017**, *12*, 1583–1584. [CrossRef]
230. Zhao, J.-L.; Zhang, M.; Liu, J.-M.; Tan, Z.; Chen, R.-D.; Xie, K.-B.; Dai, J.-G. Bioactive steroids and sorbicillinoids isolated from the endophytic fungus *Trichoderma* sp. Xy24. *J. Asian Nat. Prod. Res.* **2017**, *19*, 1028–1035. [CrossRef]
231. Liu, X.-H.; Miao, F.-P.; Liang, X.-R.; Ji, N.-Y. Ergosteroid derivatives from an algicolous strain of *Aspergillus ustus*. *Nat. Prod. Res.* **2014**, *28*, 1182–1186. [CrossRef]
232. Lee, M.K.; Hung, T.M.; Cuong, T.D.; Na, M.K.; Kim, J.C.; Kim, E.-J.; Park, H.-S.; Choi, J.S.; Lee, I.S.; Bae, K.H.; et al. Ergosta-7,22-diene-2β,3α,9α-triol from the fruit bodies of *Ganoderma lucidum* induces apoptosis in human myelocytic HL-60 cells. *Phytother. Res.* **2011**, *25*, 1579–1585. [CrossRef]
233. Zheng, M.; Tang, R.; Deng, Y.; Yang, K.; Chen, L.; Li, H. Steroids from *Ganoderma sinense* as new natural inhibitors of cancer-associated mutant IDH1. *Bioorg. Chem.* **2018**, *79*, 89–97. [CrossRef] [PubMed]
234. Xie, C.-L.; Zhang, D.; Xia, J.-M.; Hu, C.-C.; Lin, T.; Lin, Y.-K.; Wang, G.-H.; Tian, W.-J.; Li, Z.-P.; Zhang, X.-K.; et al. Steroids from the deep-sea-derived fungus *Penicillium granulatum* MCCC 3A00475 induced apoptosis via retinoid X receptor (RXR)-α pathway. *Mar. Drugs* **2019**, *17*, 178. [CrossRef]
235. Costa, T.M.; Lenzi, J.; Paganelli, C.J.; Filho, H.H.D.S.; Alberton, M.D.; Tavares, L.B.B.; de Oliveira, D. Liposoluble compounds from *Ganoderma lipsiense* grown on solid red rice medium with antiparasitic and antibacterial properties. *Biotechnol. Appl. Biochem.* **2020**, *67*, 180–185. [CrossRef] [PubMed]
236. Nhiem, N.X.; Yen, H.T.; Luyen, B.T.T.; Tai, B.H.; Van Hoan, P.; Thao, N.P.; Anh, H.L.T.; Ban, N.K.; Van Kiem, P.; Van Minh, C.; et al. Chemical components from the leaves of *Trichosanthes baviensis* and their tyrosinase inhibitory activity. *Bull. Korean Chem. Soc.* **2015**, *36*, 703–706. [CrossRef]
237. Lian, C.; Wang, C.F.; Xiao, Q.; Xiao, L.; Xu, Y.; Liu, J. The triterpenes and steroids from the fruiting body Ganoderma duripora. *Biochem. Syst. Ecol.* **2017**, *73*, 50–53. [CrossRef]
238. Nguyen, V.T.; Tung, N.T.; Cuong, T.D.; Hung, T.M.; Kim, J.A.; Woo, M.H.; Choi, J.S.; Lee, J.-H.; Min, B.S. Cytotoxic and anti-angiogenic effects of lanostane triterpenoids from *Ganoderma lucidum*. *Phytochem. Lett.* **2015**, *12*, 69–74. [CrossRef]
239. Gao, S.-S.; Li, X.-M.; Li, C.-S.; Proksch, P.; Wang, B.-G. Penicisteroids A and B, antifungal and cytotoxic polyoxygenated steroids from the marine alga-derived endophytic fungus *Penicillium chrysogenum* QEN-24S. *Bioorg. Med. Chem. Lett.* **2011**, *21*, 2894–2897. [CrossRef]
240. Niu, S.; Wang, N.; Xie, C.-L.; Fan, Z.; Luo, Z.; Chen, H.-F.; Yang, X.-W. Roquefortine J, a novel roquefortine alkaloid, from the deep-sea-derived fungus *Penicillium granulatum* MCCC 3A00475. *J. Antibiot.* **2018**, *71*, 658–661. [CrossRef]
241. Guo, J.; Yuan, Y.; Lu, D.; Du, B.; Xiong, L.; Shi, J.; Yang, L.; Liu, W.; Yuan, X.; Zhang, G.; et al. Two natural products, trans-phytol and (22E)-ergosta-6,9,22-triene-3β,5α,8α-triol, inhibit the biosynthesis of estrogen in human ovarian granulosa cells by aromatase (CYP19). *Toxicol. Appl. Pharmacol.* **2014**, *279*, 23–32. [CrossRef]
242. Kawahara, N.; Sekita, S.; Satake, M. Steroids from *Calvatia cyathiformis*. *Phytochemistry* **1994**, *37*, 213–215. [CrossRef]

243. Weng, Y.; Lu, J.; Xiang, L.; Matsuura, A.; Zhang, Y.; Huang, Q.; Qi, J. Ganodermasides C and D, two new anti-aging ergosterols from spores of the medicinal mushroom *Ganoderma lucidum*. *Biosci. Biotechnol. Biochem.* **2011**, *75*, 800–803. [CrossRef]
244. Weng, Y.; Xiang, L.; Matsuura, A.; Zhang, Y.; Huang, Q.; Qi, J. Ganodermasides A and B, two novel anti-aging ergosterols from spores of a medicinal mushroom *Ganoderma lucidum* on yeast via UTH1 gene. *Bioorg. Med. Chem.* **2010**, *18*, 999–1002. [CrossRef]
245. Zhang, F.L.; Yang, H.X.; Wu, X.; Li, J.Y.; Wang, S.Q.; He, J.; Li, Z.H.; Feng, T.; Liu, J.K. Chemical constituents and their cytotoxicities from mushroom *Tricholoma imbricatum*. *Phytochemistry* **2020**, *177*, 112431. [CrossRef] [PubMed]
246. Wu, S.H.; Huang, R.; Miao, C.P.; Chen, Y.W. Two new steroids from an endophytic fungus Phomopsis sp. *Chem. Biodivers.* **2013**, *10*, 1276–1283. [CrossRef]
247. Zhang, C.-Y.; Ji, X.; Gui, X.; Huang, B.-K. Chemical constituents from an endophytic fungus *Chaetomium globosum* Z1. *Nat. Prod. Commun.* **2013**, *8*, 1217–1218. [CrossRef] [PubMed]
248. Kikuchi, T.; Horii, Y.; Maekawa, Y.; Masumoto, Y.; In, Y.; Tomoo, K.; Sato, H.; Yamano, A.; Yamada, T.; Tanaka, R. Pleurocins A and B: Unusual 11(9→7)-abeo-ergostanes and eringiacetal B: A 13,14-seco-13,14-epoxyergostane from fruiting bodies of *Pleurotus eryngii* and their inhibitory effects on nitric oxide production. *J. Org. Chem.* **2017**, *82*, 10611–10616. [CrossRef] [PubMed]
249. Kitchawalit, S.; Kanokmedhakul, K.; Kanokmedhakul, S.; Soytong, K. A new benzyl ester and ergosterol derivatives from the fungus *Gymnoascus reessii*. *Nat. Prod. Res.* **2014**, *28*, 1045–1051. [CrossRef] [PubMed]
250. Kikuchi, T.; Masumoto, Y.; In, Y.; Tomoo, K.; Yamada, T.; Tanaka, R. Eringiacetal A, 5,6-seco-(5S,6R,7R,9S)-5,6:5,7:6,9-triepoxyergosta-8(14),22-diene-3β,7β-diol, an unusual ergostane sterol from the fruiting bodies of *Pleurotus eryngii*. *Eur. J. Org. Chem.* **2015**, *2015*, 4645–4649. [CrossRef]
251. Liu, Y.P.; Pu, C.J.; Wang, M.; He, J.; Li, Z.H.; Feng, T.; Xie, J.; Liu, J.K. Cytotoxic ergosterols from cultures of the basidiomycete *Psathyrella candolleana*. *Fitoterapia* **2019**, *138*, 104289. [CrossRef]
252. He, W.-J.; Zhou, X.-J.; Qin, X.-C.; Mai, Y.-X.; Lin, X.-P.; Liao, S.-R.; Yang, B.; Zhang, T.; Tu, Z.-C.; Wang, J.-F.; et al. Quinone/hydroquinone meroterpenoids with antitubercular and cytotoxic activities produced by the sponge-derived fungus *Gliomastix* sp. ZSDS1-F7. *Nat. Prod. Res.* **2017**, *31*, 604–609. [CrossRef]
253. Yang, S.; Ma, Q.Y.; Kong, F.D.; Xie, Q.Y.; Huang, S.Z.; Zhou, L.M.; Dai, H.F.; Yu, Z.F.; Zhao, Y.X. Two new compounds from the fruiting bodies of *Ganoderma philippii*. *J. Asian Nat. Prod. Res.* **2018**, *20*, 249–254. [CrossRef]
254. Xue, J.; Wu, P.; Xu, L.; Wei, X. Penicillitone, a potent in vitro anti-inflammatory and cytotoxic rearranged sterol with an unusual tetracycle core produced by *Penicillium purpurogenum*. *Org. Lett.* **2014**, *16*, 1518–1521. [CrossRef] [PubMed]
255. Hwang, H.; Kwon, H.C.; Kwon, J. Chemical constituents isolated from the moss-derived fungus *Talaromyces* sp. *J. Korean Magn. Reson. Soc.* **2020**, *24*, 123–128. [CrossRef]
256. Chen, H.; Chen, D.Q.; Li, Q.F.; Li, P.F.; Chen, H.; Zhao, Y.Y. Research progress on pharmacology, pharmacokinetics and determination of ergosta-4,6,8 (14),22-tetraen-3-one. *China J. Chin. Mater. Med.* **2014**, *39*, 3905–3909.
257. Lee, W.Y.; Park, Y.; Ahn, J.K. Improvement of ergone production from mycelial culture of *Polyporus umbellatus*. *Mycobiology* **2007**, *35*, 82–86. [CrossRef] [PubMed]
258. Boehme, R.M.; Kempfle, M.A. Synthesis of fluorescent 4,6,8(14)-trien-3-one steroids via 3,5,7-trien-3-ol ethers. Important probes for steroid-protein interactions. *Steroids* **1994**, *59*, 265–269. [CrossRef]
259. Quang, D.N.; Bach, D.D. Ergosta-4,6,8(14),22-tetraen-3-one from Vietnamese *Xylaria* sp. possessing inhibitory activity of nitric oxide production. *Nat. Prod. Res.* **2008**, *22*, 901–906. [CrossRef]
260. Yuan, D.; Mori, J.; Komatsu, K.I.; Makino, T.; Kano, Y. An anti-aldosteronic diuretic component (drain dampness) in *Polyporus sclerotium*. *Biol. Pharm. Bull.* **2004**, *27*, 867–870. [CrossRef]
261. Zhao, Y.Y.; Zhang, L.; Mao, J.R.; Cheng, X.H.; Lin, R.C.; Zhang, Y.; Sun, W.J. Ergosta-4,6,8(14),22-tetraen-3-one isolated from *Polyporus umbellatus* prevents early renal injury in aristolochic acid-induced nephropathy rats. *J. Pharm. Pharmacol.* **2011**, *63*, 1581–1586. [CrossRef]
262. Zhao, Y.Y.; Zhang, L.; Long, F.Y.; Cheng, X.L.; Bai, X.; Wei, F.; Lin, R.C. UPLC-Q-TOF/HSMS/MS(E)-based metabonomics for adenine-induced changes in metabolic profiles of rat faeces and intervention effects of ergosta-4,6,8(14),22-tetraen-3-one. *Chem. Biol. Interact.* **2013**, *201*, 31–38. [CrossRef]
263. Chang, C.-W.; Chen, Y.-S.; Chen, C.-C.; Chan, I.-O.; Chen, C.-C.; Sheu, S.-J.; Lin, T.-W.; Chou, S.-H.; Liu, C.-J.; Lee, T.-C.; et al. Targeting cancer initiating cells by promoting cell differentiation and restoring chemosensitivity via dual inactivation of STAT3 and Src activity using an active component of *Antrodia cinnamomea* mycelia. *Oncotarget* **2016**, *7*, 73016–73031. [CrossRef] [PubMed]
264. Fernando, D.; Adhikari, A.; Nanayakkara, C.; de Silva, E.D.; Wijesundera, R.; Soysa, P. Cytotoxic effects of ergone, a compound isolated from *Fulviformes fastuosus*. *BMC Complement. Altern. Med.* **2016**, *16*, 484. [CrossRef]
265. Wang, Z.-R.; Li, G.; Ji, L.-X.; Wang, H.-H.; Gao, H.; Peng, X.-P.; Lou, H.-X. Induced production of steroids by co-cultivation of two endophytes from *Mahonia fortunei*. *Steroids* **2019**, *145*, 1–4. [CrossRef] [PubMed]
266. Zhao, Y.-Y.; Cheng, X.-L.; Wei, F.; Bai, X.; Lin, R.-C. Ultra performance liquid chromatography coupled with electrospray and atmospheric pressure chemical ionization (ESCi)-quadrupole time-of-flight mass spectrometry with novel mass spectrometry$^{\text{Elevated Energy}}$ (MSE) data collection technique: Determination and pharmacokinetics, tissue distribution and biliary excretion study of ergone in rat. *J. Sep. Sci.* **2012**, *35*, 1619–1626. [CrossRef] [PubMed]
267. Lee, W.Y.; Park, Y.; Ahn, J.-K.; Park, S.-Y.; Lee, H.-J. Cytotoxic activity of ergosta-4,6,8(14),22-tetraen-3-one from the sclerotia of *Polyporus umbellatus*. *Bull. Korean Chem. Soc.* **2005**, *26*, 1464–1466. [CrossRef]

268. Yuan, W.-H.; Teng, M.-T.; Sun, S.-S.; Ma, L.; Yuan, B.; Ren, Q.; Zhang, P. Active metabolites from endolichenic fungus *Talaromyces* sp. *Chem. Biodivers.* **2018**, *15*, e1800371. [CrossRef]
269. Arthan, S.; Tantapakul, C.; Kanokmedhakul, K.; Soytong, K.; Kanokmedhakul, S. A new xanthone from the fungus *Apiospora montagnei*. *Nat. Prod. Res.* **2017**, *31*, 1766–1771. [CrossRef]
270. Zhao, Y.Y.; Shen, X.; Chao, X.; Ho, C.C.; Cheng, X.L.; Zhang, Y.; Lin, R.C.; Du, K.J.; Luo, W.J.; Chen, J.Y.; et al. Ergosta-4,6,8(14),22-tetraen-3-one induces G2/M cell cycle arrest and apoptosis in human hepatocellular carcinoma HepG2 cells. *Biochim. Biophys. Acta* **2011**, *1810*, 384–390. [CrossRef]
271. Nguyen, T.H.; Ho, V.D.; Do, T.T.; Bui, H.T.; Phan, V.K.; Sak, K.; Raal, A. A new lignan glycoside from the aerial parts and cytotoxic investigation of *Uvaria rufa*. *Nat. Prod. Res.* **2015**, *29*, 247–252. [CrossRef]
272. Zhang, Y.; Zhao, T.; Wang, H.; Wang, J.; Wang, R.; Bu, H.; Hu, L.; Hu, D.; Wang, S. Effects of ergosterone on lipopolysaccharide-induced acute lung injury and nucleo side-binding oligomerization domain, leucine-rich repeats and pyrin domain containing protein 3 inflammatory signaling pathway in mice. *Mater. Express* **2021**, *11*, 38–45. [CrossRef]
273. Sun, Y.; Zhao, Y.; Li, G.; Yang, S.; Hu, X.; Fan, J. Studies of interaction between ergosta-4,6,8(14),22-tetraen-3-one (ergone) and human serum albumin by molecular spectroscopy and modeling. *J. Chin. Chem. Soc.* **2011**, *58*, 602–610. [CrossRef]
274. Liang, X.; Sun, Y.; Liu, L.; Ma, X.; Hu, X.; Fan, J.; Zhao, Y. Folate-functionalized nanoparticles for controlled ergosta-4,6,8(14),22-tetraen-3-one delivery. *Int. J. Pharm.* **2013**, *441*, 1–8. [CrossRef]
275. Sun, Y.; Ji, Z.; Zhao, Y.; Liang, X.; Hu, X.; Fan, J. Enhanced distribution and anti-tumor activity of ergosta-4,6,8(14),22-tetraen-3-one by polyethylene glycol liposomalization. *J. Nanosci. Nanotechnol.* **2013**, *13*, 1435–1439. [CrossRef] [PubMed]
276. Gu, B.-B.; Jiao, F.-R.; Wu, W.; Liu, L.; Jiao, W.-H.; Sun, F.; Wang, S.-P.; Yang, F.; Lin, H.-W. Ochrasperfloroid, an ochratoxin-ergosteroid heterodimer with inhibition of IL-6 and NO production from *Aspergillus flocculosus* 16D-1. *RSC Adv.* **2019**, *9*, 7251–7256. [CrossRef]
277. Gu, B.B.; Wu, W.; Jiao, F.R.; Jiao, W.H.; Li, L.; Sun, F.; Wang, S.P.; Yang, F.; Lin, H.W. Asperflotone, an 8(14->15)-*abeo*-ergostane from the sponge-derived fungus *Aspergillus flocculosus* 16D-1. *J. Org. Chem.* **2019**, *84*, 300–306. [CrossRef] [PubMed]
278. Gu, B.-B.; Wu, W.; Jiao, F.-R.; Jiao, W.-h.; Li, L.; Sun, F.; Wang, S.-P.; Yang, F.; Lin, H.-W. Aspersecosteroids A and B, two 11(9→10)-abeo-5,10-secosteroids with a dioxatetraheterocyclic ring system from *Aspergillus flocculosus* 16D-1. *Org. Lett.* **2018**, *20*, 7957–7960. [CrossRef]
279. Tao, H.; Li, Y.; Lin, X.; Zhou, X.; Dong, J.; Liu, Y.; Yang, B. A new pentacyclic ergosteroid from fungus *Aspergillus* sp. ScSiO41211 derived of mangrove sediment sample. *Nat. Prod. Commun.* **2018**, *13*, 1629–1631.
280. Liu, L.; Duan, F.F.; Gao, Y.; Peng, X.G.; Chang, J.L.; Chen, J.; Ruan, H.L. Aspersteroids A–C, three rearranged ergostane-type steroids from *Aspergillus ustus* NRRL 275. *Org. Lett.* **2021**, *23*, 9620–9624. [CrossRef]
281. Palasarn, S.; Intereya, K.; Boonpratuang, T.; Thongpanchang, C.; Isaka, M. Ergostane triterpenoids from the cultures of basidiomycete *Favolaschia calocera* BCC 36684 and stereochemical elucidation of favolon. *Phytochem. Lett.* **2022**, *47*, 168–173. [CrossRef]
282. Pu, C.J.; Peng, Y.L.; Li, Z.H.; He, J.; Huang, R.; Feng, T.; Liu, J.K. Two highly oxygenated ergosterols from cultures of the basidiomycete *Conocybe siliginea*. *Nat. Prod. Res.* **2019**, *33*, 3037–3043. [CrossRef]
283. Yang, S.Q.; Li, X.M.; Li, X.; Chi, L.P.; Wang, B.G. Two new diketomorpholine derivatives and a new highly conjugated ergostane-type steroid from the marine algal-derived endophytic fungus *Aspergillus alabamensis* EN-547. *Mar. Drugs* **2018**, *16*, 114. [CrossRef]
284. Surup, F.; Halecker, S.; Nimtz, M.; Rodrigo, S.; Schulz, B.; Steinert, M.; Stadler, M. Hyfraxins A and B, cytotoxic ergostane-type steroid and lanostane triterpenoid glycosides from the invasive ash dieback ascomycete *Hymenoscyphus fraxineus*. *Steroids* **2018**, *135*, 92–97. [CrossRef]
285. Ji, J.-C.; Wei, P.-P.; Han, X.-Y.; Li, Z.-H.; Ai, H.-L.; Lei, X.-X. Secondary metabolites of the endophytic fungus *Chaetomium globosum* isolated from *Coptis chinensis*. *Nat. Prod. Commun.* **2021**, *16*, 1934578X211044574. [CrossRef]
286. Guo, H.; Li, Z.-H.; Feng, T.; Liu, J.-K. One new ergostane-type steroid and three new phthalide derivatives from cultures of the basidiomycete Albatrellus confluens. *J. Asian Nat. Prod. Res.* **2015**, *17*, 107–113. [CrossRef] [PubMed]
287. Chen, Z.-M.; Fan, Q.-Y.; Chen, H.-P.; Li, Z.-H.; Feng, T.; Liu, J.-K. A novel C25 sterol peroxide from the endophytic fungus *Phoma* sp. EA-122. *Z. Nat. C* **2015**, *70*, 93–96. [CrossRef]
288. Zhu, X.; Liu, Y.; Hu, Y.; Lv, X.; Shi, Z.; Yu, Y.; Jiang, X.; Feng, F.; Xu, J. Neuroprotective activities of constituents from *Phyllosticta capitalensis*, an endophyte fungus of *Loropetalum chinense* var. rubrum. *Chem. Biodivers.* **2021**, *18*, e2100314. [CrossRef]
289. Wakana, D.; Itabashi, T.; Kawai, K.-I.; Yaguchi, T.; Fukushima, K.; Goda, Y.; Hosoe, T. Cytotoxic anthrasteroid glycosides, malsterosides A–C, from *Malbranchea filamentosa*. *J. Antibiot.* **2014**, *67*, 585–588. [CrossRef]
290. Jiao, F.-R.; Gu, B.-B.; Zhu, H.-R.; Zhang, Y.; Liu, K.-C.; Zhang, W.; Han, H.; Xu, S.-H.; Lin, H.-W. Asperfloketals A and B, the first two ergostanes with rearranged a and d rings: From the sponge-associated *Aspergillus flocculosus* 16D-1. *J. Org. Chem.* **2021**, *86*, 10954–10961. [CrossRef]
291. Luo, Q.; Yang, Z.-L.; Yan, Y.-M.; Cheng, Y.-X. Ganotheaecolin A, a neurotrophic conjugated ergosterol with a naphtho[1,8-*ef*]azulene scaffold from *Ganoderma theaecolum*. *Org. Lett.* **2017**, *19*, 718–721. [CrossRef]
292. Fan, S.-Q.; Xie, C.-L.; Xia, J.-M.; Xing, C.-P.; Luo, Z.-H.; Shao, Z.; Yan, X.-J.; He, S.; Yang, X.-W. Sarocladione, a unique 5,10:8,9-diseco-steroid from the deep-sea-derived fungus *Sarocladium kiliense*. *Org. Biomol. Chem.* **2019**, *17*, 5925–5928. [CrossRef]
293. Ning, Y.; Tian, H.; Gui, J. Biogenesis-guided synthesis and structural revision of sarocladione enabled by ruthenium-catalyzed endoperoxide fragmentation. *Angew. Chem. Int. Ed.* **2021**, *60*, 11222–11226. [CrossRef]

294. Su, L.H.; Geng, C.A.; Li, T.Z.; Huang, X.Y.; Ma, Y.B.; Zhang, X.M.; Wu, G.; Yang, Z.L.; Chen, J.J. Spiroseoflosterol, a rearranged ergostane-steroid from the fruiting bodies of *Butyriboletus roseoflavus*. *J. Nat. Prod.* **2020**, *83*, 1706–1710. [CrossRef] [PubMed]
295. Anke, T.; Werle, A.; Kappe, R.; Sterner, O. Laschiatrion, a new antifungal agent from a *Favolaschia* species (Basidiomycetes) active against human pathogens. *J. Antibiot.* **2004**, *57*, 496–501. [CrossRef]
296. Cui, C.-M.; Li, X.-M.; Meng, L.; Li, C.-S.; Huang, C.-G.; Wang, B.-G. 7-Nor-ergosterolide, a pentalactone-containing norsteroid and related steroids from the marine-derived endophytic *Aspergillus ochraceus* EN-31. *J. Nat. Prod.* **2010**, *73*, 1780–1784. [CrossRef]
297. Krohn, K.; Biele, C.; Aust, H.J.; Draeger, S.; Schulz, B. Herbarulide, a ketodivinyllactone steroid with an unprecedented homo-6-oxaergostane skeleton from the endophytic fungus *Pleospora herbarum*. *J. Nat. Prod.* **1999**, *62*, 629–630.
298. Tong, Z.B.; Cui, X.H.; Wang, J.; Zhang, C.L.; Zhang, Y.Y.; Ren, Z.J. Constituents from solid-cultured *Antrodia camphorata*. *Nat. Prod. Res.* **2017**, *31*, 2564–2567. [CrossRef]
299. Duecker, F.L.; Heinze, R.C.; Mueller, M.; Zhang, S.; Heretsch, P. Synthesis of the alleged structures of fortisterol and herbarulide and structural revision of herbarulide. *Org. Lett.* **2020**, *22*, 1585–1588. [CrossRef]
300. Ratnaweera, P.B.; Williams, D.E.; Patrick, B.O.; de Silva, E.D.; Andersen, R.J. Solanioic acid, an antibacterial degraded steroid produced in culture by the fungus *Rhizoctonia solani* isolated from tubers of the medicinal plant *Cyperus rotundus*. *Org. Lett.* **2015**, *17*, 2074–2077. [CrossRef]
301. Song, Y.-P.; Shi, Z.-Z.; Miao, F.-P.; Fang, S.-T.; Yin, X.-L.; Ji, N.-Y. Tricholumin A, a highly transformed ergosterol derivative from the alga-endophytic fungus *Trichoderma asperellum*. *Org. Lett.* **2018**, *20*, 6306–6309. [CrossRef]
302. Amagata, T.; Doi, M.; Tohgo, M.; Minoura, K.; Numata, A. Dankasterone, a new class of cytotoxic steroid produced by a *Gymnascella* species from a marine sponge. *Chem. Commun.* **1999**, *14*, 1321–1322. [CrossRef]
303. Amagata, T.; Tanaka, M.; Yamada, T.; Doi, M.; Minoura, K.; Ohishi, H.; Yamori, T.; Numata, A. Variation in cytostatic constituents of a sponge-derived Gymnascella dankaliensis by manipulating the carbon source. *J. Nat. Prod.* **2007**, *70*, 1731–1740. [CrossRef] [PubMed]
304. Gao, W.; Chai, C.; He, Y.; Li, F.; Hao, X.; Cao, F.; Gu, L.; Liu, J.; Hu, Z.; Zhang, Y. Periconiastone A, an antibacterial ergosterol with a pentacyclo[8.7.0.0^{1,5}.0^{2,14}.0^{10,15}]heptadecane system from *Periconia* sp. TJ403-rc01. *Org. Lett.* **2019**, *21*, 8469–8472. [CrossRef] [PubMed]
305. Duecker, F.L.; Heinze, R.C.; Heretsch, P. Synthesis of swinhoeisterol A, dankasterone A and B, and periconiastone A by radical framework reconstruction. *J. Am. Chem. Soc.* **2020**, *142*, 104–108. [CrossRef] [PubMed]
306. Zhao, Z.Z.; Chen, H.P.; Huang, Y.; Zhang, S.B.; Li, Z.H.; Feng, T.; Liu, J.K. Bioactive polyketides and 8,14-seco-ergosterol from fruiting bodies of the ascomycete *Daldinia childiae*. *Phytochemistry* **2017**, *142*, 68–75. [CrossRef]
307. Wu, J.; Tokuyama, S.; Nagai, K.; Yasuda, N.; Noguchi, K.; Matsumoto, T.; Hirai, H.; Kawagishi, H. Strophasterols A to D with an unprecedented steroid skeleton: From the mushroom *Stropharia rugosoannulata*. *Angew. Chem. Int. Ed. Engl.* **2012**, *51*, 10820–10822. [CrossRef]
308. Sato, S.; Kuwahara, S. Synthesis of strophasterols C, E, and F. *Org. Lett.* **2020**, *22*, 1311–1315. [CrossRef]
309. Sato, S.; Taguchi, Y.; Kuwahara, S. Synthesis and stereochemistry of glaucoposterol A and strophasterol D. *Tetrahedron* **2020**, *76*, 131129. [CrossRef]
310. Lee, T.-H.; Chen, C.-C.; Chen, J.-J.; Liao, H.-F.; Chang, H.-S.; Sung, P.-J.; Tseng, M.-H.; Wang, S.-Y.; Ko, H.-H.; Kuo, Y.-H. New and cytotoxic components from *Antrodia camphorata*. *Molecules* **2014**, *19*, 21378–21385. [CrossRef]
311. Liu, X.-H.; Tang, X.-Z.; Miao, F.-P.; Ji, N.-Y. A new pyrrolidine derivative and steroids from an algicolous *Gibberella zeae* strain. *Nat. Prod. Commun.* **2011**, *6*, 1243–1246. [CrossRef]
312. Nakada, T.; Yamamura, S. Three new metabolites of hybrid strain KO 0231, derived from Penicillium citreo-viride IFO 6200 and 4692. *Tetrahedron* **2000**, *56*, 2595–2602. [CrossRef]
313. Tang, G.-H.; Lu, N.; Li, W.; Wu, M.; Chen, Y.-Y.; Zhang, H.-Y.; He, S.-Y. Mannosylxylarinolide, a new 3,4-seco-ergostane-type steroidal saponin featuring a β-D-mannose from the endophytic fungus *Xylaria* sp. *J. Asian Nat. Prod. Res.* **2020**, *22*, 397–403. [CrossRef] [PubMed]
314. Elissawy, A.M.; Ebada, S.S.; Ashour, M.L.; Ozkaya, F.C.; Ebrahim, W.; Singab, A.N.B.; Proksch, P. Spiroarthrinols a and B, two novel meroterpenoids isolated from the sponge- derived fungus *Arthrinium* sp. *Phytochem. Lett.* **2017**, *20*, 246–251. [CrossRef]
315. Yang, X.-Y.; Li, Z.-H.; Dong, Z.-J.; Feng, T.; Liu, J.-K. Three new sesquiterpenoids from cultures of the basidiomycete *Conocybe siliginea*. *J. Asian Nat. Prod. Res.* **2015**, *17*, 671–675. [CrossRef]
316. Kumla, D.; Aung, T.S.; Buttachon, S.; Dethoup, T.; Gales, L.; Pereira, J.A.; Inacio, A.; Costa, P.M.; Lee, M.; Sekeroglu, N.; et al. A new dihydrochromone dimer and other secondary metabolites from cultures of the marine sponge-associated fungi *Neosartorya fennelliae* KUFA 0811 and *Neosartorya tsunodae* KUFC 9213. *Mar. Drugs* **2017**, *15*, 375. [CrossRef]
317. Jiao, Y.; Li, G.; Wang, H.-Y.; Liu, J.; Li, X.-B.; Zhang, L.-L.; Zhao, Z.-T.; Lou, H.-X. New metabolites from endolichenic fungus *Pleosporales* sp. *Chem. Biodivers.* **2015**, *12*, 1095–1104. [CrossRef]
318. Wang, W.; Wan, X.; Liu, J.; Wang, J.; Zhu, H.; Chen, C.; Zhang, Y. Two new terpenoids from *Talaromyces purpurogenus*. *Mar. Drugs* **2018**, *16*, 150. [CrossRef]
319. Zhao, Z.-Z.; Chen, H.-P.; Wu, B.; Zhang, L.; Li, Z.-H.; Feng, T.; Liu, J.-K. Matsutakone and matsutoic acid, two (nor)steroids with unusual skeletons from the edible mushroom *Tricholoma matsutake*. *J. Org. Chem.* **2017**, *82*, 7974–7979. [CrossRef]
320. Chen, C.; Liang, F.; Chen, B.; Sun, Z.; Xue, T.; Yang, R.; Luo, D. Identification of demethylincisterol A3 as a selective inhibitor of protein tyrosine phosphatase Shp2. *Eur. J. Pharmacol.* **2017**, *795*, 124–133. [CrossRef]

321. Chen, M.; Wang, K.L.; Liu, M.; She, Z.G.; Wang, C.Y. Bioactive steroid derivatives and butyrolactone derivatives from a gorgonian-derived *Aspergillus* sp. fungus. *Chem. Biodivers.* **2015**, *12*, 1398–1406. [CrossRef]
322. Kawagishi, H.; Akachi, T.; Ogawa, T.; Masuda, K.; Yamaguchi, K.; Yazawa, K.; Takahashi, M. Chaxine A, an osteoclast-forming suppressing substance, from the mushroom *Agrocybe chaxingu*. *Heterocycles* **2006**, *69*, 253–258.
323. Choi, J.-H.; Ogawa, A.; Abe, N.; Masuda, K.; Koyama, T.; Yazawa, K.; Kawagishi, H. Chaxines B, C, D, and E from the edible mushroom *Agrocybe chaxingu*. *Tetrahedron* **2009**, *65*, 9850–9853. [CrossRef]
324. Hirata, Y.; Nakazaki, A.; Kawagishi, H.; Nishikawa, T. Biomimetic synthesis and structural revision of chaxine B and its analogues. *Org. Lett.* **2017**, *19*, 560–563. [CrossRef] [PubMed]
325. Niki, M.; Hirata, Y.; Nakazaki, A.; Wu, J.; Kawagishi, H.; Nishikawa, T. Biomimetic synthesis of chaxine and its related compounds. *J. Org. Chem.* **2020**, *85*, 4848–4860. [CrossRef] [PubMed]
326. Xiao, J.H.; Sun, Z.H.; Pan, W.D.; Lü, Y.H.; Chen, D.X.; Zhong, J.J. Jiangxienone, a new compound with potent cytotoxicity against tumor cells from traditional Chinese medicinal mushroom *Cordyceps jiangxiensis*. *Chem. Biodivers.* **2012**, *9*, 1349–1355. [CrossRef] [PubMed]
327. Chen, Z.-M.; Yang, X.-Y.; Fan, Q.-Y.; Li, Z.-H.; Wei, K.; Chen, H.-P.; Feng, T.; Liu, J.-K. Three novel degraded steroids from cultures of the Basidiomycete *Antrodiella albocinnamomea*. *Steroids* **2014**, *87*, 21–25. [CrossRef] [PubMed]
328. Chen, K.; Sun, W.; Bie, Q.; Liu, X.; Chen, C.; Liu, J.; Xue, Y.; Wang, J.; Luo, Z.; Zhu, H.; et al. Fusopoltide A and fusosterede A, A polyketide with a pentaleno[1,2-c]pyran ring system and A degraded steride, from the fungus *Fusarium solani*. *Tetrahedron Lett.* **2018**, *59*, 2679–2682. [CrossRef]
329. Amagata, T.; Tanaka, M.; Yamada, T.; Chen, Y.-P.; Minoura, K.; Numata, A. Additional cytotoxic substances isolated from the sponge-derived *Gymnascella dankaliensis*. *Tetrahedron Lett.* **2013**, *54*, 5960–5962. [CrossRef]
330. McCloskey, S.; Noppawan, S.; Mongkolthanaruk, W.; Suwannasai, N.; Senawong, T.; Prawat, U. A new cerebroside and the cytotoxic constituents isolated from *Xylaria allantoidea* SWUF76. *Nat. Prod. Res.* **2017**, *31*, 1422–1430. [CrossRef]
331. Wu, J.; Zhang, H.; He, L.-M.; Xue, Y.-Q.; Jia, J.; Wang, S.-B.; Zhu, K.-K.; Hong, K.; Cai, Y.-S. A new fusicoccane-type norditerpene and a new indone from the marine-derived fungus *Aspergillus aculeatinus* WHUF0198. *Chem. Biodivers.* **2021**, *18*, e2100562. [CrossRef]
332. An, C.L.; Kong, F.D.; Ma, Q.Y.; Xie, Q.Y.; Yuan, J.Z.; Zhou, L.M.; Dai, H.F.; Yu, Z.F.; Zhao, Y.X. Chemical constituents of the marine-derived fungus *Aspergillus* sp. SCS-KFD66. *Mar. Drugs* **2018**, *16*, 468. [CrossRef]
333. Zhang, F.L.; Shi, C.; Sun, L.T.; Yang, H.X.; He, J.; Li, Z.H.; Feng, T.; Liu, J.K. Chemical constituents and their biological activities from the mushroom *Pyropolyporus fomentarius*. *Phytochemistry* **2021**, *183*, 112625. [CrossRef] [PubMed]
334. Li, L.-N.; Wang, L.; Guo, X.-L. Chemical constituents from the culture of the fungus *Hericium alpestre*. *J. Asian Nat. Prod. Res.* **2019**, *21*, 735–741. [CrossRef] [PubMed]
335. Huang, H.-C.; Liaw, C.-C.; Yang, H.-L.; Hseu, Y.-C.; Kuo, H.-T.; Tsai, Y.-C.; Chien, S.-C.; Amagaya, S.; Chen, Y.-C.; Kuo, Y.-H. Lanostane triterpenoids and sterols from *Antrodia camphorata*. *Phytochemistry* **2012**, *84*, 177–183. [CrossRef] [PubMed]
336. Zhao, J.-Y.; Feng, T.; Li, Z.-H.; Dong, Z.-J.; Zhang, H.-B.; Liu, J.-K. Sesquiterpenoids and an ergosterol from cultures of the fungus *Daedaleopsis tricolor*. *Nat. Prod. Bioprospect.* **2013**, *3*, 271–276. [CrossRef]
337. Wen, C.-N.; Chen, H.-P.; Zhao, Z.-Z.; Hu, D.-B.; Li, Z.-H.; Feng, T.; Liu, J.-K. Two new γ-lactones from the cultures of basidiomycete *Lenzites betulinus*. *Phytochem. Lett.* **2017**, *20*, 9–12. [CrossRef]
338. Chen, S.; Liu, Z.; Chen, Y.; Tan, H.; Zhu, S.; Liu, H.; Zhang, W. Phosteoid A, a highly oxygenated norsteroid from the deep-sea-derived fungus *Phomopsis tersa* FS441. *Tetrahedron Lett.* **2020**, *61*, 151555. [CrossRef]
339. Liu, Z.; Zhao, J.-Y.; Sun, S.-F.; Li, Y.; Liu, Y.-B. Fungi: Outstanding source of novel chemical scaffolds. *J. Asian Nat. Prod. Res.* **2020**, *22*, 99–120. [CrossRef]